Throughput Maximization by Using Modulation and Coding Techniques for Free-Space Optical Links

Master's thesis

Martin Czaputa

_____

Institute for Broadband Communication
Graz University of Technology

in cooperation with the

Department of Electrical and Computer Engineering
McMaster University

Abstract

The growing demand on network capacity is an increasing issue. Free-space optical (FSO) systems are a promising communication technology. These wireless communication links use light to exchange data between two data terminals. Information transfer is carried out by modulating the light of a light emitting diode or a laser. The generated intensity signal propagates through the air. At the receiver, a photodiode converts this optical intensity signal back into an electrical signal and data is recovered. Such point-to-point free-space optical links have advantages in offering very high data rates, high security and have low installation costs. However, the quality of the communication link is influenced by various weather effects. For example, dense fog can lead to link outages which can last from several minutes to hours. One way to reduce these impairments is to use robust and simple modulation techniques such as on-off keying (OOK). These techniques are more tolerant against weather influences but lead to decreased data rates.

In this work, the effect of various modulation and coding schemes is investigated to increase data rates. First, FSO systems are considered for latency tolerant traffic applications. For such classes of data traffic, the instantaneous reliability of the link is not the primary concern, rather the average throughput of the link is important. In case of a link with 1 km distance and a low-density-parity-check coded 8-Pulse amplitude modulation, an increase of around 100% average data throughput was achieved compared to conventional used uncoded on-off keying (OOK) modulation.

In order to exploit the channel capacity more efficiently and hence to increase data rates and availability, the FSO system was extended by adaptive communication. For this technique, feedback data about the channel transmission quality are used in order to, e.g., select the right modulation type depending on the current weather condition. With an adaptive method called "adaptive coded modulation", a yearly average data throughput of 2.6 Gbps can be achieved. This is a 220% improvement over standard uncoded OOK.

In order to evaluate the performance of the tested modulation and coding schemes, a simple channel model was introduced. With the background information about the proper modulation and coding techniques, various system restrictions and the channel model, the whole system was simulated under changing channel conditions. As a basis for simulations, real world weather and visibility data from a canadian region were used. Different metrics such as data rates, availability measurements and outage behavior were utilized to evaluate and compare the different presented FSO communication systems.

Kurzfassung

Der steigende Bedarf an Netzwerkkapazitäten ist ein immer größer werdendes Problem. Eine vielversprechende Möglichkeit, diesen steigenden Bedarf zu decken, ist der Einsatz von optischen Freiraum-Übertragungssystemen (FSO). Diese kabellosen Kommunikationssysteme benützen Licht, um Daten zwischen einzelnen Terminals auszutauschen. Die Informationsübertragung erfolgt hierbei durch Modulation des Lichtes einer Leuchtdiode oder eines Lasers. Die dadurch generierten Lichtintensitätsimpulse werden in der Folge durch die Atmosphäre zum Empfänger übertragen. Empfängerseitig wandelt eine Photodiode die empfangenen Lichtimpulse wieder in ein elektrisches Signal zurück, um die gesendeten Daten zurückzugewinnen. Solche optischen Punkt-zu-Punkt-Freiraumübertragungssysteme besitzen den Vorteil, im Vergleich zu anderen drahtlosen Kommunikationssystemen hohe Datenraten zu gewährleisten. Außerdem sind sie sehr abhörsicher und kostengünstig in der Installation. Ein Nachteil dieser Technologie ist aber die Anfälligkeit bezüglich verschiedener Wettereinflüsse, die die Qualität des gesendeten optischen Signals verschlechtern. Ein Beispiel dafür ist dichter Nebel, der zu Datenübertragungsausfällen von einer Dauer zwischen Minuten bis zu Stunden führen kann. Um diese Kommunikationssysteme möglichst tolerant gegen solche Wettereinflüsse zu gestalten, werden robuste Modulationstechniken wie „On-Off Keying"(OOK) gewählt. Diese Modulationsschemata sind zwar weniger wetterempfindlich, haben jedoch verringerte Datenraten zur Folge.

In dieser Arbeit wird der Einfluss von verschiedenen Modulationsarten und zusätzlichen Kodierungsschemata untersucht, um den Datendurchsatz zu erhöhen. Der erste Teil befasst sich mit latenztoleranten Datenverkehrs-Applikationen für FSO Systeme. Für solche Datenverkehrs-Klassen ist nicht wie üblich die Verfügbarkeit, sondern der durchschnittliche Datendurchsatz wichtig. Im Falle einer ein Kilometer langen FSO Kommunikationsstrecke konnte der durchschnittliche Datendurchsatz mit einer sogenannter Low-Density-Parity-Check kodierten 8-Puls-Amplituden-Modulation (PAM) um 100% gegenüber einem herkömmlichen System mit sogenannter unkodierter On-Off-Keying-Modulation (OOK) verbessert werden.

Um die Kanalkapazität noch besser auszunutzen und dadurch Datenraten und Verfügbarkeit weiters zu erhöhen, wurde FSO durch Anwendung adaptiver Kommunikation erweitert. Für diese Technik werden Rückmeldungen über die Qualität der jeweiligen Kanalübertragung verwendet, um z.B. den Modulationstyp sende -und empfangsseitig gegenüber den momentanen Wetterverhältnissen richtig zu wählen. Eine Variante der adaptiven Kommunikation, die sogenannte „Adaptive Modulation und Kodierung", erreicht eine jährliche Durchschnitts-Datenrate von 2.6 Gbit/Sekunde. Das ergibt eine 220%ige Verbesserung relativ zu einfachen Systemen.

Zur Durchführung wurde zuerst ein einfaches Kanalmodell erstellt. Unter Verwendung von Hintergrundinformationen über verschiedene Modulationen, Kanalkodierungen und Systembeschränkungen wurde schließlich ein komplettes FSO System einschließlich sich verändernder Kanaleinflüsse simuliert. Als Datenbasis für die Berechnungen wurden tatsächliche Wetter -und Sichtdaten aus einer kanadischen Region verwendet. Verschiedene Parameter wie stündliche Datenraten, Verfügbarkeitsmessungen und Ausfallverhalten wurden herangezogen, um die Leistung der unterschiedlichen FSO Systeme zu evaluieren.

Danksagung

Die vorliegende Masterarbeit wurde zum großen Teil während eines von der Technischen Universität Graz geförderten Auslandsaufenthaltes in Kanada an der McMaster Universität erstellt. Bei der Bearbeitung wurde ich durch die Mitwirkung folgender Personen maßgeblich unterstützt, denen ich besonders danken möchte:

Für die zahlreichen fachlichen und organisatorischen Hilfestellungen danke ich Ao. Univ.-Prof. Dr. Erich Leitgeb. Für die kompetente fachliche Betreuung, die fruchtbaren Diskussionen und die vielen anregenden Ideen danke ich Prof. Dr. Steve Hranilovic von der McMaster Universität. Herzlich danken möchte ich weiters Dr. Sajid Sheikh Muhammad für gesonderte Beratungen und Herrn Awad Dabbo für diverse Hilfestellungen.

Für ihre Bemühungen bei den Korrekturarbeiten und ihre Anteilnahme möchte ich auch meiner Freundin Katharina Preßler von Herzen danken. Ein ganz besonderer Dank geht an meine lieben Eltern, ohne deren so selbstverständlich wirkenden Hilfsbereitschaft, sowohl in menschlicher als auch in finanzieller Hinsicht, der Abschluss meines Studiums bedeutend schwerer gewesen wäre.

Graz, im Dezember 2010   Martin Czaputa

EIDESSTATTLICHE ERKLÄRUNG

Ich erkläre an Eides statt, dass ich die vorliegende Arbeit selbstständig verfasst, andere als die angegebenen Quellen/Hilfsmittel nicht benutzt, und die den benutzten Quellen wörtlich und inhaltlich entnommene Stellen als solche kenntlich gemacht habe.

Graz, am ……………………………   ……………………………………………………..
                                                                                    (Unterschrift)

Englische Fassung:

STATUTORY DECLARATION

I declare that I have authored this thesis independently, that I have not used other than the declared sources / resources, and that I have explicitly marked all material which has been quoted either literally or by content from the used sources.

……………………………   ……………………………………………………..
        date   (signature)

Contents

Contents

List of Abbreviations

AM   Adaptive Modulation

ACM   Adaptive Coded Modulation

ARQ   Automatic Repeat Request

BER   Bit Error Rate

CG   Coding Gain

FEC   Forward Error Correction

FSO   Free-Space Optics

Gbps   Giga Bit Per Second

Gsps   Giga symbol per second

ISP   Internet Service Provider

LDPC   Low Density Parity Check

LED   Light Emitting Diode

LLR   Log-Likelihood Ratio

OOK   On Off Keying

P2P   Peer-to-Peer

PAM   Pulse Amplitude Modulation

PPM   Pulse Position Modulation

pdf   probability density function

RF   Radio Frequency

RS   Reed Solomon

SER   Symbol Error Rate

List of Figures

List of Tables

1 Introduction

Network size and higher data rates have been fast growing factors in telecommunication systems in the last decade. As a promising technology, wireless optical communication systems were found to be a suitable candidate to satisfy these demands in various areas. Wireless optical communication is a point-to-point communication link where the optical intensity is used to transmit data through air while a laser or light emitting diode (LED) is acting as the transmitter and a photodiode as the receiver. These systems are considered in many scenarios like indoor wireless communications [3], terrestrial links, ground-to-air, air-to-air (unmanned aerial vehicles (UAV)) [4], ground-to-satellite [5,6] and inter-satellite communications [7].

A popular and commercial application of optical wireless links is free-space optical communication (FSO) where a point-to-point link establishes communication between two stations near ground. Commercial systems are available [8,9] and are able to offer data rates from 10 Megabit/second (Mbps) to 10 Gigabit/second (Gbps) depending on link distances. Recently developed experimental links can support data rates from of 10 to 40 Gbps. Even a 1.28 Terabit/second [10] (Tbps) system was presented in December 2009.

FSO systems have a broad field of application. Due to the high data rate support, FSO has high potential to solve the so-called "last mile" problem. The issue is that major cities have already established fibre networks for broadband internet access. Unfortunately, these networks are limited in density. As a result, residential houses, buildings, companies and office buildings are not connected to a fiber network but are often only "one mile" away from fiber network terminals. Consequently, the goal is to close this gap and to integrate these users into the high speed network. Here, different solutions are considered with their advantages and disadvantages.

Newly developed DSL (digital subscriber line) standards like VDSL2 (4 - 30 Mbps) [11,12] or cable lines (8 - 100 Mbps) [13] have improved in the last years, but can not provide true broadband services in a deterministic way. Data rates of DSL suffer from the attenuation due to the copper cables as well as from the influence of their neighbor lines. On the other hand, cable modems share their capacity between television, internet and telephony service, and therefore no available bandwidth is guaranteed.

Interference aspects and limited capacity make unlicensed radio frequency (RF) links unusable. For example, a standard RF link named PTP 300 Series from Motorola, operating in a 5.4 frequency band, can achieve data rates only up to 25 Mbps [14]. Licensed RF technology points, with higher capacity but initial costs and limited number of carriers per area, make it relatively difficult to implement.

Furthermore, millimeter wave point-to-point radio technology in the range of 50-86 GHz has gained big attention in recent years. Already available systems, for instance the Aire-Beam$^{\text{TM}}$G60 manufactured by LightPointe$^{\text{TM}}$ [15], can offer data rates of 1.25 Gbps over a distance of 800 meters (m). They operate in the license-free 57-64 GHz spectrum. However, radio waves in this spectrum are significantly affected by signal attenuations during rain events. For example, by medium to heavy rain fall, a loss of 20-50 dB/km can occur [16]. This impairment as well as the high costs are not negligible challenges for this technology.

The most reliable and rate perspective solution would be the extension of the existing fibre structure. Usually, fibre cables are installed in existing shafts or pipes e.g. sewer, while in case of fibre-to-the-home (FTTH) telephone connection tubes are used. Often the mentioned possibilities don't exist or are too difficult to access in urban areas. As a consequence, installing fibre cables is very expensive mainly because of necessary digging work. For example, as it was reported in a case study [17], deployment costs for a small area increased up to $\approx$ \$400.000 and higher instead of \$14.200 just for a short range link with 1.25 Gbps [18].

Compared to RF communication systems with a bandwidth of maximum 70 Mbps, FSO links could accomplish much higher data rates, i.e. 160 Gbps [19], with the advantage that no spectrum license is needed for the optical infrared band. In contradiction to RF links operating between 50 and 86 GHz, FSO systems are less influenced during rain events [16]

and are cheaper by a factor of two. In addition, FSO links hold the benefit not to interfere with other devices due to the small beam width and exhibit high data security.

Another application of short link FSO systems consists in using them to extend local area networks (LAN), e.g. for inter-company or inter-office connectability. Moreover, this technology could be used to establish LAN-to-LAN networks, inter-campus connections, metro extensions or network backhaul connections. In rural areas, where the installation of fibre cables is impossible or impractical, FSO links are a preferable solution.
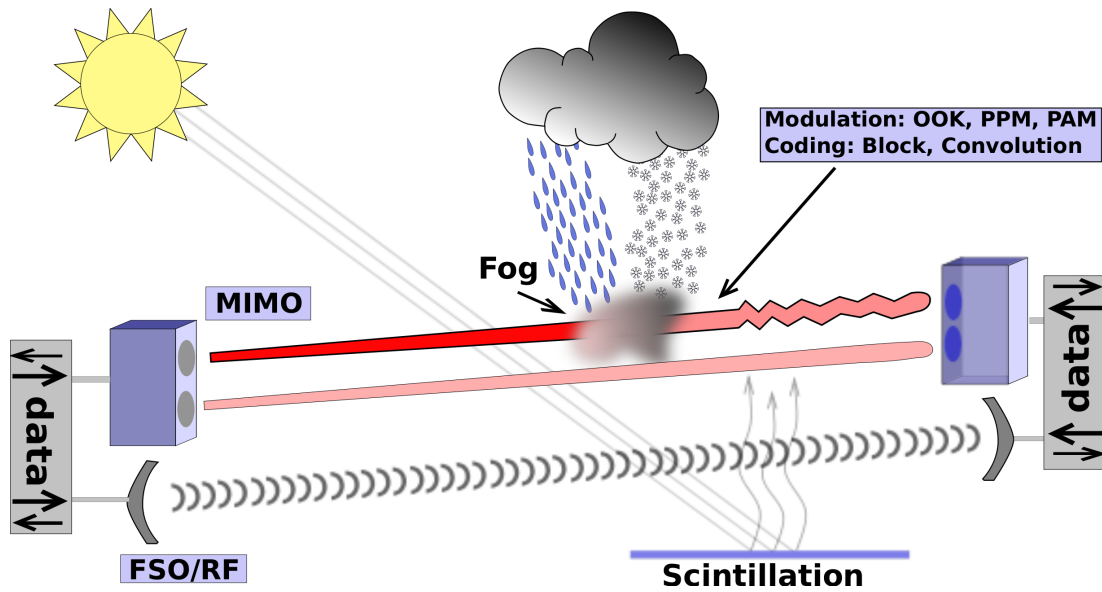
Figure 1.1: Techniques to mitigate various weather techniques of FSO links

The features of FSO have been very attractive in the field of military communication since the late 60's. FSO is considered to establish secure communication links between different stations in the battlefield. Recent activities are dealing with UAV's where FSO is used as a wireless link to control vehicles from ground or as a communication technique between UAV's in a swarm. Another important application is disaster management. If terrestrial network structures are not available or got destroyed, a mobile broadband network could get established between operating emergency stations. As a solution, a combination of satellite/FSO/WLAN systems is considered to establish the necessary network structure [4].

Each technology has its advantages and disadvantages with regard to different applications.

The disadvantages of fibre and RF networks were illustrated above. However, it is also important to expose the challenges for FSO systems. Link distance, data rate and reliability of such links are limited due to atmospheric impairments. Weather situations like fog or snow, dependent on their intensity, can decrease the communication link performance. For example, in a typical dense continental fog event, the signal attenuation due to scattering is in the order of hundreds of dB/km on average [20]. Additionally, scintillation induced fading of the received optical signal is caused by atmospheric turbulence and can often limit the range and reliability of links [21]. Due to eye safety reasons, the allowed optical transmitted power is limited and this makes it even more difficult to achieve good link performance. As a consequence of the sensitivity of FSO links to atmospheric effects, communication system design is centred on improving the reliability of the link. Simple binary modulation schemes like on-off-keying (OOK) and M-ary pulse position modulation (M-PPM) [22] are often used in commercial systems due to their power efficiency. Higher orders of M-ary PPM, often coupled with error control coding [23], can significantly increase the robustness against atmospheric attenuation at the cost of bandwidth efficiency. In contrast, multilevel modulation schemes, such as pulse amplitude modulation (PAM), although more bandwidth efficient, are not widely used due to lower power efficiency and increased sensitivity to channel loss [24]. Other techniques to improve the reliability of FSO links include channel coding [25–28], spatial diversity [29,30] and hybrid RF/FSO links [31,32]. However, such techniques increase system complexity and cost due to additional signal processing and optics.

1.1 Motivation

The usual goal to design highly reliable FSO systems has the disadvantage of an insufficient use of the available bandwidth, and hence reduces the desired data rates substantially. One key factor in communication systems to improve reliability and rate as well lies in proper modulation and error control coding. In this thesis, two different ways of average throughput maximization techniques for FSO systems are presented using the right choice under several modulation and coding strategies. In both cases the available channel capacity is better exploited than in standard systems which leads to an increase in average throughput.

First, the idea of utilizing FSO links for latency tolerant traffic has to be considered.

4

Latency tolerant traffic can easily be shifted onto free space optical links particularly in the last mile within the high capacity network. Here, average data rates are the centre of interest while data link outages can be tolerated. The goal is to select a modulation and coding scheme to maximize the average data rates for this traffic class.

Second, the idea of throughput maximization on the free space optical links can be extended by introducing adaptive modulation and adaptive coding techniques. Here, additional channel measurements are used to adapt the system to the current channel conditions. In nice weather conditions, higher data rates can be achieved while in the case of atmospheric turbulence scenarios data rates are lowered by adaptive control of modulation and coding.

1.2 Thesis Structure

This thesis presents novel contributions to FSO modulation design, its combination with coding algorithms and illustrates FSO as a new application. The corresponding structure is presented as follows. In Chapter 2, the general design of the communication model for a free space optical link is discussed, followed by a simple and established channel model. The physical background of each of the channel model parameters is provided and the practical model of those are shown. Big attenuators such as fog, snow and rain are modeled with empirical formulas. For turbulence impairments, the lognormal model is considered as a statistical fading model. Background about the used modulation and coding techniques follows in Chapter 3. Signal formulation, bit error and symbol error curves are provided for M-ary PAM and M-ary PPM. This chapter closes with a short discussion on channel capacity and information rates. Chapter 4 first introduces the idea of using FSO links for latency tolerant traffic applications followed by the complete presentation of the simulation model. Different modulations and combined coding were investigated to maximize the average throughput of such systems. To quantify the FSO design for this special kind of traffic, different metrics are considered for comparison. Spectrally efficient communication design is discussed in Chapter 5. It starts with adaptive modulation, where only the constellation size and type is changed according to feedback information. Additionally, the influence of adaptive coded modulation is studied. Finally, the most important facts and outcomes are concluded in Chapter 6.

2 Channel Structure and Transmission Losses

In the past, several approaches were made to characterize the transmission of optical intensity signals through air. It was observed that different weather situations, e.g. fog, snow, or rain which are highly correlated with the actual visibility, have a deep impact on the availability and the range of the link. Additionally, atmospheric turbulence effects are decreasing the link performance further. It has to be kept in mind that the occurrence of these impairments is mainly dependent on the actual climate and physical characteristics of the FSO installation location. In case of fog, attenuation measurements with FSO systems in Graz, Austria and in LaTurbie, France are showing significant differences in the attenuation peaks and behaviour [33]. The main target of this work was to maximize the average throughput of FSO systems by investigating different modulation and coding schemes and their combinations, taking into account a wide variety of weather characteristics. Thus, the first task was to develop a convenient and practical channel model which should reflect the attenuation and scattering effects of free-space on the communication channel.

This chapter is organized as follows: First, the technology to transmit the FSO data is discussed. Second, a general and established channel model is presented and its parameters are described. Afterwards, models are given for the most significant impairments and are discussed in Sec. 2.3, Sec. 2.4 and Sec. 2.5.

2.1 Basic Transmission Technology

Generally, a free-space optical wireless link consists of multiple transmitters and multiple receivers. The input data stream is processed in the electrical domain and is then converted to an optical signal which propagates through air. To generate this optical signal, multiple laser diodes (LD) or light emitting diodes (LED) are used. Both elements have their "field

of application" [34]. Additional lenses and mirrors help to form the outgoing beam. At the receiver, lenses and mirrors focus the incoming optical signal on the detectors areas. Multiple photo receivers have the task to detect the transmitted light signal and convert it back into an electrical signal. Commonly two different kinds of receivers are considered, namely p-i-n photo diodes (PIN) and avalanche photo diodes (APD). The advantages of APDs have higher sensitivity and higher level gain compared to PIN diodes usually used. But, they are not as widely used as their PIN counterparts because of several disadvantages, e.g. the output is non-linear, a much higher operating voltage may be required and ADPs produce more noise than PIN diodes. Optical transmitters utilized in FSO systems often are operating in the
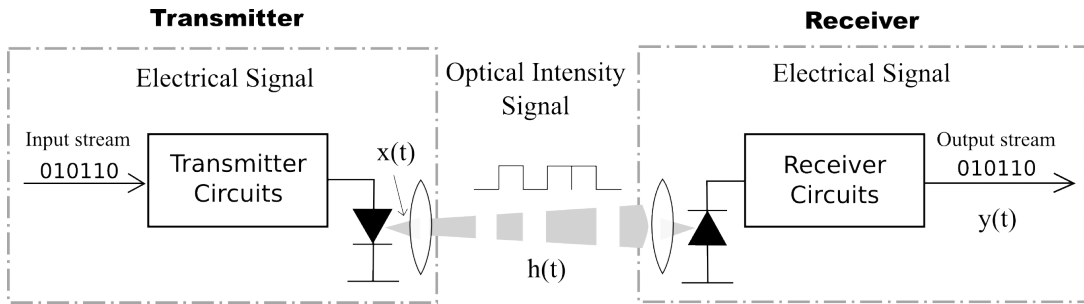
Figure 2.1: Block diagram of an optical wireless system

850 nm or 1550 nm wavelength area. The common use of these bands has different reasons e.g. low wavelength attenuation dependency, eye safety reasons, low price, etc.. When light propagates through the atmosphere, the molecules and particles contained in the air are causing signal impairments, e.g. frequency selective fading, absorption and scattering. The attenuation at the wavelengths mentioned above can be neglected.

Eye safety must be taken into account when dealing with lasers. Lasers can cause tremendous damage on the retina depending on the emitted power and wavelength. A commonly used standard concerning eye safety was created by the International Electrotechnical Commission (IEC) [35] which specifies different laser classes and their limitations. The standard allows an average optical power transmission of 1 mW/cm^2 for 850 nm while for 1550 nm 100 mW/cm^2 are specified. The reason for this difference is that visible light and light close to that region is propagating through pupil and lens and is focused on the retina while other wavelengths are absorbed by other parts of the eye before hitting the retina. The sensitiv-

ity as well as the price at 1550 nm behave worse compared to 850 nm, but higher allowed emitting power compensates this disadvantage.

2.2 FSO Channel Model

The block diagram of a wireless optical communication system is shown in Fig. 2.1. The electrical input stream modulates the light source intensity to generate the optical signal. This process is known as *intensity modulation*. On the receiver side, the incident photons are collected and converted to a current $y(t)$ proportional to the light intensity by means of a photodiode, i.e., *direct detection*. In literature, this conventional method of transmission is called a *intensity modulation direct detection* (IM/DD) system. Hence, the signal output of the receiver is proportional to the received optical power. The optical power is reduced when it passes through telescopes and lenses both on the transmitter and the receiver. This influence is specified as the optics efficiency γ which multiplies the signal $x(t)$. Without loss of generality, the optics efficiency is set to unity in all further considerations, since this only scales the signal-to-noise ratio and is small compared to other losses. A general and justified channel model is given in [3,36] and forms to

$$y(t) = x(t)h(t)R_d\,\gamma + n(t), \tag{2.1}$$

where $y(t)$ is the generated photocurrent, $x(t)$ is the transmitted optical intensity signal , $h(t)$ models the random fluctuations through the medium, R_d is the responsivity of the detector and $n(t)$ describes the noise. In FSO, ambient light interference and the circuit noise are the main reasons for noise [3] in the system. While on lower data rates (10 Mbps) the produced shot noise through ambient light is dominant, it can be neglected at higher rates (1 Gbps) against circuit noise. Under the assumption that the received signal has a high intensity, this noise can be modeled as a signal-independent additive white Gaussian noise with variance σ_n^2 and zero mean.

The channel state $h(t)$ is time-variant, and is here considered as a frequency-nonselective (flat-fading), slowly fading process [37]. A channel is stated flat when all used signal frequencies are equally magnified. In other words, the coherence bandwidth ΔH [37] of the channel is greater than the signal bandwidth W. This and the time-variance results in a

multiplicative distortion of the transmitted signal $x(t)$ [37]. As mentioned above, a FSO channel has also the attribute of slow-fading. Actually, this is true if the coherence time of the channel state h(t) is longer than the symbol duration of a transmitted intensity signal. The coherence time is defined as the time interval within which the state factor of the channel stays nearly constant. The free space optical channel is slow fading since the symbol duration T_s is usually around 10^{-9} s and the coherence time of the fading process is in the range of 1 ms - 100 ms. As a consequence, the channel state h stays approximately constant over many symbol periods.

In order to perform numerical simulations, it is helpful to have an equivalent discrete-time representation of the channel model. A discrete time representation [38] equivalent to equation (2.1) is given as

$$y = xhR_d + n. \tag{2.2}$$

As mentioned above, the channel state h represents the optical intensity fluctuations and is separated into three factors: the atmospheric influence h_l, the geometric factor h_g and the atmospheric turbulence fading h_s (scintillation). The channel state h follows as

$$h = h_l h_g h_s. \tag{2.3}$$

Two signal constraints have to be taken in account when dealing with this channel. First, the optical intensity signal $x(t)$ must always stay positive. This is because the transmit power can physically never be negative [24].

$$x(t) \geq 0 \tag{2.4}$$

Second, due to the described eye-safety reasons in Sec. 2.1, the sent average optical power P is limited and follows as

$$\lim_{T \to \infty} \frac{1}{T} \int_0^T x(t)dt \leq P \tag{2.5}$$

where T is the symbol period time. In statistics equation (2.5) can be rewritten as the expected value of $x(t)$

$$\mathbb{E}\{x(t)\} \leq P. \tag{2.6}$$

Consequently, the average of the optical intensity signal is constrained. Note that the constraint in equation (2.4) is treated differently from that in the radio frequency (RF) area. In RF, negative amplitudes can exist.

2.3 Atmospheric Attenuations

Mainly, optical wave propagation through the atmosphere is impaired by scattering and absorption processes. Light is interacting with different types of gaseous molecules and small particles, called aerosols. The density, varying spatially and temporally, and the type of these particles determine the degree of absorption and scattering. Fog is one example for attenuation due to scattering processes. Dense fog can cause attenuations in the order of hundreds of dB/km and leads often to total link outages. Latter mentioned impairments are not the only influencing factors degrading the link performance. Air domains with different temperature and pressure are refracting the passing light beam through the atmosphere. These atmospheric turbulence effects, also called scintillation, result in fading at the receiver which can cause attenuations up to 30 dB/km. Another limiting factor is the geometric loss. With an increasing link distance the optical beam is broadening and the optical power per unit area reduces. As a consequence of the fixed receiver aperture size, only a part of the transmitted optical intensity signal can be received.

Several attenuation factors, for example fog or rain, are often highly correlated with the visibility V. Thus, comprehensive visibility measurements, available from airport databases, can be used together with empirical developed models to simulate the influence of different attenuating factors. Visibility itself can be defined as follows [39]: "The human eye is sensitive to the difference relative to the overall intensity level detecting the contrast: reducing the contrast between object and background the object tends to be less distinct and when it becomes small, the object will no longer be visible". The distance from the human eye to the distinct object is called visibility.

The reduction of the FSO optical power signal through the atmosphere is characterized by the Beer-Lambert law as follows [40],

$$h_l = \frac{P(z)}{P(0)} = e^{-z\sigma} \tag{2.7}$$

, where h_l is the transmittance, $P(z)$ is the transmitted power at the link distance z, and σ represents the attenuation coefficient in km^{-1}. In literature, the exponent σz is also known as the *optical thickness* τ. The attenuation coefficient σ includes all influences of absorption

and scattering from molecules and aerosols [1, 41]. It is given by,

$$\sigma(\lambda) = \alpha_m(\lambda) + \alpha_a(\lambda) + \beta_m(\lambda) + \beta_a(\lambda), \qquad (2.8)$$

where α_m, α_a represent the absorption coefficient of molecules and aerosols, β_m, β_a are the scattering coefficients, respectively, and λ is the laser transmission wavelength in use.

Absorption can occur when propagating photons interact with molecules along the path. Their energy is preferentially converted into heat. Different types of molecules, especially O_3, H_2O and CO_2, absorb at their characterisitcal optical wavelengths [42], hence the absorption coefficient is frequency-selective. This means that there exist some optical frequency bands where nearly no absorption occurs, while other wavelengths get highly attenuated. By using these preferable bands, for example 1550 nm, the absorption can be neglected against scattering.

Scattering is the redistribution of incident photons on atmospheric particles in directions with angles different from the line-of-sight axis. The kind of scattering is determined by the size of the particle according to the used transmission wavelength. The established size parameter α (not to be confused with α in (2.8)) , given in [1], is often used to describe this effect in literature, follows as

$$\alpha = \frac{2\pi r}{\lambda}, \qquad (2.9)$$

where r is the particle radius. With this parameter, scattering can be classified into three different scattering processes (see also Fig. 2.2 for 785 nm and 1550 nm). If $\lambda << r$, it is termed Rayleigh scattering, if $\lambda \approx r$, Mie scattering theory applies, and if $\lambda >> r$ it is specified as geometric or non-selective scattering. Latter can be imagined as follows: a laser beam hits a water droplet resulting in diffraction and reflection of the optical signal.

With this background in mind, the most important attenuation factors are described in the following paragraphs. For easier comparison, the different attenuation factors are compared in terms of total attenuation (in dB) and specific attenuation (in dB/km). The total attenuation a_{tot} in decibel forms to

$$a_{tot} = \mathrm{dB}(1/h) = 10\log_{10}(1/h) = \frac{10}{\ln(10)}\sigma z \qquad (2.10)$$

and the specific attenuation a_{spec} in dB/km is defined as follows
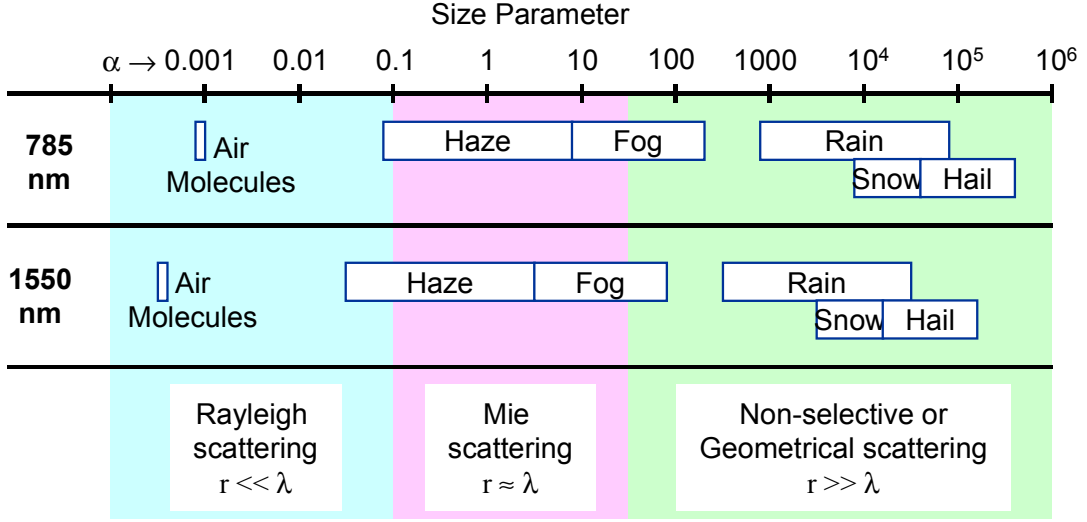
Size Parameter

Figure 2.2: Size parameters of scattering particles for 785 nm and 1550 nm [1]

$$a_{spec} = \frac{\mathrm{dB}(1/h)}{z} = \frac{10 \log_{10}(1/h)}{z} = \frac{10\,\sigma z}{\ln(10)z} = \frac{10}{\ln(10)}\sigma. \tag{2.11}$$

Fog

Measurements [33] have shown that fog is one of the most attenuating factors for FSO systems. The system availability suffers severe under long event durations (several minutes to hours) and spatial spread of fog. In other words, such weather impairments don not have high temporal attenuation fluctuations compared to the transmitted symbol duration but are causing either total link outages or not. Depending on the type of fog [43], its events can lead to attenuations in range of several to hundreds of dB/km [33] causing non-negligible link outages. Many years of research in the area of fog accomplished different mathematical models. With radii of fog droplets in the range of 1-20 μm, the Mie theory is used to described the behavior of fog events. Unfortunately, calculation of the attenuation using this theory proves to be difficult [41] in respect of various fog particle sizes and shapes. As there is a strong correlation between fog and visibility, and considering the fact that visibility data is available since the late 60's (measured on airports), empirical models have been proposed to predict the attenuation due to fog for different wavelengths [43]. Several empirical models were created. However, the most established empirical formula is given by Kim [1]. This

model is used in the case of no precipitation (sunny, cloudy or foggy weather) and it follows as

$$\sigma_{\text{no-precip}} = \frac{3.91}{V} \left(\frac{\lambda}{550}\right)^{-q}, \tag{2.12}$$

where V is the visibility in km, λ is the wavelength in nm and q is a parameter depending on the visibility which can be computed as follows

$$q = \begin{cases} 1.6 & V > 50\text{km} \\ 1.3 & 6\text{km} < V < 50\text{km} \\ 0.16V + 0.34 & 1\text{km} < V < 6\text{km} \\ 0.5V & 0.5\text{km} < V < 1\text{km} \\ 0 & V < 0.5\text{km} \end{cases} . \tag{2.13}$$

Notice that for low visibility ($V < 0.5$km) the attenuation is equal for all optical wavelengths. For visibility values higher than 0.5 km, q gets frequency selective. In Fig. 2.3, the specific attenuation a_{spec} (2.11) is calculated for $\sigma_{no-precip}$ against the visibility in kilometers. In
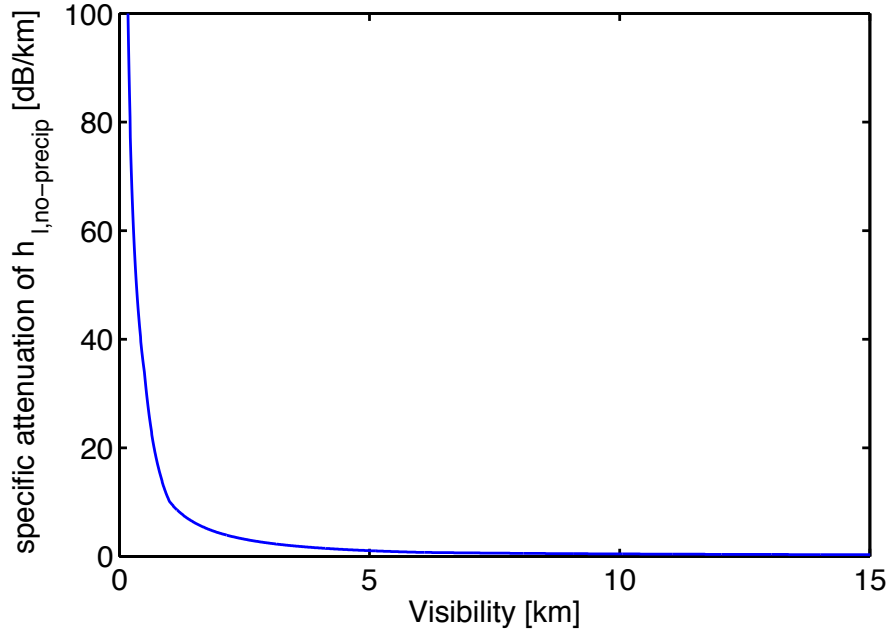
Figure 2.3: Specific attenuation a_{spec} in the case of fog (KIM model)

usual fog events, the visibility decreases enormously from only several to some hundred meters. The high attenuation during heavy fog events is also reflected by the KIM model.

13

Rain

Rain is another attenuator which effects the link quality. Since the raindrop size (diameter may vary from 0.1 to 5 mm) is much bigger than the used optical wavelengths, rain scattering is classified as *non-selective*. Here the optical waves are refracted and reflected if they hit a rain drop. Size, number, shape and distribution of these determine the overall scattering of the optical beam. Unlike fog, heavy rainfall can only cause 20-30 dB/km [16] maximum signal attenuation. Statistical and empirical models exist to predict the attenuation during rainfall. As the system model is based on measured visibility data, the focus lies on "easy-to-use" models which are connected to the visibility and therefore are easy processable. For rainy weather, an empirical value for σ is [44],

$$\sigma_{\mathrm{rain}} = 2.9/V. \qquad (2.14)$$

Again, the specific attenuation is plotted for σ_{rain} in Fig. 2.4. The curve looks similar to a_{spec} of fog. The main difference is that usual visibilities are in the 1 km range in heavy rainfall events. Thus, rain with an average rainfall rate causes only several dB/km.
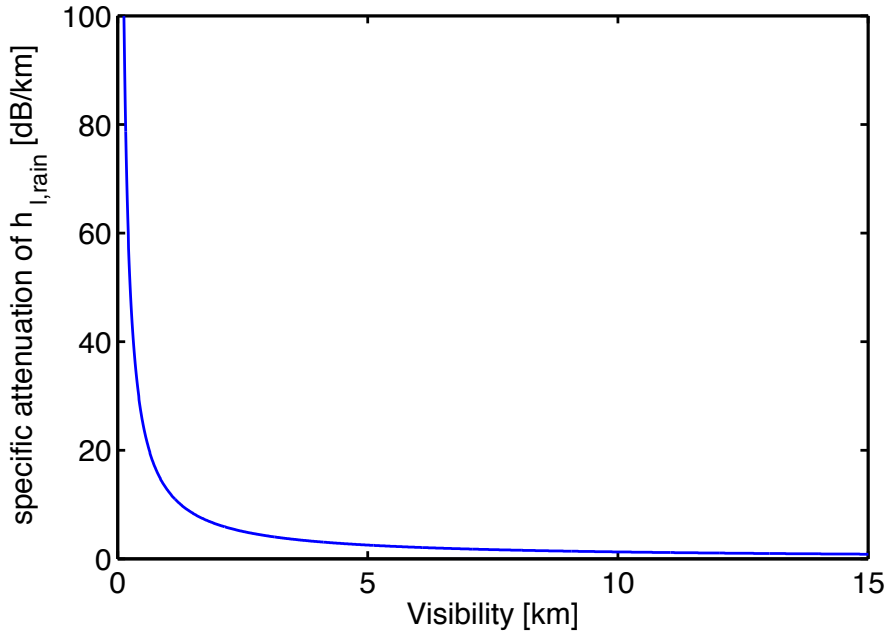
Figure 2.4: Specific attenuation a_{spec} in the case of rain

Snow

Snowfall is more complicated to describe than rainfall with respect to statistics because of the existence of different sorts of snowflakes and because of their different shapes and sizes. Especially the consistence of snow (wet/dry) has an impact on scattering and attenuation. Wet snow has more influence on optical signals than dry snow due to its increased moisture. As a consequence, separate models for wet and dry snow exist. For snowy weather, σ is approximated [45] and chosen to

$$\sigma_{\text{snow}} = 15 \, \sigma_{\text{rain}}. \tag{2.15}$$

This is reasonable since snow flakes can be modelled as large rain particles. Given equation (2.14), notice that σ_{snow} is a scaled version of σ_{rain}. The scaling factor depends on the flake size as well as on the consistency of the snow (wet/dry) [46]. In Fig. 2.5, the attenuation is given for σ_{snow}.
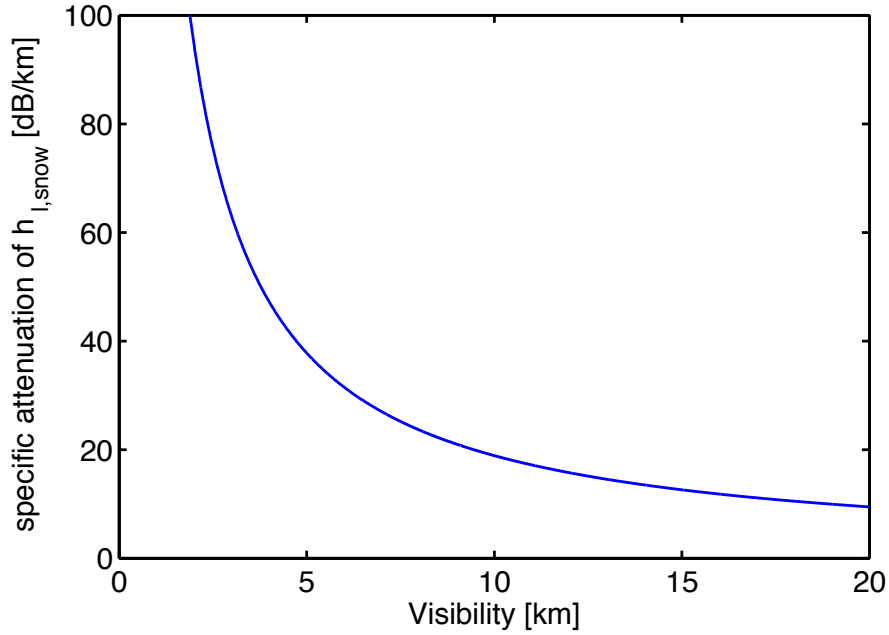
Figure 2.5: Specific attenuation a_{spec} in the case of snow

As compared to Fig. 2.3, Fig. 2.4 snow has a much higher attenuation than fog and rain for the same visibility. For example, for a visibility $V = 5$ km, the loss is 1.04 dB/km in no precipitation, 2.52 dB/km in rain events and 37.8 dB/km during snowfall. According to

Table 2.1: Relation between C_n^2 and Visibility V [2]

Weather Condition	$C_n^2 \times 10^{-14}$ $(m^{-\frac{2}{3}})$	V(km)
Clear	2	> 10
Light Haze	1.8	4-10
Haze	1.5	2-4
Thin fog	1	1-2
Light fog	0.5	< 1

measured visibility data, moderate snow events exhibit visibilities in order of 5-10 km while heavy snowfall causes $V < 5$ km. This snow model is overestimating the actual loss, which ensures the worst case snow scenarios in following simulations.

2.4 Scintillation

In FSO systems, scintillation arises due to varying temperatures and pressures along the propagation path. These variations create air pockets with different refractive indices [47]. As a result, the amplitude and phase of the optical intensity signal fluctuates causing fading with a temporal variation in order of 1 ms -100 ms at the receiver [2,47]. For weak turbulences and distances less than 1 km, fluctuations in the intensity of the received signal can be modelled by the log-normal distribution [47],

$$f_{hs}(h_s) = \frac{1}{2h_s\sqrt{2\pi\sigma_x^2}} \exp{-\frac{(\ln(h_s) + 2\sigma_x^2)^2}{8\sigma_x^2}} \tag{2.16}$$

where, σ_x^2 is given by [48],

$$\sigma_x^2 = 0.30545 \left(\frac{2\pi}{\lambda}\right)^{7/6} C_n^2 z^{11/6}, \tag{2.17}$$

and C_n^2 is the refractive index structure parameter [47], which represents the severity of the atmospheric turbulence. Although there is no explicit relationship between C_n^2 and V, Table 2.1 presents some typical values found in the literature and adapted from [38].

2.5 Geometric Loss

In FSO systems, geometric loss is due to the divergence of the transmitted beam. This loss increases with distance and the geometric factor can be expressed as,

$$h_g = \left(\frac{d}{\phi z}\right)^2 \tag{2.18}$$

where d is the diameter of the receive aperture, ϕ is the beam divergence and z is the link distance. This beam divergence is usually adjusted by the transmitter optics and measured in millirads (mrad). Choosing the right effective beam divergence angle depends on two considerations. FSO systems should receive most of their transmitted power. One factor in achieving this is to choose a small beam divergence, so most of the power can be received by the fixed size receiver aperture. On the other hand, atmospheric turbulence effects and pointing-loss [49] can deflect the optical beam, which than can not reach the receiver anymore. Therefore, a tradeoff has to be made between receiving power maximizing the signal to noise ratio (small beam width) and the ruggedness against pointing losses (large beam width).

3 Modulation, Coding and Information rates

In general, modulation and coding are key factors for improving performance in every communication system. Especially in free-space optical systems, where strong weather impacts are causing significant link degradation, the combination of modulation and coding has shown [23] meaningful improvements against moderate attenuation effects. In the past, investigations were made to adapt modulations used in RF applications directly to unexplored wireless optical communication areas. This turned out to be difficult since FSO has different system limitations. As mentioned in Sec. 2.1, usually the amplitude of the intensity signal is directly detected by photodiodes. The positive amplitude and optical power constrain limit the choice of modulation schemes for optical communication. This is the reason why primarily digital transmission schemes are used. The most popular transmission schemes are binary modulations because they are easy to implement and are tolerant against several influencing weather effects. Two of these popular schemes are binary on-off-keying (OOK) and pulse-position-modulation (PPM). Additionally, channel coding was considered in order to increase the availability during channel fading events. Codes such as Reed Solomon [50], Turbo [27], LDPC [51] and other families of codes were studied with OOK and PPM during heavy fog, snow and rain events [43, 52]. One possibility to quantify the performance of modulation and coding schemes is to evaluate information rates [37]. Explained in a simple manner, these rates determine the maximal achievable data rates for a given type of modulation and for a specified channel according to a given SNR.

In the following sections, a brief overview about the implemented modulation schemes and coding structures is given and a comparison between them is carried out in terms of symbol-error-rates (SER), bit-error-rates (BER) and information rates.

3.1 Modulation

For FSO systems, modulation is normally done by the transformation of electronically stored data bits into an optical intensity signal with a specific chronical structure. The most commonly used technique is accomplished by binary modulation schemes. These modulation techniques only consist of two different intensity levels to represent the binary information to be transmitted. Due to their simplicity and ease of implementation they became very popular in commercial systems. Two of these favored schemes are OOK and PPM which are discussed in Sec. 3.1.1 and Sec. 3.1.2, respectively. On the other hand, multilevel schemes are not widely utilized in FSO due to their liability to fading events. But in case of no weather turbulence, these schemes have the ability to achieve higher data rates compared to binary schemes because of their bandwidth efficiency and are discussed in Sec. 3.1.3. Conventional modems have system limits on the maximal impulse frequency they can generate. In order to establish a fair comparison of different modulations, it is assumed that the modulator in consideration owns a fixed bandwidth R_{rect} given in GHz. That is, it can output rectangular pulses of a fixed time duration T_{rect}. The following equations of used modulation schemes are based on [24, Chapter 3.3].

3.1.1 On-off-keying

On-off-keying is one of the simplest binary modulation schemes in FSO. This scheme uses two different intensity levels where each of them is equiprobable chosen during each symbol interval. For OOK, the symbols have either a constant intensity of $2P$ or zero intensity. Hence, an OOK modulated signal $x(t)$ is presented by a basis function

$$\phi_{\mathrm{OOK}} = \frac{1}{\sqrt{T_s}}\mathrm{rect}\left(\frac{t}{T_s}\right) \tag{3.1}$$

and follows as

$$x(t) = \sum_{k=-\infty}^{\infty} 2P\sqrt{T_s}A[k]\phi_{\mathrm{OOK}}(t - kT_s), \tag{3.2}$$

where $A[k] \in \{0, 1\}$ is uniformly distributed, T_s is the symbol duration, P is the average optical power and $\mathrm{rect}(\cdot)$ is the rectangular function defined as

$$\text{rect}(t) \begin{cases} 1 & : 0 < t < 1 \\ 0 & : \text{otherwise} \ . \end{cases} \tag{3.3}$$

As seen in equation (3.2), the average power is P and fulfills therefore the average power constrain in (2.5). As an example, a bit sequence $\mathbf{b} = [1, 0, 1, 1, 0, 0, 1, 0]$ is OOK modulated and illustrated in Fig. 3.1(a). A zero bit equals to zero intensity of OOK and a one bit equals to an intensity level of $2P$.

One important quantity to compare the performance of communication techniques is the bit error rate (BER). It gives information about the probability that a bit error occurs for a given signal to noise ratio. Empirically, a well working communication system would operate at a BER rate around 10^{-9} while a BER $= 10^{-1}$ results in incorrect transmission. An analytical form of BER for OOK over an additive white Gaussian noise (AWGN) channel is

$$P_{b,\text{OOK}} = Q\left(\frac{PRh}{\sqrt{R_s \sigma_n^2}}\right), \tag{3.4}$$

where Q{.} is the probability tail function given as

$$Q(x) = \frac{1}{\sqrt{2\pi}} \int_x^\infty \exp\left(-\frac{u^2}{2}\right) du \ . \tag{3.5}$$

To achieve $P_{b,OOK}$, also numerical Monte Carlo simulations can be performed [37]. To calculate the BER numerically, the number of incorrect received bits N_e is divided by the total number of bits N_s sent [53]

$$P_b = \lim_{N_s \to \infty} N_e / N_s. \tag{3.6}$$

This procedure is valid for all further uncoded and coded modulation schemes presented. In simulations P_b can be estimated using a finite number of N_s. Another indicator of link performance is the symbol error rate (SER) which can be numerically calculated alike computing the BER rate in (3.6), but using the number of sent and erroneous symbols. For OOK, where one symbol correspondents to one bit, BER and SER are equal, $P_s = P_b$. Figure 3.2 shows the theoretical (3.4) and the simulated BER curve, where SNR Γ is defined as

$$\Gamma = \frac{PhR_d}{\sigma}. \tag{3.7}$$
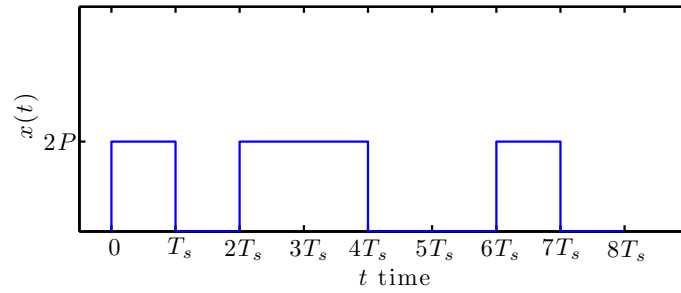
(a) OOK modulated signal
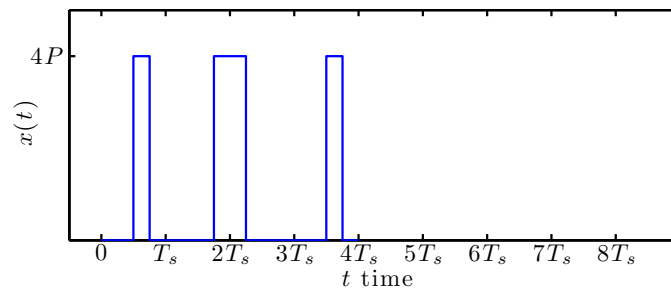
(b) PPM modulated signal with higher bandwidth
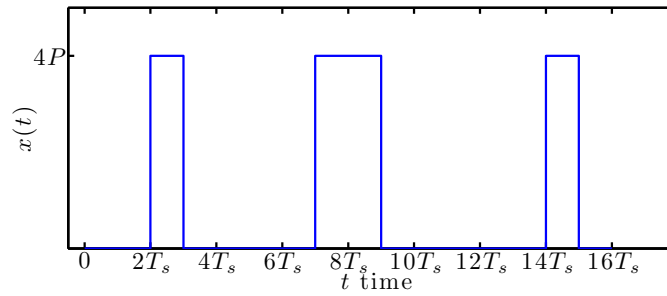
(c) PPM modulated signal using the same bandwidth as OOK
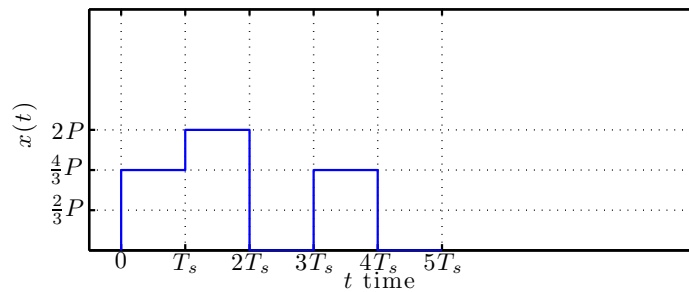
(d) PAM modulated signal.

Figure 3.1: A OOK, PPM and PAM modulated random bit sequence

21

and for a symbol rate of $R_s = R_{rect}$ Giga symbol per second (Gsps), where $R_{rect} = 1$ GHz. The Y-axes is the BER rate given in logarithmic scale while the X-axes are the optical SNR in decibel. This typical curve shape indicates a high bit error probability for a SNR value of 45 dB and lower, and almost error free transmission at SNR ≈ 51.8 dB and higher. Both, the closed form solution and numerical simulation show approximately equal BER curves.
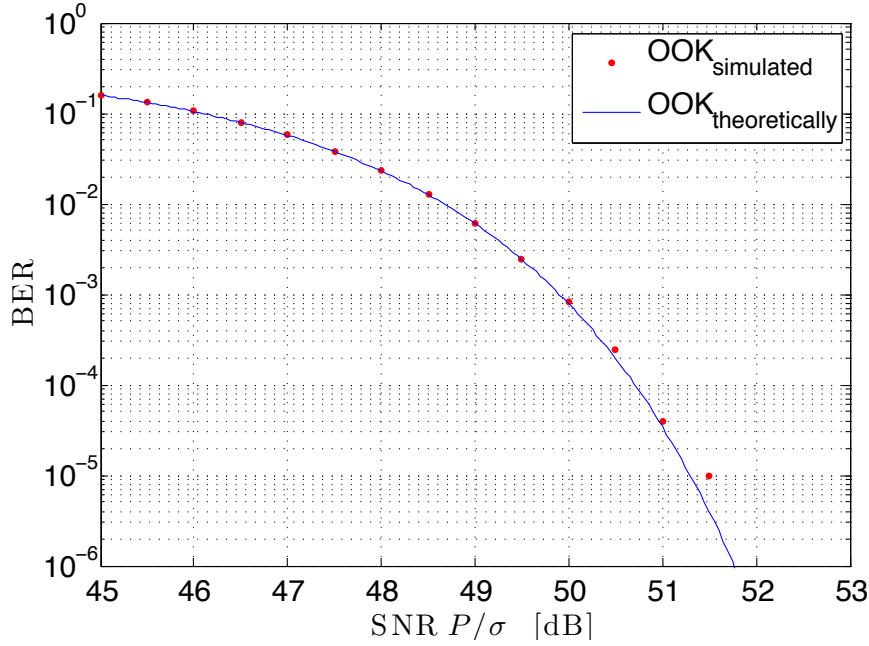
Figure 3.2: Numerically and theoretically BER rate for OOK

3.1.2 Pulse-position-modulation

PPM is also a favored binary modulation technique in optical communication. In M-ary PPM, one PPM symbol of duration T_s is divided into M subintervals (also called chips) with duration T_c. Information is transmitted by applying a positive optical intensity to one chip duration while the rest of the intervals are kept to zero. One viable basis function for M-PPM forms to

$$\phi_{\mathrm{m}} = \sqrt{\frac{M}{T_s}}\mathrm{rect}\left(\frac{t - (T_s/M)\cdot(m-1)}{T_s/M}\right),\tag{3.8}$$

where $m \in M$. The time representation of a PPM signal follows as

$$x(t) = \sum_{k=-\infty}^{\infty} MPhR_d\sqrt{\frac{T_s}{M}}\phi_{A[k]}(t - kT_s), \tag{3.9}$$

where A[k] chooses the symbol equiprobable in M [24]. The position of the impulse in a symbol is used to transmit information. The same bit sequence **b** as given in Sec. 3.1.1 was modulated with 4-PPM and is demonstrated in Fig. 3.1(b). Compared to OOK Fig. 3.1(a), 4-PPM can transmit two bits/T_s but requires more bandwidth [24] due to the shorter chip duration. Also note the higher intensity level of $4P$ which has the benefit to achieve a higher SNR compared to OOK. PPM can also be seen as a coded OOK, where one chip has positive intensity during T_s while the rest of the $(M - 1)T_s$ intervals remain dark. This fact will be important for later simulations in Chapter 4, because system restrictions limit the available transmission rate. Such a signal with a symbol rate of $R_s = R_{rect}/M = 10^9/4$ bits/s is illustrated in Fig. 3.1(c). Notice that this signal is only a scaled version of Fig. 3.1(b) with $T_c = T_s$. In addition, the symbol error probability shapes to

$$P_{s,PPM}(h) \approx (M - 1)Q\left(PR_sh\sqrt{\frac{M}{2R_s\sigma_n^2}}\right) \tag{3.10}$$

and with the bit rate $R_b = R_s\log_2(M)$, the bit error probability forms to

$$P_{b,PPM}(h) \approx \frac{M}{2} \cdot Q\left(PR_dh\sqrt{\frac{M\log_2(M)}{2R_b\sigma_n^2}}\right). \tag{3.11}$$

Note that equations 3.10 and 3.11 provide only true values for high SNR. Figure 3.3 illustrates the BER rate for PPM with a constellation size of $M = 2^i, i = 1, 2, \ldots, 6$ and SER rate Fig. 3.4, respectively. Notice, the symbol rate for PPM in this simulation is $R_s = R_{rect}/M$, so that PPM and PAM are fairly compared by using the same bandwidth. Beside the decrease in data rates, the SNR level where error free transmission is attained reduces with increasing signal constellation size M.

3.1.3 Pulse-amplitude-modulation

Pulse amplitude modulation is a bandwidth efficient modulation scheme and is usually considered in radio communication. This multilevel scheme has its benefits in higher bandwidth
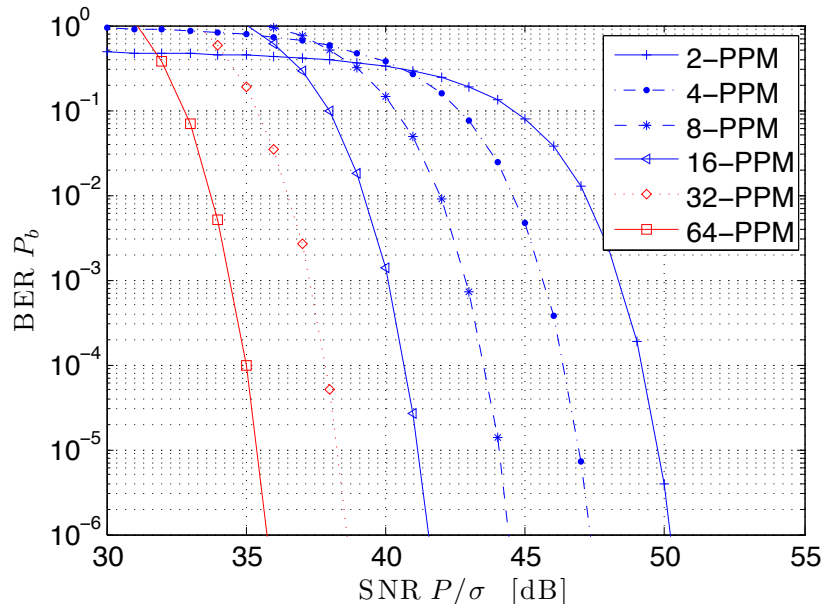
Figure 3.3: BER rate of various PPM modulation schemes
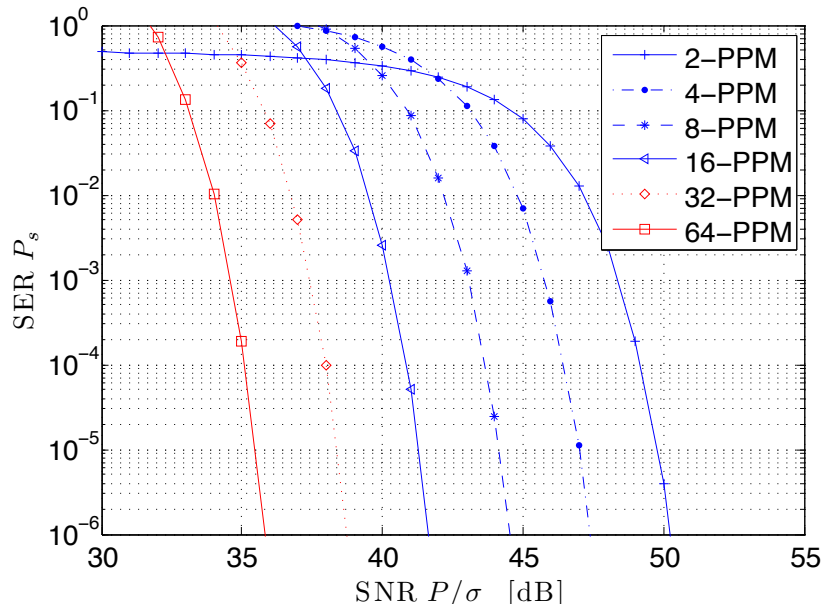
Figure 3.4: SER rate of various PPM modulation schemes

efficiency compared to the previous explained binary power efficient modulation schemes. Every PAM symbol with duration T_s is created by scaling the amplitude of the intensity by M different factors. Assuming uniformly distributed input data, the symbols are equiprobable and the average power constrain holds. The signal basis set for rectangular PAM is the same as it is in OOK $\phi_{\text{OOK}} = \phi_{\text{PAM}}$, where the signal $x(t)$ follows as

$$x(t) = \sum_{k=-\infty}^{\infty} \frac{2P}{M-1} \sqrt{T_s}(A[k]-1)\phi_{\text{PAM}}(t-kT_s), \tag{3.12}$$

and where $A[k]$ has a uniform distribution over M. The bit sequence $\mathbf{b}$ is 4-PAM modulated (see Fig. 3.1(d)). Compared to Fig. 3.1(a) and Fig. 3.1(c) only four symbol durations T_s were required to transmit the message. However with increasing number of intensity levels M, the sensitivity against noise increases. The SER is determined by

$$P_{\text{s,PAM}}(h) = \frac{2}{M}(M-1)Q\left(\frac{PR_dh}{M-1}\frac{1}{\sqrt{R_s\sigma_n^2}}\right), \tag{3.13}$$

where equiprobable PAM symbols are considered. By assuming Gray coding [54], the bit error rate becomes to

$$P_{\text{b,PAM}}(h) = \frac{2}{M\log_2(M)}(M-1)Q\left(\frac{PR_dh}{M-1}\sqrt{\frac{\log_2(M)}{R_b\sigma_n^2}}\right), \tag{3.14}$$

where the bit rate is $R_b = R_s\log_2$. Equations (3.13) and (3.14) were used to produce the BER and SER rate (Fig. 3.5 and in Fig. 3.6). Notice that with the increasing number of intensity levels M, the needed SNR to achieve, for example, a BER rate of 10^{-6} is also increasing.

3.1.4 Receiver Characteristics

Consider the channel model in (2.1). The transmitted intensity signal is converted by a photo diode into a noisy current y. A matched filter with an impulse response of $\phi(-t)$ is used to minimize the influence of noise. A following sampler samples at multiple T_s to convert the continuous signal into a discrete time signal. In this case, timing recovery is requested to obtain symbol synchronization which is even more important at higher data rates. Two main possibilities are available to regain the sent symbols, hard decision and soft decision. Hard decision is frequently used in commercial systems due to its simplicity. For M-PAM signals this matches to a threshold detector, which maps the noisy samples to the predefined
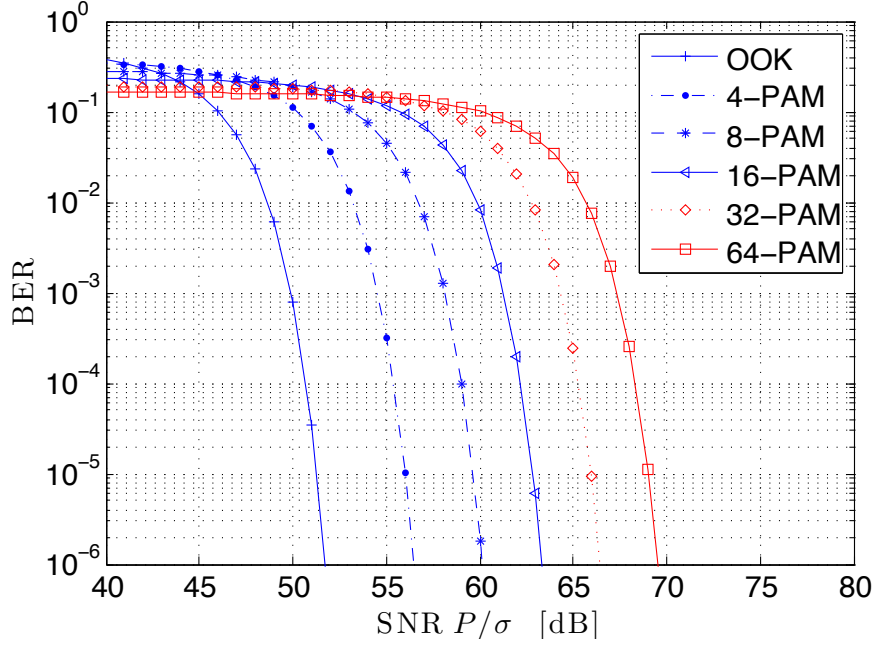
Figure 3.5: BER rate for various PAM modulation schemes

M-PAM levels. Since PPM uses the position of an impulse to transmit information, hard detection is utilized by identifying the sample with the maximum peak value in one symbol interval. If symbols are detected by hard decision, valuable information gets lost. Thus, soft information is often extracted in form of log-likelihood ratios (LLR) [37]. The LLR of each transmitted bit b is defined [55] as

$$L(b) = \ln\left(\frac{\Pr(b = 0|y)}{\Pr(b = 1|y)}\right), \qquad (3.15)$$

where $\Pr(\cdot)$ is the probability operator. For an AWGN channel and the assumption of equiprobable symbols the LLR becomes to

$$L(b) = \ln\left(\frac{\sum\limits_{s \in S_0} \exp\left(-\frac{1}{\sigma_n^2}||y - s||\right)}{\sum\limits_{s \in S_1} \exp\left(-\frac{1}{\sigma_n^2}||y - s||\right)}\right), \qquad (3.16)$$

where S_0 is the aggregate of all ideal symbols (constellation points) with the bit *zero* at the given bit position, S_1 is the aggregate of all ideal symbols with the bit *one* at the given bit position in the symbol, y is the received noisy symbol vector and s is an ideal constellation
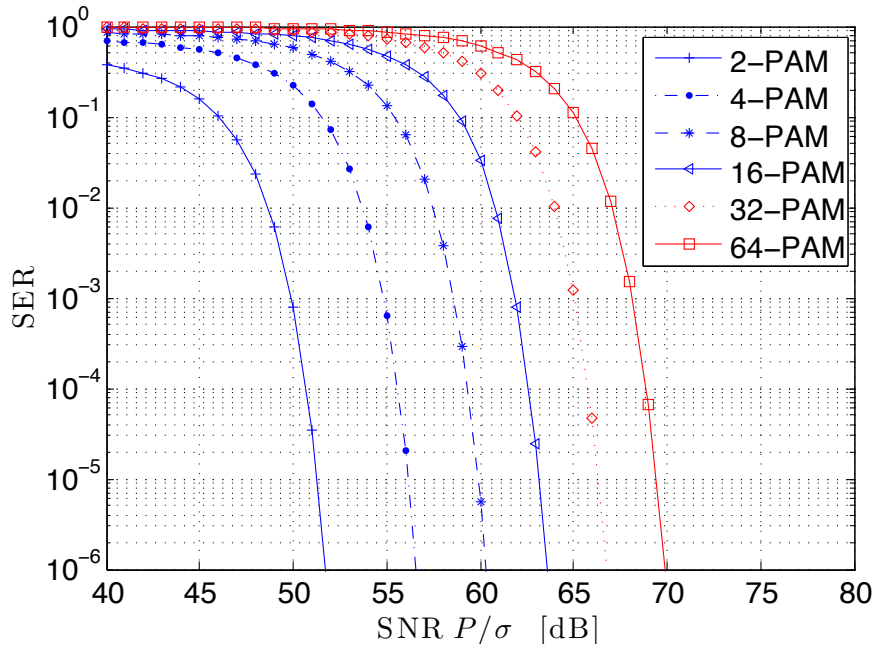
Figure 3.6: SER rate for various PAM modulation schemes

point.

3.2 Channel Coding

Error detection and error correction is one key factor in improving reliability of corrupted communication channels. The idea of channel coding is to add redundancy to the information bits in form of parity bits to be transmitted. With these additional parity bits it is possible to detect and even correct corrupted received information bits depending on the channel code, code length and the channel itself. As more redundancy is added, less information bits can be sent at the same time. As a consequence, depending on the system requirements, there is always a tradeoff between data throughput and error correction. Additionally, different combinations of modulation and coding have a different effect on the communication system. Therefore impacts on various combinations of modulation and coding proceedings, effecting FSO systems, have to be investigated. Reed Solomon and Turbo coded 256-PPM was suggested [43] to counter strong fog attenuations. The use of RS codes has shown to

provide a natural combination for higher state PPM schemes and a robust technique in terrestrial FSO links. The recent interest to combat scintillation induced fading led to various combinations of error correction coding and modulation schemes. These combinations range from coded OFDM [56], coded MIMO [57] to rateless coding [58]. The selection of channel codes shall ideally be based on the physical characterization of the atmospheric FSO channel. However, coded modulation or any other system design enhancements can not combat very high attenuation caused by fog [43]. Concerning the major FSO attenuators and the goal of throughput maximization, the choice of the channel coding techniques was limited to only RS [50] and LDPC codes [51] because of their simple implementation in current systems and the benefit of their high coding gains.

3.2.1 Reed Solomon Codes

Reed Solomon block codes are non-binary cyclic BCH codes and were invented in 1960 [50]. Particularly, the capability in correcting burst errors as well as random symbol errors have been found to be very useful for error correction in communication and data storage systems. RS codes belong to systematic linear block codes. Information bits are unified in blocks with a fixed length. These blocks are further divided into so called symbols, which are m-bits long. Because this code is operating at a symbol basis, error correction information is added in form of parity symbols. A full RS codeword consists of the actual information symbols including the attached parity symbols.

The construction of RS codes is based on Galois fields $\mathrm{GF}(2^m)$. These finite fields have the special property that any defined operation on the finite field element results again in another element of the field. Consequently, a finite field has a finite number of elements unlike, for example, the infinite field of integers. A big benefit of these Galois fields is that no problems arise due to over-flow or under-flow exceptions. A detailed explanation of RS codes can be found in [54]. An RS (n, k) code, where n is the total number of code symbols, and k is the number data symbols being encoded, may correct any errors up to $t = \lfloor \frac{n-k}{2} \rfloor$ in a coding block [54]. If more than t errors occur, symbols may be decoded incorrectly. The RS decoded symbol error probability, $P_{\mathrm{s,RS}}$, can be written as

$$P_{\mathrm{s,RS}} \approx \frac{1}{2^m - 1} \sum_{j=t+1}^{2^m - 1} j \binom{2^m - 1}{j} P_s (1 - P_s)^{2^m - 1 - j} \qquad (3.17)$$

where P_s is the symbol error probability of the used modulation scheme. Reed-Solomon codes correct up to t symbols, no matter how many bits got corrupted in any of these t symbols during transmission, and therefore it is outstanding in correcting burst errors. However, if only one bit error occurs in each of $t + 1$ symbols, the codeword can not be decoded correctly. So, the fact that RS codes are correcting on a symbol base has both, its advantages and disadvantages. As an example, the SER rate is plotted for 256-PAM including RS coded rates in Fig. 3.7. The related coding gains (CG) are given in Tab. 3.1
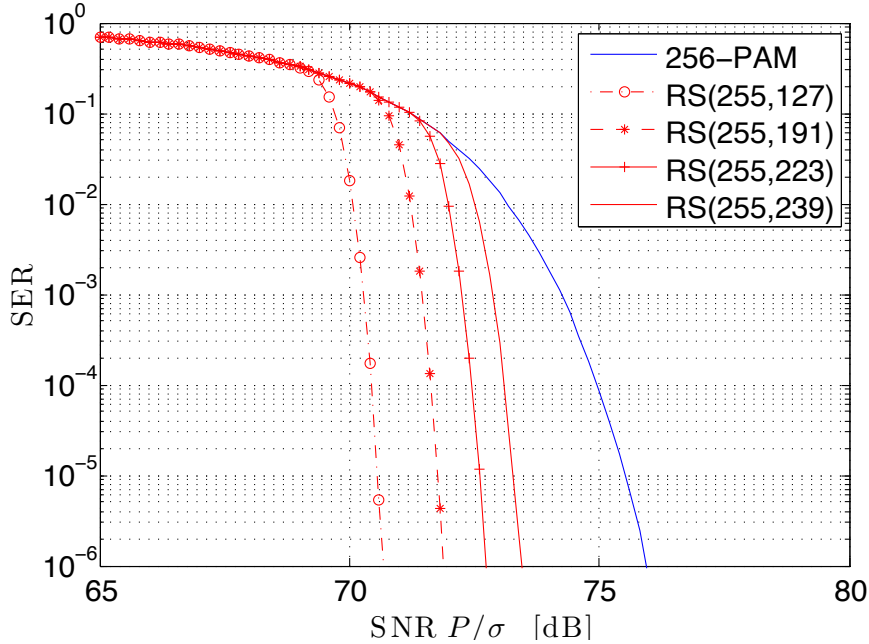
Figure 3.7: BER rate for LDPC coded OOK with three different rates of 1/2, 2/3, 5/6

RS codes have got big attention in the research field of FSO communications [52]. The benefits range from well tested RS decoders and good coding gain to the ability to simply match the alphabet size of RS codes to the constellation size of M-PPM or M-PAM schemes. Also, currently available low hardware-complexity decoders [59] achieve throughputs of up to 12.8 Gbps, which makes the RS codes one of the favorites for utilization in optical wireless

communications.

Table 3.1: Coding gain of RS coded 256-PAM at a SER rate of $P_s = 10^{-6}$

Modulation	256-PAM	RS(255,127)	RS(255,191)	RS(255,223)	RS(255,239)
SNR in dB	75.95	70.7	71.85	72.75	73.45
CG in dB	0	5.25	4.1	3.2	2.5

3.2.2 Low-density-parity-check Codes

The LDPC codes invented by Gallager [51], and rediscovered in recent times, are proven to provide very high coding gains. Usually the LDPC codeword length is very long, so that the encoding and decoding speed was way to slow in the past. Improved hardware and decoding algorithms have made it possible to design reasonable time efficient LDPC codes. LDPC codes have been proposed in the DVB-S2 standard (Digital Video Broadcast - Satellite) [60] as an inner code for forward error correction. The maximum decoder speed for the DVB-S2 LDPC codes was recently improved up to 1 Gbps [61]. Shorter codes with a Shift-LDPC decoder design already reach the 5.4 Gbps level. This rapid progress in the design of LDPC codes make them an attractive choice for FSO systems. However, DVB-S2 LDPC codes are linear block codes specified by a sparse matrix $H_{(n-k) \times k}$, where k is the number of information bits which are encoded to a codeword with length n. Conventionally, this matrix is represented by a bipartite graph. This graph consists of two different nodes, check nodes, which correspondent to $n - k$ parity check equations, and variable nodes associated with the n bits in the codeword. Each variable node i is connected to a check node j, if the parity check matrix entry $h_{i,j}$ equals to a one. Actually, this graphical presentation had a significant advantage to develop efficient decoding algorithm like the sum product algorithm or the message passing algorithm [54]. The DVB-S2 standard specifies eleven different code rates, ranging from 1/4 to 9/10, for fixed codeword length of $n = 64800$ bits. It also provides the algorithm to generate the parity check matrix H for each of these rates. In this work, the LDPC structure from the DVB- S2 standard was utilized, and soft information as input for

the message passing algorithm was used to decode the received codewords. For simulations, 30 LDPC decoder cycles are obtained. As an example for the performance of these codes, the BER is demonstrated for LDPC coded OOK in Fig. 3.8. At a BER of $P_b = 10^{-6}$ a coding gain of 6.15 dB, 5.15 dB and 4.15 dB for coding rates of 1/2, 2/3 and 5/6 can be achieved. Noticeable is the abrupt drop of the bit error rate for LDPC coded schemes.
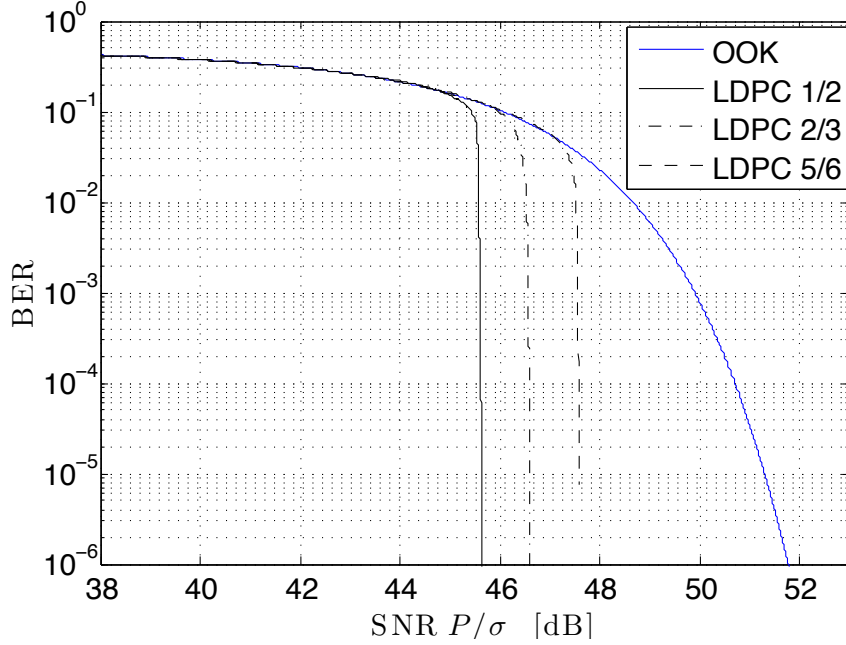
Figure 3.8: BER rate for LDPC coded OOK with three different rates of 1/2, 2/3, 5/6

3.3 Information Rates

The mathematical fundamentals to characterize information rate limits in communication systems were introduced by Shannon [37]. In general, the capacity of a communication channel is the maximum achievable data rate while error free transmission remains achievable [53]. In information theory, capacity is the maximum mutual information between channel input and output over all possible input distributions fulfilling all input constraints. For given input constraints of the optical channel, the capacity forms to

$$C = \max_{f_{\mathbf{X}}(x)} I(\mathbf{X}; \mathbf{Y}), \tag{3.18}$$

where $f_{\mathbf{X}}(x)$ are all possible input distributions, $\mathbf{X}$ is the discrete input and $\mathbf{Y}$ the channel output. The unit of the capacity is given in bits per channel use, and is often presented in dependency of SNR. The exact channel capacity for an optical intensity channel is not known. Only upper and lower bounds for the capacity have been found so far [62]. Nevertheless, in this work the information rates (capacity for a selected input distribution) of M-PAM and M-PPM are of main interest because of two reasons. First, those schemes can be compared in terms of the maximum achievable data rate for a given SNR. Second, a suitable coding scheme and rate can actually be determined and be applied to the system to guarantee error free transmission. Consider the discrete channel model in (2.4), R_d and h is set to unity in this case,

$$y = x + n \tag{3.19}$$

The discrete channel input signal set is $\mathbf{X} = \{X_0, X_1, \ldots, X_{N-1}\}$, where each entry correspondents to one constellation size point. The information rates for a memoryless discrete input and for a continuous output channel [63] yields

$$I_r = log_2(N) - \frac{1}{N} \sum_{j=0}^{N-1} \mathbb{E} \left\{ \log_2 \sum_{i=0}^{N-1} \exp\left[-\frac{|X_j + n - X_i|^2 - |n|^2}{2\sigma^2} \right] \right\}. \tag{3.20}$$

Using Monte Carlo averaging, I_r has been examined as a function of SNR for M-PAM and M-PPM signals. For instance, for 4-PAM, the input signal points are $\mathbf{X} = \{X_0, X_1, X_2, X_3\} \cdot [2P\sqrt{Ts}/(M-1)]$ and finally turn into $\mathbf{X} = \{0, 1, 2, 3\} \cdot [2 \cdot 1/(4)]$ with $M = N$. In Fig. 3.9, OOK (2-PAM), 4-PAM and 8-PAM is illustrated. On-off-keying is only able to transmit a maximum number of one bit per channel use. Furthermore, 4-PAM can not exceed the limit of 2 bits per channel use. Note, as the SNR decreases, less information can be sent over the channel. For example at SNR = 6 dB, OOK is at his rate limit but 4-PAM would be able to transmit 1.51 bits per channel use, assuming unlimited coding and decoding effort [63]. The big difference for this feature is that OOK can transmit less bits at this given SNR, but does not need any additional channel coding compared to 4-PAM. In Fig. 3.10, the information rate curves are given for PPM signals. It can be observed that with an increasing modulation order the maximum achievable rate decreases, but the robustness improves at
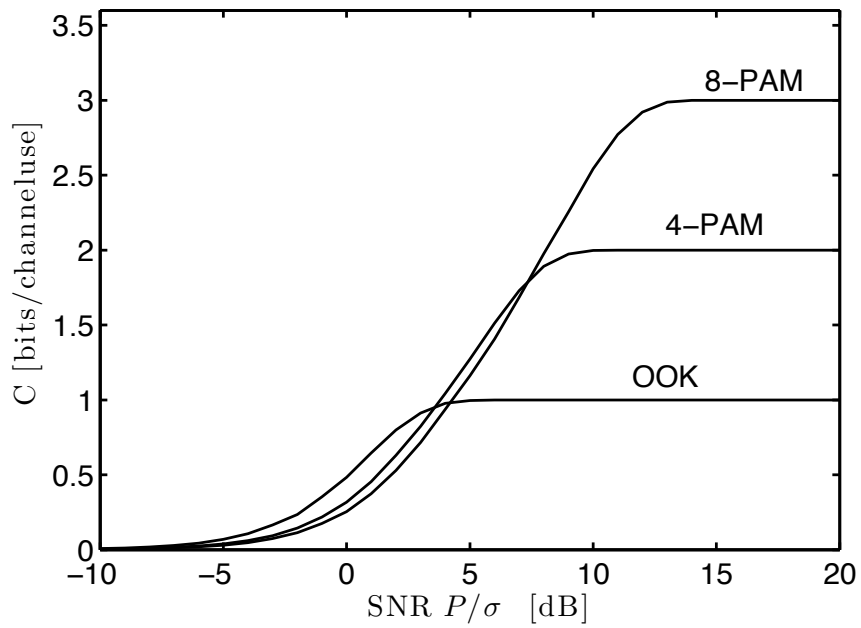
Figure 3.9: Information rate curves for selected PAM signals on an AWGN channel
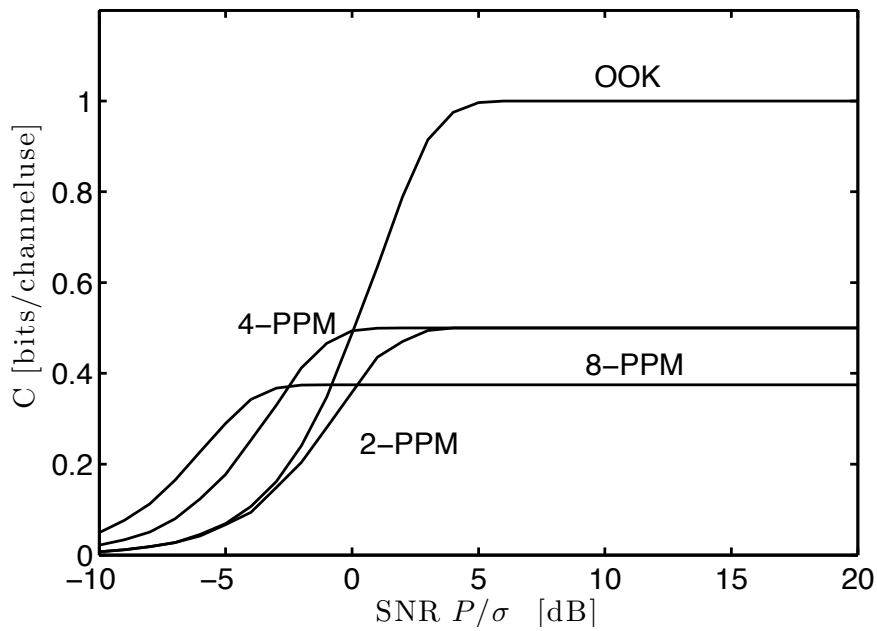
Figure 3.10: Information rate curves for selected PPM signals on an AWGN channel

the same time. As a consequence, OOK and PPM is often used in commercial systems due to their availability in low SNR regimes, but at the cost of bandwidth efficiency (higher PAM).

4 Throughput Maximization

The reliability of FSO links is inherently limited due to the variability and large scale loss in atmospheric channels [64]. In this chapter, a fundamentally different approach is proposed in terms of the design and application of FSO links. Rather than designing FSO links to improve reliability in all weather conditions, FSO links are considered for latency-tolerant traffic which can tolerate outages. The goal of system design is then not to improve the instantaneous reliability, but rather to maximize throughput of the link [64].
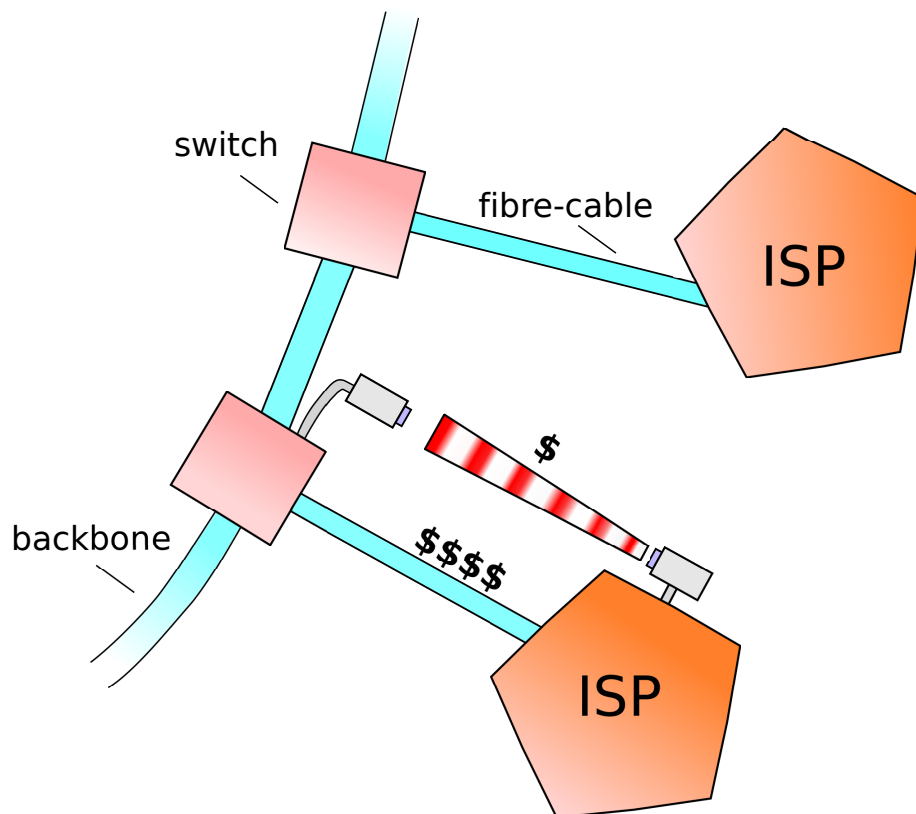
Figure 4.1: Simplified diagram demonstrating an inexpensive parallel FSO system for ISPs

Consider the connection of an internet service provider (ISP) to a backbone network in Fig. 4.1. According to a recent study [65], in 2008 nearly 35% of the aggregate traffic on the Internet consisted of P2P file-sharing, storage, back-up services and email. These classes of traffic are not real-time and are termed *latency-tolerant*. The average P2P traffic is nearly constant throughout a day [65]. Due to the high traffic caused by latency-tolerant traffic, ISPs backhaul costs are increasing while affecting the performance of other applications. Many methods, including traffic shaping, have been applied to control the priority of specific kinds of traffic [66]. Backup and storage traffic have a similar impact as P2P file sharing. Bulk data transfers range in size from GBytes to many TBytes and are transmitted from commercial users to servers causing constant high data traffic over a period of days.

This work considers the installation of a parallel FSO link to connect the ISP to the backbone (see Fig. 4.1). The FSO link is far less expensive than the fibre link and can be used to carry latency-tolerant traffic. Since the typical download/upload duration of such traffic is on the order of days, total FSO link failures in the range of hours can be tolerated. Thus, the FSO link offers a differentiated Quality of Service (QoS) for latency-tolerant traffic which frees the reliable, and expensive, fibre connection to handle real-time data. Even here, the selection of modulation for the FSO link is considered to maximize the average rate and not the reliability of the link. It is shown that the use of bandwidth-efficient modulation for this goal decreases the instantaneous reliability, but will result in a higher average throughput. This technique can also be considered for companies and universities where congestion occurs due to latency-tolerant traffic. The following simulations provide information about the data rate behavior over one full year. Metrics, such as outage and cumulative distribution, will help to evaluate the impact of the investigated modulation and coding techniques on data rates.

The structure of this chapter is organized as follows. Simulation parameters, metrics for system design and the system model are presented in Sec. 4.1. Simulations for binary and multilevel modulation schemes using measured climate data are presented in Sec. 4.2 and are extended with channel coding in Sec. 4.3.

4.1 Constraints, Rates and Simulation model

Real world FSO systems experience various system restrictions and limitations. These parameters must be determined in order to simulate and evaluate the required data rates.

4.1.1 System Constrains

Generally, FSO systems are used in communication networks where packets of the length L are transmitted. A cyclic redundancy check (CRC) code is applied to each packet to ensure that any packets corrupted during transmission are discarded. Hence, here the overall channel model is a packet erasure channel. Current systems usually support the IEEE 802.3 Gigabit Ethernet standard. In order to build the system model, hourly estimates of the visibility were obtained from [67]. Applying (2.7), h_l is obtained for each hour. In the simulations, it is assumed that the weather remains constant throughout this hour and the time scale of weather change is denoted $T_{\mathrm{atm}} = 1$ hour. While h_g is constant, h_s varies on the order of 1-100 ms. For simplicity, the scintillation coherence time is chosen to be 10 ms, $T_{\mathrm{scint}} = 10^{(-2)}/3600$ hours. Because h_l is the dominant factor, h is averaged in a period of T_{atm} to derive the average transmission rates. Additionally, define $T_{\mathrm{year}} = 8784$ hours as length of the year 2008. Consider the application of bandwidth-efficient PAM and power-efficient PPM modulation to FSO links. In order to have a fair comparison of different modulations, we assume that the modulator has a fixed bandwidth $R_{rect} = 1$ GHz , that is, it can output rectangular pulses of a fixed time duration. Define the symbol rate, and accordingly the bit rate for OOK as $R_{rect} = R_s = R_{b,\mathrm{OOK}} = 1/T_s = 10^9$ bits/s where T_s is the symbol duration. Although M-PAM has the same R_s, the bit rate varies as $R_{b,\mathrm{PAM}} = R_s \log_2(M)$ where M is the modulation order. On-off keying is a special case of a M-PAM ($M = 2$). For PPM, the chip duration is set to T_s, and correspondingly the bit rate is $R_{b,\mathrm{PPM}} = R_s \log_2(M)/M$.

4.1.2 Data Rates

Notice that all modulations satisfy the non-negativity constraint, $x \geq 0$, as well as the average optical power constraint $E\{x\} \leq P$. The symbol error rate for an AWGN channel for M-ary PAM and M-ary PPM with equiprobable signaling is given in Equation 3.13 and

3.10. Since most commercial systems perform packet transmission, a packet erasure channel is assumed with erasure probability

$$p_{\text{packet}}(h) = (1 - P_s(h)^{\frac{L}{\log_2(M)}} . \tag{4.1}$$

Notice that this is the probability that all symbols in the L-bit packet are received without error. Further, this quantity depends strongly on the particular weather condition and scintillation. Since the variation of h_s is small compared to h_l, the probability p_{packet} is averaged over a period of T_{atm} to yield

$$\bar{p}_{\text{packet}} = \frac{1}{N} \sum_{i=1}^{N} p_{\text{packet}}(h_i) \tag{4.2}$$

where $N = T_{\text{atm}}/T_{\text{scint}}$ (assumed to be integer) and h_i changes every T_{scint}.

As the main interest is subjected to throughput maximization, actual data rates over the year must be calculated.The average rate R_b per hour for PAM is

$$R_b[k] = \bar{p}_{\text{packet}}[k] \, R_{b,\text{PAM}} \tag{4.3}$$

where k is a discrete time variable indexing each hour. Equation (4.3) can be easily extended for PPM schemes where $R_{b,\text{PPM}}$ is substituted with $R_{b,\text{PAM}}$.

Because download periods are assumed to be in the order of days, instantaneous rates are of less interest than the average hourly rate. Define the average rate per hour for a 24 hour period as

$$\tilde{R}_b[k] = \frac{1}{24} \sum_{l=0}^{23} R_b[k - l]. \tag{4.4}$$

To evaluate the reliability and variability of the average daily rate, define

$$\text{Pr}_{\text{rate}}(R_0) = \text{Prob}\{\tilde{R}_b \geq R_0\}, \tag{4.5}$$

where R_0 is a fixed bit rate. This probability contains information about the certainty that a rate $\tilde{R}_b$ or higher can be achieved. As a matter of fact, averaged rates such as R_b and $\tilde{R}_b$ hold no obvious information about link outages. As a consequence, $\text{Pr}_{\text{out}}(t_{\text{out}})$ is defined as probability that the rate R_b falls below a certain limit R_{limit} for exactly t_{out} hours.

4.1.3 Simulation Model

Again, in the following simulations, various modulation and coding types are investigated to improve throughput for latency tolerant traffic rather to increase reliability of the link. Primarily, the interest is orientated on the highest average throughput. As a consequence, various parameters such as the the yearly mean of data rates, the hourly rates and distribution of data rates over time are evaluated. The schemata, which result in high throughput, are preferable. Nevertheless, system designer must examine the distribution, number and maximal length of outages in order to choose the right modulation scheme with the right code in respect to the installation location of the FSO link. Link outages, which are in the order of days, are not tolerable. In this work, more bandwidth efficient modulations are investigated and compared to commonly used OOK if they can improve throughput and keep link outages small enough. Only this analysis could make it possible to design FSO systems suitable for latency tolerant traffic applications. In the following sections, M-PAM and M-PPM with and without forward error correction is evaluated, on the previous discussed metrics, with the help of measured visibility data from one location over one year.

In the channel model of Sec. 2.2, snow, rain and fog present very large attenuation. Even in clear conditions, although scattering losses are low, scintillation may be high [47]. The simulations are based on the hourly-recorded weather data for Hamilton, Ontario, Canada [67]. This city is 80 km away from Toronto and borders on Lake Ontario. The climate of Hamilton is usually warm and rainy in the summer, and very snowy and cold in the winter. With approximately 11% of snow, 9% of rain and 5% of fog over the year, this location poses large challenges for FSO links. The system parameters are illustrated in Table 4.1 [8, 38]. While σ_n^2 consists of electrical circuit noise and background illumination interference, here circuit noise is assumed to dominate [3]. The value of σ_n^2 was chosen accordingly to [38] and adjusted to achieve a $\text{BER}_{\text{OOK}} = 10^{-9}$ with 1.5 dB link margin as is established in commercial systems [8]. With the given system restrictions and parameters the simulations are carried out in the following way. A graphical illustration of the simulation model is given in Fig. 4.2. First, hourly measured visibility data and the associated weather conditions (fog, snow, rain, hail, sunny, etc.) are used to determine the channel state h (see (2.3)). The general occurring weather situations are categorized into snow, rain and no-precipitation.
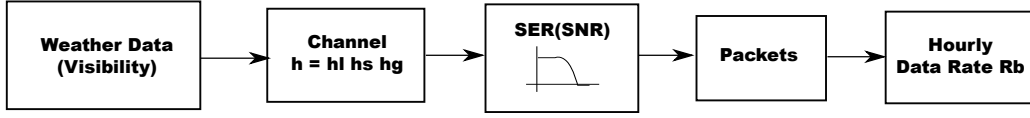
Figure 4.2: FSO simulation model

Consequently h_l is calculated by (2.3) where σ is chosen dependent on the weather situation. The probability density function (pdf) of the scintillation factor h_s changes according to the refractive index parameter C_n (see Tab. 2.1) while h_s itself varies every 10 ms. With constant h_g and the predefined system parameters, the SER can be calculated for every time step. Without coding, (3.13) and (3.10) are considered, whereas when forward error correction is applied, when the SER rate value is determined by Monte Carlo simulations. Furthermore, the number of correctly received packets as well as the hourly data rate is finally determined. Note that this procedure is different from conventional channel simulations where bits are encoded, modulated, sent over the channel and then are decoded and demodulated. If simulations are performed for a long period of time, the method to use the recalculated SER values is more time efficient than to use the usually applied method. Furthermore, during link outages no packets could be received. Therefore, in real applications the channel must be estimated to determine if a link outage occurs or not. In case of an outage, this information must be transmitted over a wired data line to switch off the FSO transmitter. The traffic shaping device will consequently route the traffic only to the wired data connection. In simulations, this is done automatically, since packet ratios are zero if the SER probability is too high (see equ. (4.1)).

4.2 Throughput Maximization without Coding

Both M-PAM and M-PPM, where $M = 2^i$, are simulated to determine a modulation type with the highest average daily rate over the year for a given distance.

Link distances of 0.2, 0.5, 1 and 2 km were considered. The daily average rate per hour $\tilde{R}_b$ is shown for standard OOK in Fig. 4.3. As expected, snow, rain and fog cause strong fluctuations during the winter while rain attenuates the signal in spring and summer. In the summer and autumn months, the maximum rate of 1 Gbps is quite reliably achieved and

Table 4.1: System Parameters

System parameter	Value	Unit	Symbol
Wavelength	1550	nm	λ
Symbol rate	1	GSymbols/s	R_s
Transmitted power	500	mW	P_{fso}
Receiver responsivity	0.5	A/W	R
Receiver aperture	20	cm	d
Laser divergence angle	2	mrad	ϕ
Standard deviation of noise	10^{-8}	A	N_{fso}

hence, attenuation is only effected due to scintillation variations.

Figure 4.4, presents the average rate over the year for a variety of PAM and PPM modulation schemes and ranges (see also Tab. A.1 for more accurate values). Notice that for a range of 1 km, 4-PAM has the highest average rate per year which is a 70% improvement over the use of OOK. It is important to note that this improvement in average rate is only useful for the latency-tolerant traffic considered here. Although 4-PAM has a high average rate, data rate of the link suffers from larger fluctuations as compared to OOK or PPM modulation. For short distances, bandwidth efficient modulations offer an enormous increase in throughput. For example, 64-PAM at a distance of $z = 200$ m has an average throughput of 5.65 Gbps. When increasing the link distance, bandwidth-efficient schemes suffer due to the low SNR. PPM schemes are more robust against low SNR, but have a lower throughput than bandwidth-efficient techniques. Additionally, the average rates for a "nice" and a "bad" month are given in Fig. 4.2. In December 4.5(b), where bad weather conditions dominate, data rates using PAM schemes drop noticeable compared to data rates in August 4.5(a) where clear conditions occur. In August and at a link distance of 200 m, 64-PAM achieves its maximum possible rate of about 6 Gbps. Commercial systems do not consider such high constellation PAM in their small range systems which is surprising according to the mentioned result. One issue could be that in inconstant weather conditions like in December, too many packet errors occur, which is not tolerable. For latency tolerant traffic, the issue of link outages is relaxed and multilevel schemes promise an improvement of several Gbps (depending on the link distance) in data rate. The results also show the robustness for PPM
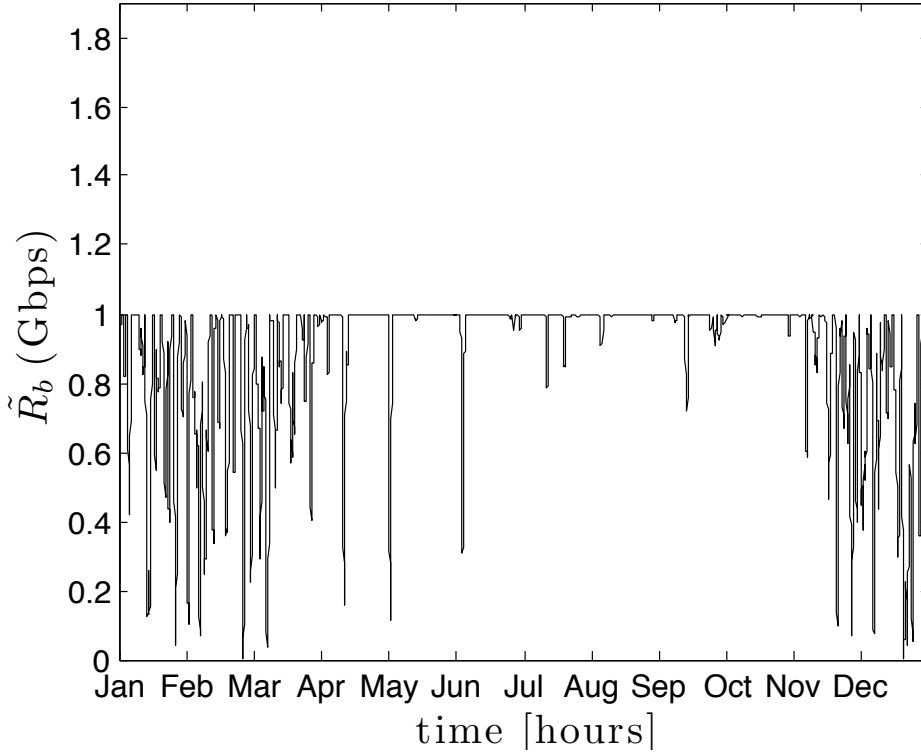
Figure 4.3: $\tilde{R}_b$ per hour using OOK with $R_s = 1\,\mathrm{Gsps}$ at 1 km distance

schemes. For link distances of 1 km and smaller, higher PPM modulations do not suffer as strong as PAM schemes do under weather impairments, as it can be observed in Fig. 4.2. As rate is the important factor for this application and not reliability, binary modulations seem to be not the right choice.

In order to quantify the data rate variations, the cumulative distribution of the rate, $\mathrm{Pr_{rate}}(R_0)$ (4.5), is shown for all modulations in Figs. 4.6 and 4.7. The corresponding mean values are given in Fig. 4.4 while the link distance is 1 km. Using 4-PAM results in the highest mean rate of 1.49 Gbps and can achieve rates $\tilde{R}_b > 0.8$ Gbps in 90% of the time and $\tilde{R}_b > 1.25$ Gbps in 80% of the time. Higher order PAM performs worse, on average, due to its increased sensitivity to loss at a range of 1 km. For OOK, the availability is $\tilde{R}_b > 0.55$ Gbps in 90% of the time and the yearly average is 0.88 Gbps. Furthermore, $\mathrm{Pr_{rate}}(R_0)$ is illustrated for a summer and a winter month (Fig. 4.2). As expected, OOK
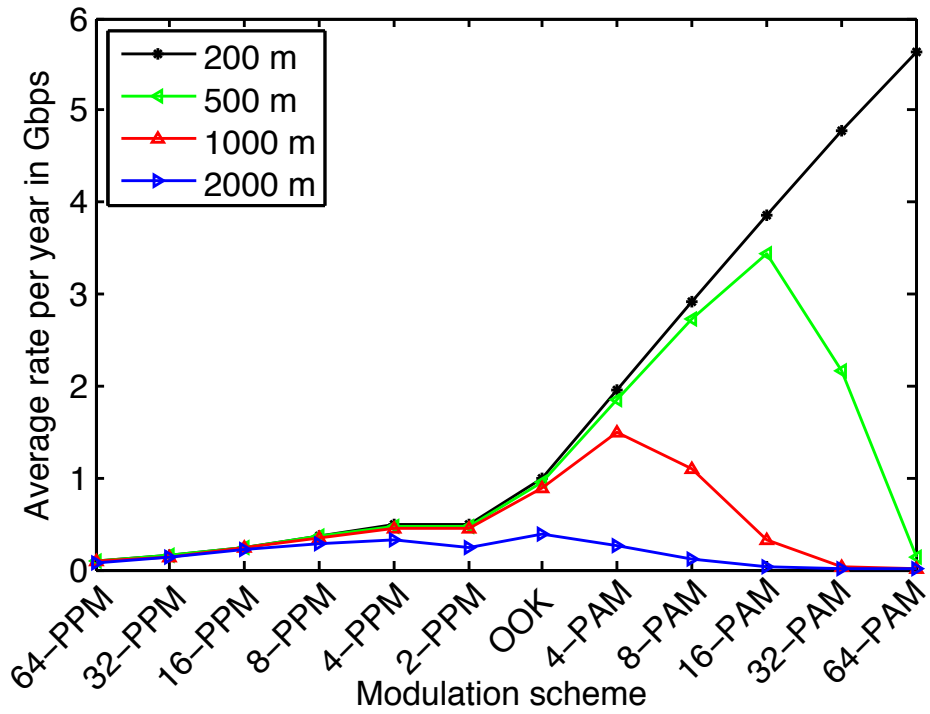
Figure 4.4: Average rate per year for various modulation types and different link distances
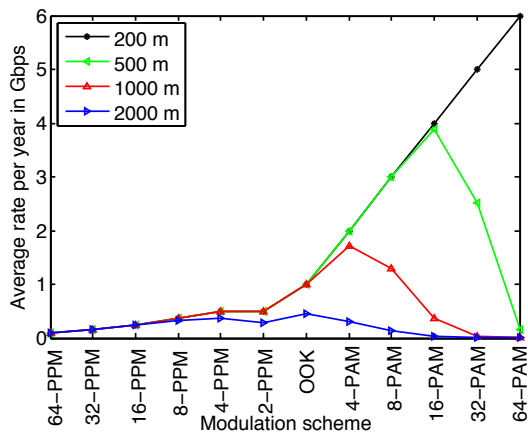
(a) Average rate in August
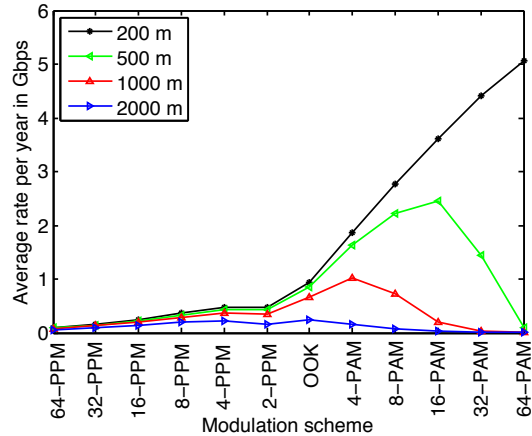
(b) Average rate in December

Figure 4.5: Average rate for selected Months (Gbps)
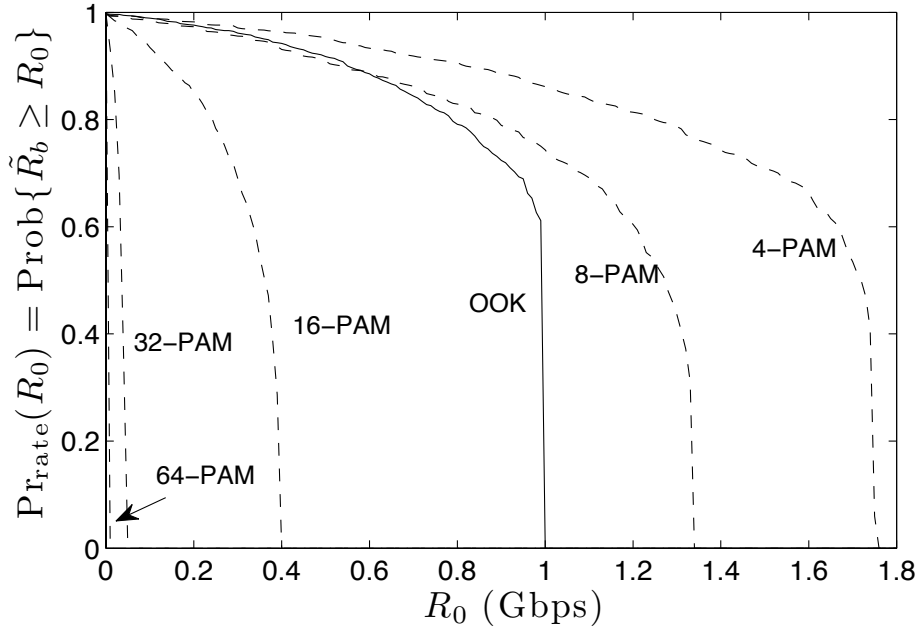
Figure 4.6: Cumulative distribution of $\tilde{R}_b$ in (4.5) for various PAM schemes at 1 km distance

4.8(a) can achieve rates of $\tilde{R}_b > 1$ Gbps in 90% of the time in August which is the maximal rate it can support. But it only achieves $\tilde{R}_b > 0.22$ Gbps in 90% of the time in December. The pathway of 4-PAM is similar to that of OOK. The availability for 4-PAM in August is $\tilde{R}_b > 1.68$ Gbps in 90% of the time and $\tilde{R}_b > 0.3$ Gbps in 90% of the time. Note that the maximum achieved rate of 4-PAM (maximum rate is 2 Gbps) is 1.76 Gbps. This results from that even in nice weather conditions at SNR = 53 dB, the BER probability is around $P_b = 1.3 \cdot 10^{-2}$. As mentioned before, the influence on rate of PPM modulations is smaller compared to that of PAM. However, no evaluated modulation scheme is available during heavy weather fluctuations. All in all, PPM gives a low rate link which is less variable, while PAM gives a higher instantaneous rate which changes more often and results in a higher average rate.

As $\mathrm{Pr_{rate}}(R_0)$ gives no information about the length of outages, $\mathrm{Pr_{out}}$ is calculated by choosing $R_{\mathrm{limit}} = 100$ Mbps and is shown in Fig. 4.9. Outages of near one hour are most likely, while failures greater than 12 hours are rare. From Table 4.2 first row, the statistical variance of outage length increases with bandwidth-efficiency. The mean behaves similarly
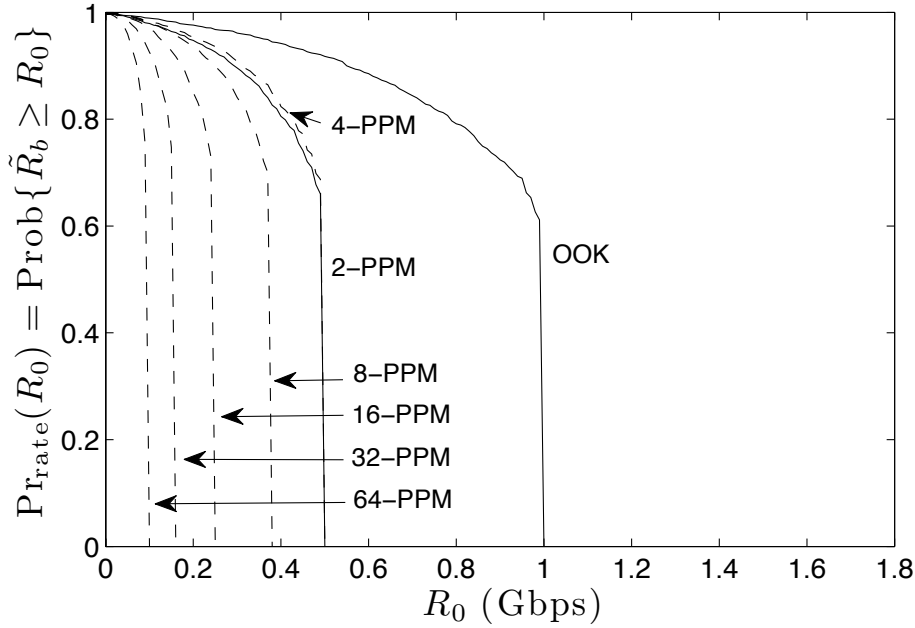
Figure 4.7: Cumulative distribution of $\tilde{R}_b$ in (4.5) for various PPM schemes at 1 km distance

with some exceptions. The outage duration of 4-PAM is always equal or greater than that of OOK, however, a greater number of short duration outages occurs for 4-PAM resulting in a lower mean outage time.   The second and third rows of Tbl. 4.2 present the mean

Table 4.2: Mean and St. Dev. of Outage Lengths in Hours ($z = 1$km)

Modulation	OOK	4-PAM	8-PAM	4-PPM
mean / st.dev. (year)	5.3 / 5.70	5.2 / 5.9	5.53 / 6.5	4.9 / 5.0
mean / max. (Aug.)	2 / 2	1.5 / 2	1.25 / 2	2 / 2
mean / max. (Dec.)	5.3 / 30	5.6 / 31	6.6 / 33	4.3 / 21

and maximum outage lengths for the best and worst month in terms of outage, respectively. In August, the number of outages is OOK = 1, 4-PAM = 2, 4-PPM = 1 each with a short length which results in a small mean value. In contrast, there is a high number of outages of variable length in December (number of outages: OOK = 38, 4-PAM = 40, 4-PPM = 37). This results in a higher mean and standard deviation. The maximum outage length for PAM is 31 hours which is still on the order of usual download times. Considering average
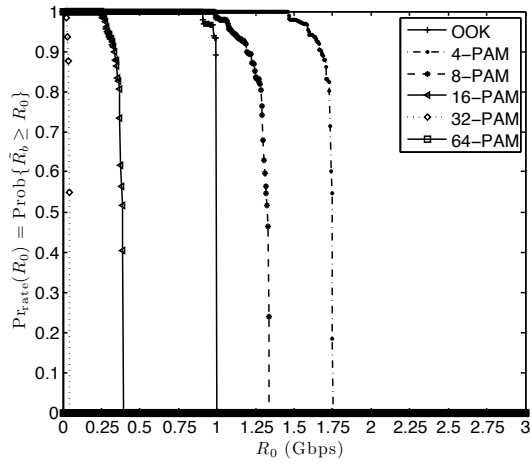
(a) $\mathrm{Pr_{rate}}(R_0)$ for PAM schemes in August
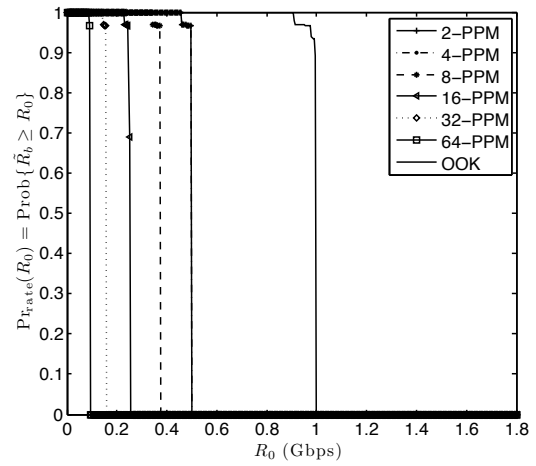
(b) $\mathrm{Pr_{rate}}(R_0)$ for PPM schemes in August
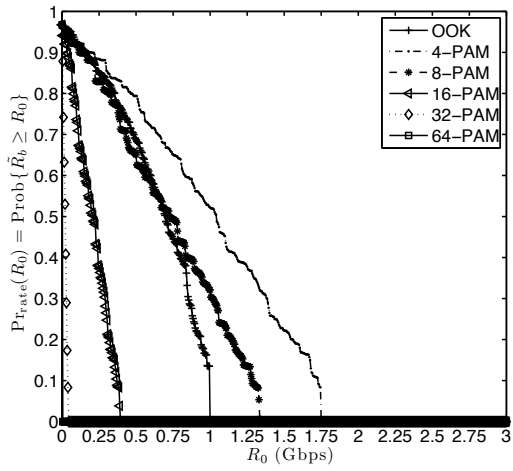
(c) $\mathrm{Pr_{rate}}(R_0)$ for PAM schemes in December
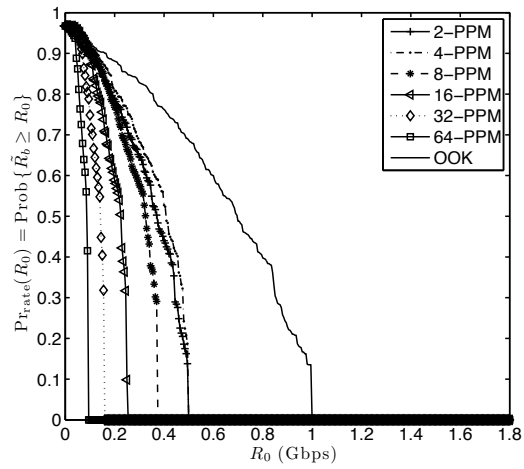
(d) $\mathrm{Pr_{rate}}(R_0)$ for PPM schemes in December

Figure 4.8: Cumulative distribution of $\tilde{R}_b$ in (4.5) for various months
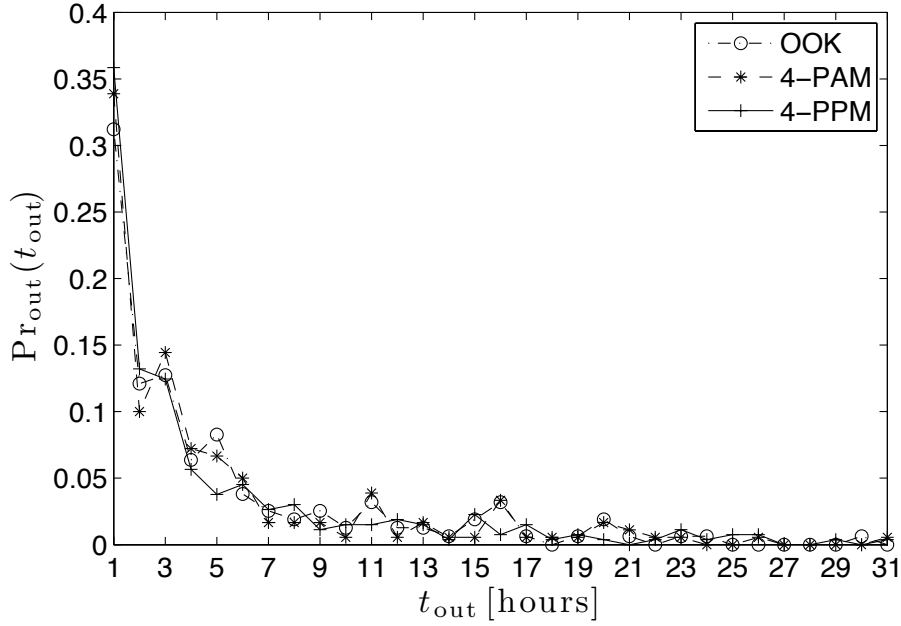
Figure 4.9: Distribution of outage durations , $\mathrm{Pr}_{\mathrm{out}}[k]$, with $R_{\mathrm{limit}} = 100$ Mbps

rate, availability and outages, uncoded 4-PAM is an effective and simple choice to maximize throughput for latency tolerant traffic as long as the outage length can be tolerated.

4.3 Throughput Maximization with Channel Coding

In Sec. 4.2, simulations were carried out by exploring different modulation types and the resulting effects on the FSO link. In this section, additional forward error correction is used in the communication structure. Two benefits are expected by doing this: 1) Increase in the average throughput and 2) To control and to reduce the length and number of outages. As mentioned in Sec. 3.2, two promising code families are selected for this application. Reed Solomon codes, namely RS(255,239), RS(255,223), RS(255,191) and RS(255,127) are applied which have a broad field of application and are well studied. Furthermore, LDPC codes gained big attention in recent years and are used in the upcoming "Third Generation Communication" standards. LDPC codes are utilized with limited code rates of 9/10, 8/9, 5/6, 4/5, 3/4, 3/5, 2/3 and 1/2. The combinations of modulation and coding schemes are

studied in terms of average throughput, availability and outage behavior.

In case of used forward error correction coding (FEC), data rate calculation slightly differs from that without coding. Here, no packet transmission with CRC check is required since FEC is used for error correction. Furthermore, a bit error limit $\text{BER}_0 = 10^{-3}$ assures in simulation that the system is switched off if data transmission is too erroneous. The data rate of this system is calculated as

$$\bar{R}_b(h) = (1 - P_b(h))r R_{b,\text{PAM}}, \tag{4.6}$$

where r is the code rate. The hourly rate follows with (4.6) to

$$R_b[k] = \frac{1}{N} \sum_{i=1+(k-1)N}^{kN} \bar{R}_b(h_i), \tag{4.7}$$

where i is a discrete time variable indexing each T_{scint} and k is a discrete time variable indexing each hour. Equation (4.7) can be easily extended for PPM schemes where $R_{b,\text{PAM}}$ is substituted with $R_{b,\text{PPM}}$. The average hourly rate, availability and outage calculations are equally determined as in the uncoded case (Sec. 4.1.2).

As Sec. 4.2 has shown, PAM modulations are outperforming PPM schemes in terms of average rate and are therefore primarily considered in this section. The chosen code rates where selected by simulation, so that the used modulation has the highest average throughput per year. The average rate for RS coded and LDPC coded PAM with a link distance of 1 km is illustrated in Fig. 4.10(a) and Fig. 4.10(b). However, the maximum average throughput of uncoded 4-PAM could not be exceeded with the usage of RS codes. The average yearly rate decreased for OOK, with RS(255,239), to 0.83 Gbps and for 4-PAM to 1.47 Gbps. Higher modulations, such as 8-PAM, have not been reliable without coding. The additional use of channel coding results in an increase of rate if the number of symbol errors is smaller as or equal to the number of correctable symbols by the code. For 8-PAM, an average rate of 1.32 is given while for 16-PAM and higher constellations only small improvements are noted. The DVB-S2 LDPC are strong codes which are operating close to the channel capacity. The arising high coding gains have an obvious effect on the rates. The modulations 4-PAM and 8-PAM show an increase in rate to 1.52 and 1.77 Gbps. Furthermore, the LDPC coded 8-PAM with code rate of $r = 4/5$ has the highest yearly throughput of all tested coded

(a) RS coded.   (b) LDPC coded.
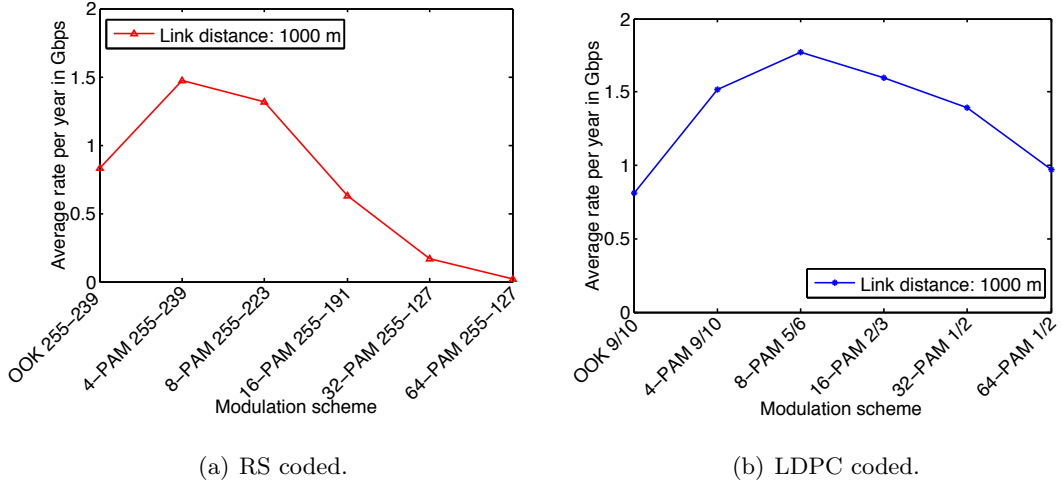
Figure 4.10: Average rate per year for coded PAM signals (Gbps)

modulations. There are also improvements for higher PAM schemes, but outage calculation will show later that they may not be usable for this application. Again, a decrease of OOK with a 9/10 LDPC code from 0.88 to 0.81 Gbps can be observed. This decrease is also visible for all simulated PPM schemes. Generally, such modulations as OOK are fully reliable and operate at maximum transmission rate when no weather impairments occur. If now a code with a specific code rate is applied, availability improves, while the maximum achievable rate and hence the yearly average rate decreases according to the chosen code rate.

The cumulative distribution of $\tilde{R}_b$ is presented in Fig. 4.11 for selected RS coded modulations. The corresponding mean values are given in Tab. A.4. The availability for OOK and 4-PAM could not be improved because RS coding reduced the rate during nice weather (due to added redundant bits), but the coding gain was not large enough to counter deep fades during bad weather conditons. Whereas 8-PAM (with RS(255,23)) had a noticeable change in availability where $\tilde{R}_b > 1.07$ Gbps in 80% and $\tilde{R}_b > 0.66$ Gbps 90% of the time. Although additional RS coding was applied, the modulation with the highest availability is still uncoded 4-PAM. Furthermore, a high rate LDPC ($r = 9/10$) code enhances the availability (see Fig. 4.12) of 4-PAM, $\tilde{R}_b > 1.32$ Gbps in 80% and $\tilde{R}_b > 0.88$ Gbps in 90% of the time, and as well as the average throughput to 1.52 Gbps. This advancement can also be observed for 8-PAM where the availability follows to: $\tilde{R}_b > 1.41$ Gbps in 80% and $\tilde{R}_b > 0.91$

Gbps in 90% of the time. Although 8-PAM results in a high average rate, the data rate of
the link suffers from larger fluctuations as compared to OOK or PPM modulation.
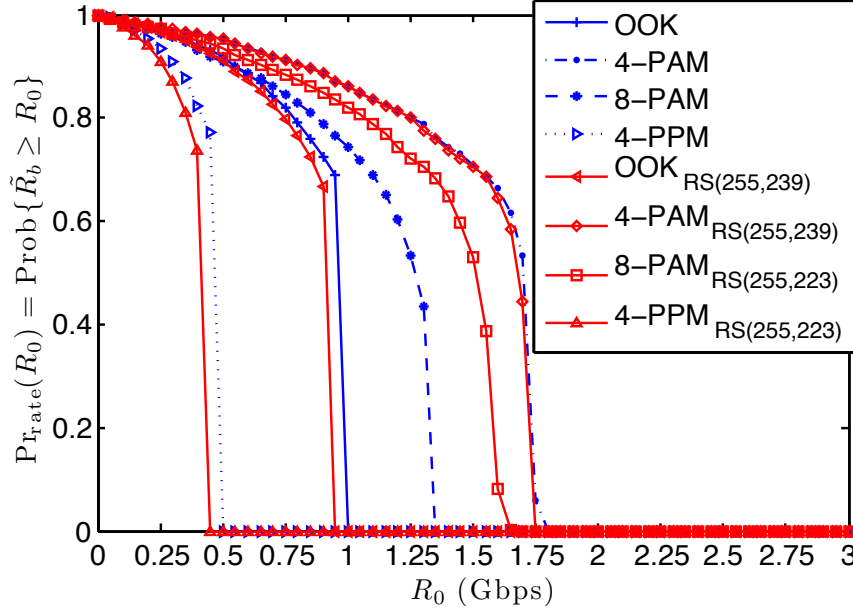
Figure 4.11: $\mathrm{Pr}_{\mathrm{rate}}(R_0)$ in (4.5) for various selected RS coded PAM and PPM schemes

Compared to uncoded schemes, additional coding reduces the outage events for all consid-
ered modulations. The mean and standard deviation of outages for the year and for selected
months is given in Tab. A.5 and Tab. 4.3, respectively. First, the influence of RS codes is
investigated. In the case of 4-PAM with RS(255,239), a mean of 4.9 and a standard devia-
tion of 5.7 can be achieved while the number of outages increased from 180 (uncoded) to 197
overall outages. This curious outcome is explained as follows. Channel coding enables the
communication system in some hours during one long outage event. As a result, the long
outage event splits into one or several smaller outages. This explanation is confirmed by
the decreasing mean and standard deviation compared to uncoded 4-PAM. For OOK, also
improvements are noticeable (mean $= 5.3$, std. dev. $= 5.6$, number of out. $= 151$) while the
decrease in data rate has to be kept in mind. The higher coding gains of LDPC codes are
also remarkable in terms of outages.

The mean and standard deviations for coded modulations are 4-PAM$_{LDPC(9/10)} = 5.18/5.87$,
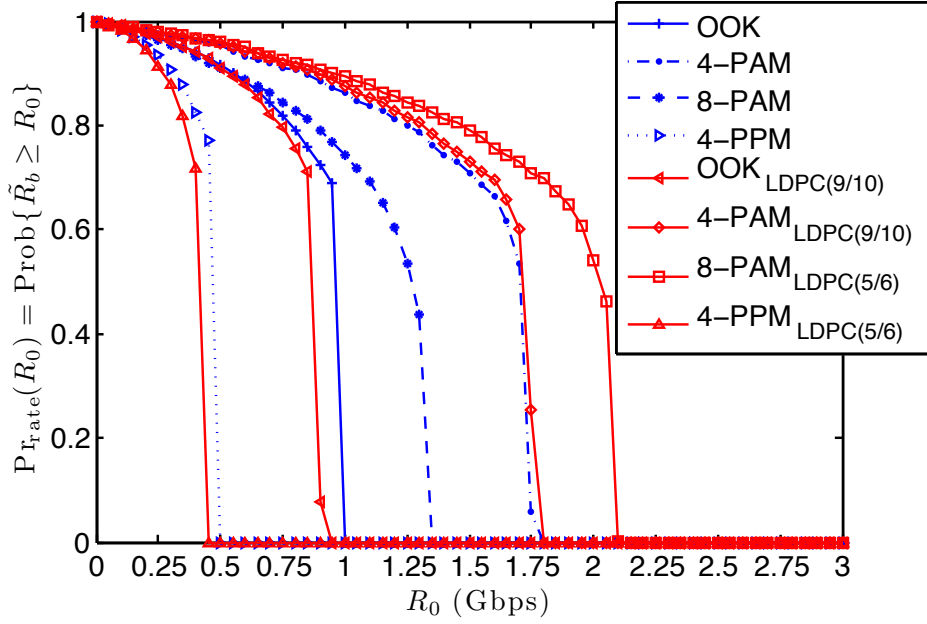
Figure 4.12: $\mathrm{Pr_{rate}}(R_0)$ in (4.5) for various selected LDPC coded PAM and PPM schemes

8-PAM$_{LDPC(5/6)}$ = 5.36/6.22 and 4-PPM$_{LDPC(5/6)}$ = 4.84/4.97, respectively. The maximum outage (max. out.) length of 4-PAM is 31 hours and the number of outages became to 170. The maximal outage length is still in the range of tolerance. Furthermore, 8-PAM with a code rate $r = 5/6$ has a maximal outage length of 36 hours in February. This may become critical in terms of link unavailability and is considered as unusable in this month. However in other months, 8-PAM has smaller outage lengths and less overall outages. Due to its high data rate support, it may also considered as a suitable modulation scheme for latency tolerant traffic transport. With coding, PPM can be made even more robust, but at the cost of data rate. The mean and standard deviation is 4.8/4.5 and the maximal outage length and the entire number of outages follow to be 24/147.

As it was presented in the previous two sections, OOK, 4-PAM and 8-PAM are possible candidates to increase throughput of latency tolerant traffic. Especially LDPC coded 4-PAM had a high average rate of 1.51 Gbps while outages are still tolerable. An extension for this application would be to use higher PAM modulations in the summer where less outages occur while in the winter the link is fixed switched to a PPM scheme to mitigate stronger

attenuation effects.

Table 4.3: Outage metrics in hours of $\mathrm{Pr_{out}}$ (hours) per month, $z = 1$ km)

Outage metrics / Modulation	mean	maximal outage event	number of outages
RS coded	August		
OOK 239/255	2	2	1
4-PAM 239/255	2	2	1
8-PAM 223/255	1.5	2	2
16-PAM 191/255	2	3	2
4-PPM 223/255	2	2	1
LDPC coded			
OOK 9/10	2	2	1
4-PAM 9/10	2	2	1
8-PAM 5/6	2	2	1
16-PAM 2/3	2	2	1
4-PPM 5/6	2	2	1
RS coded	December		
OOK 239/255	4.6	22	37
4-PAM 239/255	5.2	28	37
8-PAM 223/255	5.2	31	50
16-PAM 191/255	6.5	33	46
4-PPM 223/255	3.9	19	40
LDPC coded			
OOK 9/10	4.2	18	37
4-PAM 9/10	4.9	28	36
8-PAM 5/6	5.0	30	40
16-PAM 2/3	5.1	31	39
4-PPM 5/6	3.8	14	33

5 Adaptive Communication in FSO

In Chapter 4, the idea of using FSO links for latency tolerant traffic application was presented. It was shown that usually not considered bandwidth efficient PAM modulation schemes, such as 4-PAM, outperform conventionally used schemes in terms of throughput, especially during nice weather conditions. By contrast, PPM modulations are tolerant against atmospheric turbulence effects but provide lower data rates. For instance, average throughput can be improved by switching between different modulation schemes depending on the channel condition, what is called *adaptive modulation* (AM). Such a technique is, for example, specified in the new satellite communication standard [60]. Adaptive modulation is only one possibility in the wide field of application of adaptive communication. By using channel side information sent over a feedback path, different parameters of the transmitter can be modified, such as transmitting power, transmission rate, constellation size, coding rate/scheme, modulation scheme or any combination of these parameters. However, current commercial systems use fixed modulations and do not consider any adaptive scheme mentioned above. Adaptive communication for FSO is a relatively unexplored topic. Recently, first steps have been done to mitigate scintillation issues by using rateless coding [58] and adaptive coded modulation [68] (ACM). In this chapter, two adaptive schemes are presented and refined to simplify the implementation and to diminish the system complexity. First, a simple adaptive modulation (variable rate) system is discussed in Sec. 5.1. An adaptive coded modulation technique follows in Sec. 5.2. The main goal of these adaptive schemes is to increase data rates by efficiently exploiting the available channel capacity while keeping the reliability as high as possible.

5.1 Adaptive Modulation

In todays communication applications there is an increasing demand on data rates while bandwidth limitations still apply. To satisfy these desires, communication systems need to become more spectrally efficient to exploit the channel capacity without using more bandwidth. As mentioned before, different parameters of the transmitter can be modified in order to improve the spectral efficiency. Previously, variable power and variable rate techniques [69] were considered in wireless RF communication applications. Here, power and constellation size is varied according to the actual fading level to achieve a certain bit error limit while improving the spectral efficiency. These techniques can be applied to FSO systems. As the system should be kept practicable and simple, a constant power, variable data rate design is investigated in this work to improve throughput. Consequently, the considered design only changes the constellation size of the modulation scheme while the bandwidth R_{rect} is still fixed. The AM communication model is presented in Fig. 5.1. Several solutions are obtained
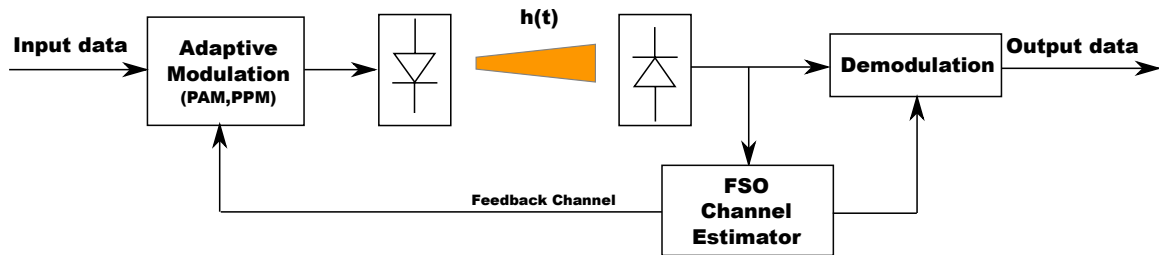
Figure 5.1: Adaptive modulation system model with feedback channel

for the feedback channel. FSO links usually have on either end both a transmitter and a receiver, so they can communicate with each other in both directions. This is called a *full duplex* system. As a consequence, the system itself can be used to send feedback information. However, in the case of atmospheric turbulence where outages disturb the communication link before the system can adapt to the conditions, feedback can be unfavorable. Link instability is the consequence. RF backup links are sometimes coupled with FSO systems and may also be a suitable candidate to deliver feedback information to the transmitter. The third option is to use existing wired cables in combination with FSO links. Some kind of wired network is often available and has high reliability in terms of data transmission. Due to

the lack of evaluation of the mentioned feedback paths for FSO links, it is hard to select the solution which results in the best performance. Thus, no specific feedback channel is chosen in this work but it is assumed that at least one is available. First, the channel estimator estimates the channel condition. Then, this estimate is transmitted over the feedback channel. It is assumed that the feedback path doesn't introduce errors which is assured by the use of an ARQ transmission protocol [69]. After extracting the channel state information out of the received packets, a decision on the modulation type and constellation size is made. The restricted modulation schemes, discussed in Sec. 4.2, are M-PAM and M-PPM. By using these two schemes, there is only a minor increase in system complexity because M-PPM is just coded 2-PAM. The benefit by using the additional M-PPM scheme lies in errorless transmission in low SNR conditions, where M-PAM schemes are not reliable. Notice that with increasing size M of PAM there is an increase in data rate as well as an increase of the required SNR to achieve a certain BER limit. In the case of M-PPM, data rate and the required SNR for a certain BER limit decreases with increasing constellation size M.

5.1.1 Adaptive System Modeling

The following section deals with the design of the adaptive modulation model. First, the constellation sizes are restricted to $M_{\mathrm{PPM},j} = 2^{N_{\mathrm{PPM}}+1-j}$, $j = 1, 2, \ldots, N_{\mathrm{PPM}}$ for PPM signals, to $M_{\mathrm{PAM},j} = 2^{j-N_{\mathrm{PPM}}}$, $j = N_{\mathrm{PPM}} + 1, N_{\mathrm{PPM}} + 2, \ldots, N_{\mathrm{PPM}} + N_{\mathrm{PAM}}$ for PAM signals and for no data transmission $M_{\mathrm{off},j}$, $j = 0$. Summarized, this equals to $M_j =:$ $\{M_{\mathrm{off},j}, M_{\mathrm{PPM},j}, M_{\mathrm{PAM},j} : j = 0, 1, \ldots, N\}$, where $N = N_{\mathrm{PPM}} + N_{\mathrm{PAM}}$.

Consider now the time-discrete channel model given in Sec. 2.2. The instantaneous SNR is obtained to $\Gamma = (PRh)/\sigma$, where h is estimated at every multiple of T_{est} (time of the adaptation interval). Assume the estimated channel state $\hat{h}$, the estimated received SNR follows as $\hat{\Gamma} = (PR\hat{h})/\sigma$. Furthermore, perfect channel estimation and a delay free feedback is assumed. For every SNR value, the constellation M_j, which correspondents on the highest capacity, has to be chosen to achieve a BER requirement $\mathrm{BER} < \mathrm{BER}_0$, where BER_0 is a specified bit error target. As a consequence, the SNR is quantized into $N+1$ intervals. Their range is defined from 0 to ∞. The borders of these SNR regions $\mathrm{SNR}_{0,j}$ are determined for all M_j, so they satisfy $P_b(\mathrm{SNR}_{0,j}) = \mathrm{BER}_0$, where P_b is the BER equation for PAM

Table 5.1: Percentage of time of used modulation scheme (AM) over the year

Modulation	64-PPM	32-PPM	16-PPM	8-PPM	4-PPM	2-PPM	link-off
%	0.68	0.7	0.88	1.01	1.79	1.84	6.3
Modulation	OOK	4-PAM	8-PAM	16-PAM	32-PAM	64-PAM	-
%	27.45	**41.8**	15.4	1.77	0.07	0.00	-

and PPM given in [24]. The actual constellation M_j is determined by finding j such that $\mathrm{SNR}_{0,j} \leq \hat{\Gamma} < \mathrm{SNR}_{0,j+1}$ is satisfied. This rule guarantees that a certain bit error probability or higher is achieved during communication, excluded the case that no constellation can fulfill the latter statement.

5.1.2 Simulation of the Adaptive Modulation Scheme

The system parameters stay the same as mentioned in Sec. 4.2. The BER limit is first set to $\mathrm{BER}_0 = 10^{-6}$. In order to limit the calculation requirements to simulate the general case, where infinity constellation points (M_j) are existing, the signal set was restricted first to $\{M_j : j = 0, 1, \ldots, 16\}$ with $N_{\mathrm{PPM}} = N_{\mathrm{PAM}} = 8$. This results in the largest possible constellation to 65536-PAM and to 65536-PPM. The channel estimate T_{est} is determined every 10 ms by simulation and fed back to the transmitter. In a look-up table, modulation scheme and order are stored togehter with the according BER limits. So, the modulator and demodulator can adapt to the current channel condition. To evaluate the performance, this scheme is compared to *non*-adaptive maximizing modulation schemes given in Sec. 4.2 with the difference that this system increases the rate while keeping the reliability higher. First, AM was compared in terms of available data rates as shown in Fig. 5.3. As it may be in evidence by intuition, that AM has a higher mean rate than all other schemes and has the lowest outage events. Compared to uncoded 4-PAM, AM has an increased averaged throughput of 1.67 Gbps. In 80% of the time, a data rate of $\tilde{R}_b > 1.44$ is available. By changing $\mathrm{BER}_0 = 10^{-3}$, the system operates closer to the channel capacity. Hence, average data rates ($\bar{R}_b = 1.92$ Gbps) and availability ($\tilde{R}_b > 1.66$ in 80% of the time) increased. Notice that this lower BER also implicates higher sensitivity, if only imperfect channel estimation is provided. Here, the

quantity of constellation sizes was reduced for a more practical implementation. The amount of time when a modulation scheme was in use is presented in Tab. 5.1 for unreduced AM. The table includes only schemes up to a maximum of 64 constellation points since higher constellation schemes are hardly selected. In 84% of the time, OOK, 4-PAM and 8-PAM were considered while in 6.6 % the link is not available. The modulation 8-PAM operates only under nice weather conditions, while OOK is primarily selected if light attenuation occurs. In moderate attenuation conditions, PPM schemes are power efficient enough to operate with low bit error rates. During dense fog and heavy snow fall, high data rates are not achievable anymore. Hence, the use of high order PPM schemes is unuseful and also impractical. As a consequence of the outcome presented in Tab. 5.1, OOK, 4-PAM and 8-PAM are chosen for high throughput and 4-PPM and 32-PPM are taken to deal with moderate attenuations. Hence, the system reduces the amount of modulation schemes to only a number of *five*. Considering Fig. 5.3, adaptive modulations with the selected schemes (AM-S) for $\text{BER}_0 = 10^{-3}, \text{BER}_0 = 10^{-6}$ have neglectable degradation in link performance compared to AM.

In addition, the information rate curve of AM-S ($P_b = 10^{-6}$), together with information rate curves for each individual selected modulation for $R_{rect} = 1$ Gbps, is plotted in Fig. 5.2. Also, the SNR value at which uncoded transmission achieves $P_b = 10^{-6}$ is indicated. The information rate curve of AM-S correspondents to some kind of a step function. Whenever the SNR gets smaller than the lower SNR region limit, the curve makes a jump down to the next "more tolerant" modulation and jumps up if the SNR is greater than the upper limit. This results in an always higher BER rate than BER_0, and in better utilization of the capacity compared to use one fixed modulation.

The amount of outages in AM is controlled by using the most reliable modulation scheme. In the case of AM-S, this scheme is 32-PPM with a $P_b = 10^{-6}$ at SNR = 38.63 dB. If the SNR is below this value, the link is not available. The mean, 4.15, and standard deviation, 4.58, of the years outage behavior for AM and AM-S (for both BER_0 10^{-3} and 10^6) are approximately the same. Consequently, in order to reduce outages, a higher PPM scheme with less throughput but more robustness must be considered in modeling practical AM. However, during strong link attenuations, as already discussed, no signal is able to be received
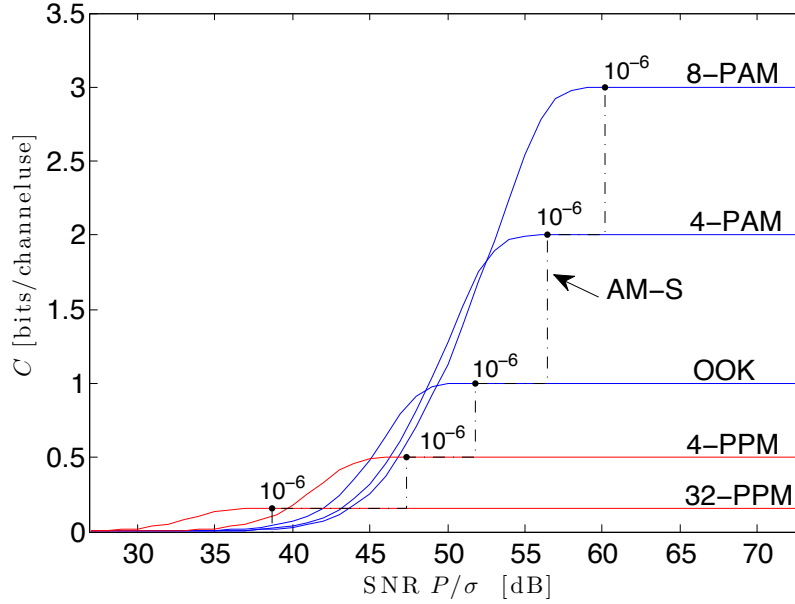
Figure 5.2: Information rate curves for various modulation schemes

and the link is not available.

5.2 Adaptive Coded Modulation

In Chapter 5.1, an adaptive modulation scheme was proposed to increase data throughput. As it was illustrated in Fig. 5.2, the available capacity was better utilized by AM compared to only one fixed modulation. Nevertheless, the information rate of AM has still some room for improvement. The maximum achievable rate for the given input distributions of M-PAM and M-PPM, respectively, is to switch to a modulation scheme with the highest information rate for a given SNR and to apply channel coding to achieve this rate. In any adapting interval, the selection of the modulation constellation and the code rate is repeated. In this thesis, this scheme is defined as *adaptive coded modulation* (ACM). In wireless channels, ACM is utilized to enable robust and spectrally efficient high data rate transmission over time-varying and fading channels [70]. ACM has been recently proposed [68] to combat strong atmospheric turbulence in free space optical channels. In simulation it was shown that the proposed adaptive LDPC-coded modulation can tolerate deep fades of the order of
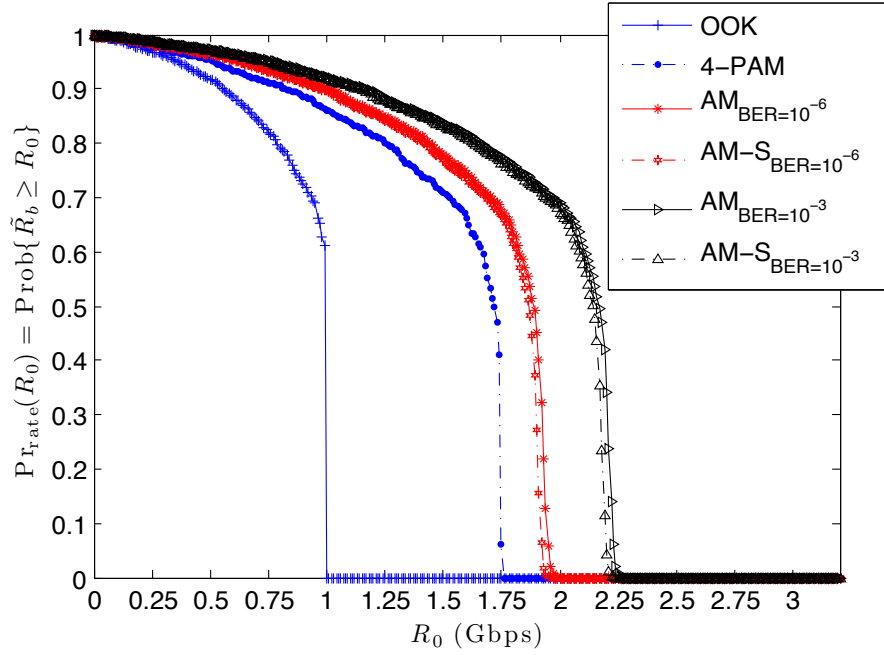
Figure 5.3: Cumulative distribution of $\tilde{R}_b$ in (4.5) of AM

30 dB. An RF feedback channel has been utilized to feed the channel estimate back to the transmitter for the necessary adaptation relative to the channel conditions.

In this work, the design of the ACM system differs from that in [68] as here the channel code rates are variable and are selected according to SNR and used modulation type. Furthermore, not only scintillation induced fading but also atmospheric attenuators are considered in the evaluation. The goal of this design is to improve data rates with reasonable increase in system complexity and price, so the enhanced system can be implemented in current developing terrestrial FSO systems.

5.2.1 Adaptive Coded Modulation Model

Consider the communication model in Fig. 5.4. The designed adaptive coded modulation system uses LDPC codes, owing to their high coding gain, in combination with adaptive modulation. The suggested design adapts both, the modulation and the code rate. In order to determine both parameters, the modulation scheme with the highest information rate for the instantaneous estimated SNR $\hat{\Gamma}$ is utilized. For example, in Fig. 5.2 the maximizing
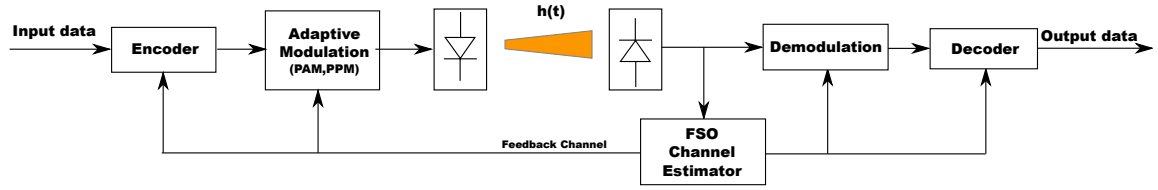
Figure 5.4: Adaptive coded modulation system model with a feedback channel

modulation scheme for SNR = 55 dB is 8-PAM with an information rate of around 2.5 bit/T and a code rate $r = 2.5/3 = 0.8\dot{3}$. Because only a discrete set of LDPC codes is available, the code rate in the discrete set is used which is closest and which is smaller to the one calculated. Discrete code alphabet sets and practical limitations of decoders require the use of additional link margins. As indicated by simulations, an additional SNR margin of 0.9 dB is suitable to operate with low transmission errors. In Fig. 5.4, the proposed ACM model is presented. The channel estimation is repeated at an interval of T_{est} and fed back to the transmitter. According to the selected code rate, the information is encoded and cached in a buffer. From the buffer $\log_2(M_j)$ bits are taken to choose a corresponding constellation point. The modulated data is then transmitted over the atmosphere. At the receiver, soft information is extracted from the received signal and sent to the LDPC decoder.

	AM	AM-S	AM	AM-S	ACM	ACM-S
BER_0	10^{-3}	10^{-3}	10^{-6}	10^{-6}	-	-
avg. R_b	1.92	1.89	1.67	1.65	2.6	2.5
$> 80\%$	1.66	1.64	1.44	1.42	2.26	2.21
$> 90\%$	1.17	1.15	1.01	0.99	1.6	1.58
mean/std.dev.	4.18/4.6	4.18/4.6	4.15/4.58	4.15/4.58	4.15/4.54	4.15/ 4.57

Table 5.2: Summary of different metrics for AM and ACM schemes

5.2.2 Simulation of the Adaptive Coded Modulation Scheme

In this section, the performance of ACM is evaluated with the help of computer simulations. The system is restricted to $\{M_j : j = 0, 1, \ldots, 12\}$ with $N_{PPM} = N_{PAM} = 6$ (constellations from 64-PPM to 2-PPM and OOK to 64-PAM) and LDPC code rates form 1/2 to 9/10.

Again, the channel estimate procedure is repeated in an interval of $T_{est} = 10$ ms. With ACM, the average throughput of the year had an increase of approximately 35% to 2.6 Gbps against uncoded AM and a boost of 220% compared to standard OOK. The availability $\tilde{R}_b$ is greater or equal to 2.26 Gbps in 80% of the time (see Fig. 5.5). The outage improved to 4.1/4.3 for a yearly mean and standard deviation as a result of the additional coding gain for high order PPM schemes. In Tab. 5.2.1 the most important metrics are summarized for AM and ACM. The use of several different code rates increases the complexity of the LDPC decoder noticeable. One opportunity to keep complexity in tolerable limits would be to use the method of puncturing [71, 72]. This method is using one mother code to generate other codes with different code rates. As a consequence, the decoder must only decode codewords generated by one code. The only increase in this system is the puncturing and depuncturing algorithm. Another method used in [68, 70] is to use only one channel code. Experimentally, the code set was reduced to only one with code rate $r = 4/5$. In order to distinguish between ACM, with a code set greater than one, and ACM with just one applied error correction code, the latter scheme is named *adaptive coded modulation selection* (ACM-S). Comparing ACM with ACM-S in Fig. 5.5, the reduction in availability is negligible. This design considerably reduces system complexity as only a single code can be applied to the AM scheme to achieve a robust FSO link that operates at very high throughput. Note that the selection of just one code decreases flexibility which may result in decreased data rates if the installation location of the FSO link changes. Consequently, the optimal code rate may vary from location to location.

5.3 Practical Challenges

The previous assumption of channel estimation without delay and error is not valid in real world systems. Delay is mainly introduced by the feedback path (+ARQ) and the processing time of the channel estimation. The impact of the delay and estimation error may be most critical in atmospheric turbulence induced fading conditions since this is the most frequently changing channel factor. As discussed before, slow fading is assumed where the coherence time of scintillation induced fading is of the order of 1-100 ms. As a consequence, the time to estimate the channel state to send this information to the receiver and to optionally encode
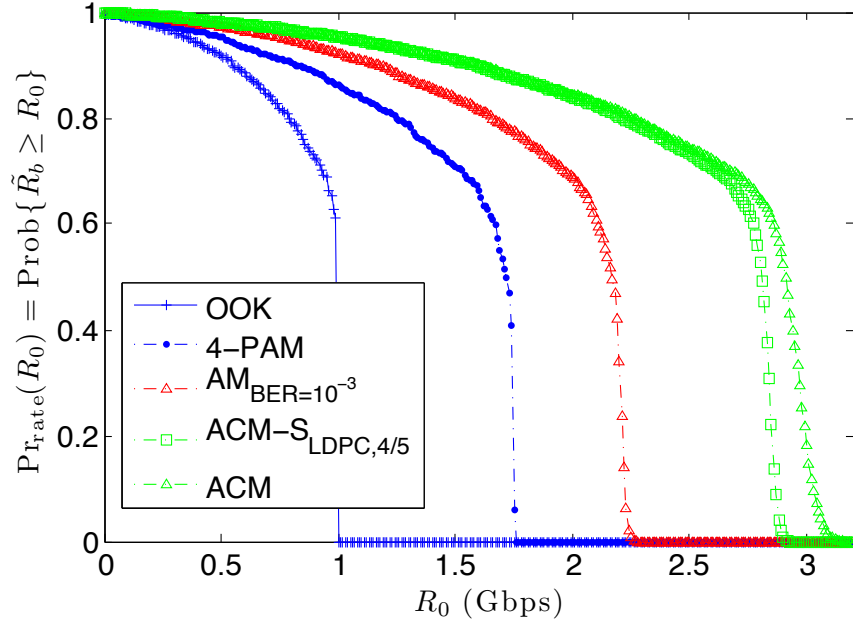
Figure 5.5: Availability comparison between AM, AM-S, ACM and ACM-S

the information bits to be sent, must be at least smaller than 1 ms. For example, the time to send optical symbols over the feedback path through a 1 km link distance takes approximately $\tau_f = 3.3\,\mu$s. Also, the time for the feedback symbols τ_s must be added to this time. For instance, if OOK, transmitting at 1 Gbps and with 32 Bits (to transmit the estimate), is used, the additional time is $\tau_s = 32 \cdot 10^{-9} = 32$ ns. Therefore, the receiver must wait a minimum of $2(\tau_f + \tau_s) = 6.664\,\mu$s to change rate and modulation type. The rest of the time ($\approx 1000\mu s - 6.7\mu s$) is left for channel estimation and encoding at the transmitter. Notice, longer codewords result in longer latency. In the case of the DVB-S2-LDPC code, where a codeword has 64800 bits, all bits must be send before a new code rate can be applied. One can assume here an minimum additional delay of 64.8 μs. A criterium to optimally estimate the channel state is given in [58]. In their paper, they determine channel state information only from received samples without any additional signaling algorithm. They also determine the optimal number of how much samples have to be observed to make an accurate decision on the channel state value. Such a technique is proposed as to be very accurate and can be used in practical FSO systems.

6 Conclusions

Popular applications such as P2P file sharing, data backup and large FTP exchanges generate a large proportion of data traffic on today's networks. This class of traffic is latency-tolerant as typical download times are on the order of days. The use of inexpensive FSO links was proposed to supplement current backhaul and provide a differentiated quality of service for these links. The use of bandwidth-efficient PAM is beneficial in the case of latency-tolerant traffic since it provides a high average rate with moderate outage periods. Thus, although 4-PAM makes the FSO link less reliable for real-time traffic, it is very well suited for latency-tolerant traffic due to its higher throughput. For a 1 km distance link, 4-PAM has an average yearly rate of 1.49 Gbps, nearly 70% higher than OOK, and an average daily throughput greater than 0.8 Gbps, 90% of the time. Average outage times are on the order of 5 hours in a year using both OOK and 4-PAM. The additional usage of FEC reduces the rate for already rate saturated schemes, as OOK or M-ary PPM, but also lowers the duration and number of outages. With LDPC codes specified in DVB-S2 standard, we achieved a higher data rate for 4-PAM up to 1.52 Gbps. The coded modulation scheme with the highest average throughput turned out to be 8-PAM with 1.76 Gbps and a daily throughput greater than 1.41 Gbps, 80% of the time. Although the rate improvement of 8-PAM is significantly high, long outage lengths and higher number of outages makes it questionable to use this scheme for latency tolerant traffic application.

The idea of throughput maximization for latency tolerant traffic was extended by introducing adaptive feedback communication techniques for all kinds of traffic. The use of adaptive modulation or adaptive coded modulation is required to counter deep fades during poor weather conditions and take advantage of the channel capacity when no channel impairments occur. The well-known fact that implementation of communication systems utilizing

feedback information increases hardware complexity, led us to keep our design simple so that it may remain practical for FSO systems under development. In the case of ACM, we restrained to a few modulation constellations and only one code was applied to all of them. This design had an improvement of 220% in average data rate compared to conventional used OOK.

Future research must consider the effects of imperfect channel estimation, as well as the delay of computing CSI and sending this information back to the transmitter. This would inevitably result in a slightly degraded system performance. One key to extend the presented results is to take real world measurements sampled every 1 ms as a basis, so that also small fading variations can be covered. A real test system should be set up. Hence, the system has to be driven using different types of feedback channels to verify the simulation results. Furthermore, the performance enhancements of LDPC coded modulations should be evaluated by implementing this technique in a real world system. Such communication systems are often just simulated, but are usually not tested in practice.

Bibliography

[1] I. I. Kim, B. McArthurand, and E. Korevaar, "Comparison of laser beam propagation at 785 nm and 1550 nm in fog and haze for optical wireless communications," *Proc. SPIE*, vol. 4214, pp. 26–37, Feb. 2001.

[2] I. I. Kim, E. L. Woodbridge, V. J. Chan, and B. R. Strickland, "Scintillation measurements performed during the limited-visibility lasercom experiment," vol. 3266, pp. 209–220, SPIE, 1998.

[3] J. Kahn and J. Barry, "Wireless infrared communications," *Proceedings of the IEEE*, vol. 85, pp. 265 –298, feb 1997.

[4] C. Chlestil, E. Leitgeb, N. Schmitt, S. Sheikh Muhammad, K. Zettl, and W. Rehm, "Reliable optical wireless links within UAV swarms," in *Transparent Optical Networks, 2006 International Conference on*, vol. 4, pp. 39 –42, 18-22 2006.

[5] M. Toyoshima, Y. Takayama, T. Takahashi, K. Suzuki, S. Kimura, K. Takizawa, T. Kuri, W. Klaus, M. Toyoda, H. Kunimori, T. Jono, and K. Arai, "Ground-to-satellite laser communication experiments," *Aerospace and Electronic Systems Magazine, IEEE*, vol. 23, pp. 10 –18, aug. 2008.

[6] A. Alonso, M. Reyes, and Z. Sodnik, "Performance of satellite-to-ground communications link between artemis and the optical ground station," vol. 5572, pp. 372–383, SPIE, 2004.

[7] S. Betti, V. Carrozzo, and E. Duca, "Optical intersatellite system based on DPSK modulation," in *Wireless Communication Systems, 2005. 2nd International Symposium on*, pp. 817 –821, 7-7 2005.

[8] fSONA Networks Corp. , "fSONA datasheets [online]." `http://www.fsona.com`, last checked: Jul. 2010.

[9] MRV Communications , "MRV datasheets [online]." `http://www.mrv.com`, last checked: Jul. 2010.

[10] E. Ciaramella, Y. Arimoto, G. Contestabile, M. Presi, A. D'Errico, V. Guarino, and M. Matsumoto, "1.28 Terabit/s (32x40 gbit/s) WDM transmission system for free space optical communications," *Selected Areas in Communications, IEEE Journal on*, vol. 27, pp. 1639 –1645, december 2009.

[11] International Telecommunication Union, "VDSL2 [online]." `http://www.itu.int`, last checked: Jul. 2010.

[12] Telekom Austria GmBH, "Gigaspeed Internet [online]." `http://www.telekom.at`, last checked: Jul. 2010.

[13] UPC, "Cable Internet [online]." `http://www.upc.at/internet/`, last checked: Jul. 2010.

[14] Motorola, "PTP 300 Series data sheet." `http://http://motorola.com`, last checked: Dec. 2010.

[15] Lightpointe Inc., "Lightpointe FSO datasheets [online]." `http://www.lightpointe.com`, last checked: Jul. 2010.

[16] F. Nadeem, V. Kvicera, M. Awan, E. Leitgeb, S. Muhammad, and G. Kandus, "Weather effects on hybrid FSO/RF communication link," *Selected Areas in Communications, IEEE Journal on*, vol. 27, pp. 1687 –1697, december 2009.

[17] H. Willebrand and B. Ghuman, "Fiber optics without fiber," *Spectrum, IEEE*, vol. 38, pp. 40 –45, aug 2001.

[18] Canon Inc., "Canobeam dt-130 datasheet [online]." `http://www.tessco.com`, last checked: Jul. 2010.

[19] P.-L. Chen, S.-T. Chang, S.-T. Ji, S.-C. Lin, H.-H. Lin, H.-L. Tsay, P.-H. Huang, W.-C. Chiang, W.-C. Lin, S.-L. Lee, H.-W. Tsao, J.-P. Wu, and J. Wu, "Demonstration of 16 channels 10 GB/s WDM free space transmission over 2.16 km," in *IEEE/LEOS Summer Topical Meetings, 2008 Digest of the*, pp. 235 –236, 21-23 2008.

[20] B. Flecker, M. Gebhart, E. Leitgeb, and S. S. Muhammad, "Results of attenuation measurements for optical wireless channels under dense fog conditions regarding different wavelengths," *Proc. SPIE*, vol. 6303, pp. 1–11, Aug. 2006.

[21] R. Lawrence and J. Strohbehn, "A survey of clear-air propagation effects relevant to optical communications," *Proceedings of the IEEE*, vol. 58, pp. 1523 – 1545, oct. 1970.

[22] H. Park and J. Barry, "Modulation analysis for wireless infrared communications," in *Communications, 1995. ICC '95 Seattle, 'Gateway to Globalization', 1995 IEEE International Conference on*, vol. 2, pp. 1182 –1186 vol.2, 18-22 1995.

[23] S. Muhammad, T. Javornik, I. Jelovcan, E. Leitgeb, E.b, and O. Koudelka, "Reed solomon coded PPM for terrestrial FSO links," in *Electrical Engineering, 2007. ICEE '07. International Conference on*, pp. 1 –5, 11-12 2007.

[24] S. Hranilovic, *Wireless Optical Communication Systems*. New York: Springer, 2005.

[25] R. McEliece, "Practical codes for photon communication," *Information Theory, IEEE Transactions on*, vol. 27, pp. 393 – 398, jul 1981.

[26] J. Massey, "Capacity, cutoff rate, and coding for a direct-detection optical channel," *Communications, IEEE Transactions on*, vol. 29, pp. 1615 – 1621, nov 1981.

[27] J. Hamkins, "Performance of binary turbo coded 256-ary pulse position modulation," *TMO progress report 42-138*, pp. 1–15, Aug. 1999.

[28] G. Pottie, "Trellis codes for the optical direct-detection channel," *Communications, IEEE Transactions on*, vol. 39, pp. 1182 –1183, aug 1991.

[29] E. Lee and V. Chan, "Part 1: Optical communication over the clear turbulent atmospheric channel using diversity," *Selected Areas in Communications, IEEE Journal on*, vol. 22, pp. 1896 – 1906, nov. 2004.

[30] W. Popoola, Z. Ghassemlooy, J. Allen, E. Leitgeb, and S. Gao, "Free-space optical communication employing subcarrier modulation and spatial diversity in atmospheric turbulence channel," *Optoelectronics, IET*, vol. 2, pp. 16 –23, feb. 2008.

[31] I. I. Kim and E. J. Korevaar, "Availability of free space optics (FSO) and hybrid FSO/RF systems," *Proc. SPIE*, vol. 4530, pp. 84–95, Nov. 2001.

[32] E. Leitgeb, M. Gebhart, U. Birnbacher, W. Kogler, and P. Schrotter, "High availability of hybrid wireless networks," *Proc. SPIE*, vol. 5465, pp. 238–249, Apr. 2004.

[33] E. Leitgeb, S. Muhammad, B. Flecker, C. Chlestil, M. Gebhart, and T. Javornik, "The influence of dense fog on optical wireless systems, analysed by measurements in Graz for improving the link-reliability," vol. 3, pp. 154 –159, jun. 2006.

[34] ClearMesh Networks Inc., "LEDs vs. Laser Diodes for Wireless Optical Communication[online]." `http://www.clearmesh.com`, last checked: Aug. 2010.

[35] International Electrotechnical Commission, "Safety of laser products – Part 1: Equipment classification, requirements and user's guide. Group safety publication, reference number 825-1." 1993.

[36] X. Zhu and J. Kahn, "Free-space optical communication through atmospheric turbulence channels," *Communications, IEEE Transactions on*, vol. 50, pp. 1293 – 1300, August 2002.

[37] J. Proakis, *Digital Communications*. McGraw-Hill Science/Engineering/Math, 4 ed., August 2000.

[38] W. Zhang, S. Hranilovic, and C. Shi, "Soft-switching hybrid FSO/RF links using short-length raptor codes: design and implementation," *Selected Areas in Communications, IEEE Journal on*, vol. 27, pp. 1698 –1708, december 2009.

[39] D. Mandich, "A comparison between free space optics and 70 GHz short haul links behavior based on propagation model and measured data," in *Wireless Technology, 2004. 7th European Conference on*, pp. 85 – 88, 2004.

[40] E. J. McCartney, *Optics of the Atmosphere*. Wiley press, 1976.

[41] W. Popoola, Z. Ghassemlooy, M. S. Awan, and E. Leitgeb, "Atmospheric channel effects on terrestrial free space optical communication links," 2009.

[42] P. Fasser, E. Leitgeb, and T. Plank, "Optische Nachrichtentechnik - Skriptum," 2007.

[43] S. S. Muhammad, B. Flecker, E. Leitgeb, and M. Gebhart, "Characterization of fog attenuation in terrestrial free space optical links," *Optical Engineering*, vol. 46, no. 6, p. 066001, 2007.

[44] D. Atlas, "Optical extinction by rainfall," *Journal of Meteorology*, vol. 10, no. 6, pp. 486–488, 1953.

[45] H. W. O'Brien, "Visibility and light attenuation in falling snow," *Journal of Applied Meteorology*, vol. 9, no. 4, pp. 671–683, 1970.

[46] M. Awan, E. Leitgeb, R. Nebuloni, F. Nadeem, and M. Khan, "Optical wireless ground-link attenuation statistics of fog and snow conditions," in *Wireless and Optical Communications Networks, 2009. WOCN '09. IFIP International Conference on*, pp. 1 –5, 2009.

[47] L. C. Andrews and R. L. Phillips, *Laser Beam Propagation Through Random Media*. WA: SPIE, 1998.

[48] S. Karp, R. Gagliardi, S. Moran, and L. Stotts, *Optical Channels*. New York: Plenum, 1988.

[49] W. Gappmair, S. Hranilovic, and E. Leitgeb, "Performance of PPM on terrestrial FSO links with turbulence and pointing errors," *Communications Letters, IEEE*, vol. 14, pp. 468 –470, May 2010.

[50] I. S. Reed and G. Solomon, "Polynomial codes over certain finite fields," *Journal of the Society for Industrial and Applied Mathematics*, vol. 8, no. 2, pp. pp. 300–304, 1960.

[51] R. Gallager, "Low-density parity-check codes," *Information Theory, IRE Transactions on*, vol. 8, pp. 21 –28, Jan. 1962.

[52] S. S. Muhammad, T. Javornik, I. Jelovčan, Z. Ghassemlooy, and E. Leitgeb, "Comparison of hard-decision and soft-decision channel coded M-ary PPM performance over free space optical links," *European Transactions on Telecommunications*, vol. 20, 2009.

[53] S. Haykin, *Digital communications*. New York, NY, USA: John Wiley & Sons, Inc., 1988.

[54] S. Lin and D. J. Costello, *Error Control Coding, Second Edition*. Upper Saddle River, NJ, USA: Prentice-Hall, Inc., 2004.

[55] MathWorks, "Log Likelihood Calculation." `http://http://www.mathworks.com/help/toolbox/comm/ug/bqwswmc-1.html`, last checked: Dec. 2010.

[56] I. B. Djordjevic, B. Vasic, and M. A. Neifeld, "LDPC coded OFDM over the atmospheric turbulence channel," *Opt. Express*, vol. 15, no. 10, pp. 6336–6350, 2007.

[57] I. Djordjevic, S. Denic, J. Anguita, B. Vasic, and M. Neifeld, "LDPC-coded MIMO optical communication over the atmospheric turbulence channel," *Lightwave Technology, Journal of*, vol. 26, pp. 478 –487, March 2008.

[58] J. Anguita, M. Neifeld, B. Hildner, and B. Vasic, "Rateless coding on experimental temporally correlated fso channels," *Lightwave Technology, Journal of*, vol. 28, pp. 990 –1002, April 2010.

[59] C.-S. Choi and H. Lee, "High throughput four-parallel RS decoder architecture for 60GHz mmWAVE WPAN systems," in *Consumer Electronics (ICCE), 2010 Digest of Technical Papers International Conference on*, pp. 225 –226, Jan. 2010.

[60] ETSI, "Digital video broadcasting (DVB); second generation framing structure, channel coding and modulation systems for broadcasting, interactive services, news gathering and other broadband satellite applications." EN 302 307, V1. 1. 1, Jun. 2004.

[61] S.-M. Kim, C.-S. Park, and S.-Y. Hwang, "A novel partially parallel architecture for high-throughput ldpc decoder for dvb-s2," *Consumer Electronics, IEEE Transactions on*, vol. 56, pp. 820 –825, May 2010.

[62] A. A. Farid and S. Hranilovic, "Capacity bounds for wireless optical intensity channels with gaussian noise," *Information Theory, IEEE Transactions on*, vol. 56, no. 12, pp. 6066 –6077, 2010.

[63] G. Ungerboeck, "Channel coding with multilevel/phase signals," *Information Theory, IEEE Transactions on*, vol. 28, pp. 55 – 67, Jan. 1982.

[64] M. Czaputa, S. Hranilovic, and E. Leitgeb, "On the use of free-space optical links for latency-tolerant traffic applications," in *Communication Systems Networks and Digital Signal Processing (CSNDSP), 2010 7th International Symposium on*, pp. 588 –592, July 2010.

[65] Sandvine Incorporated, "Research report: 2009 Global Broadband Phenomena [online]." `http://www.sandvine.com`, last checked: Jan. 2010.

[66] R. L. Pereira and T. V. ao, "On the impact of P2P file sharing traffic restrictions on user perceived performance," *ICOIN 2008*, pp. 1–5, jan 2008.

[67] E. Canada, "National climate data and information archive [online]." `http://climate.weatheroffice.gc.ca`, last checked: Jan. 2010.

[68] I. B. Djordjevic, "Adaptive modulation and coding for free-space optical channels," *Optical Communications and Networking, IEEE/OSA Journal of*, vol. 2, pp. 221 –229, May 2010.

[69] A. Goldsmith and S.-G. Chua, "Variable-rate variable-power MQAM for fading channels," *Communications, IEEE Transactions on*, vol. 45, pp. 1218 –1230, Oct. 1997.

[70] A. Goldsmith and S.-G. Chua, "Adaptive coded modulation for fading channels," *Communications, IEEE Transactions on*, vol. 46, pp. 595 –602, May 1998.

[71] E. Choi, S.-B. Suh, and J. Kim, "Rate-compatible puncturing for low-density parity-check codes with dual-diagonal parity structure," in *Personal, Indoor and Mobile Radio Communications, 2005. PIMRC 2005. IEEE 16th International Symposium on*, vol. 4, pp. 2642 –2646 Vol. 4, 2005.

[72] M. Smolnikar, T. Javornik, M. Mohorcic, S. Papaharalabos, and P. Mathiopoulos, "Rate-compatible punctured DVB-S2 LDPC codes for DVB-SH applications," in *Satellite and Space Communications, 2009. IWSSC 2009. International Workshop on*, pp. 13 –17, 2009.

[73] MathWorks, "Matlab [online]." `http://www.mathworks.com`, last checked: Dec. 2010.

A Basic Simulation Results

This section provides basic results used for analysis in Chapter 4. A short description for this material is given in the following paragraph. Table A.1 presents values instead of graphical points as shown in Fig. 4.4. In this table, the yearly average data rate is given for selected modulation schemes and various link distances. Related outage metrics, such as the mean, the standard deviation (std. dev.), the maximum outage duration (max. out.) and the number of outages (number of out.) for a year are given in Tab. A.2. An outage occurs if the hourly data rate falls below a specified data rate limit R_{limit}. In this case, the limit is $R_{limit} = 100$ MBit/s. For example, OOK has a mean and a std. dev. of 5.31/5.74, a longest outage event of 30 hours and a total number of outages (containing every event of outages) of 157. In Tab. A.3 the mean and the standard deviation of outages of some modulation schemes are given for all months. The columns a refer to the mean outage and columns b refer to the standard deviation per month. The average yearly rate for coded PAM modulations and a 1 km link distance is given in Tab. A.4. The first column represents the used code rate. Outage metrics for coded modulation are given in Tab. A.5.

Table A.1: Average rate per year (Gbps)

Modulation / Link distance	200 m	500 m	1000 m	2000 m
64-PAM	**5.65**	0.14	0.001	0.001
32-PAM	4.8	2.16	0.031	0.007
16-PAM	3.66	**3.43**	0.31	0.03
8-PAM	2.9	2.73	1.10	0.1
4-PAM	1.96	1.86	**1.49**	0.25
OOK	0.98	0.95	0.88	**0.38**
2-PPM	0.49	0.47	0.45	0.24
4-PPM	0.49	0.48	0.45	0.32
8-PPM	0.37	0.36	0.34	0.29
16-PPM	0.25	0.24	0.23	0.21
32-PPM	0.16	0.15	0.14	0.13
64-PPM	0.09	0.09	0.09	0.08

Table A.2: Mean and standard deviation of in hours of Pr_{out} (hours) per year ($z = 1$ km)

Outage metrics / Modulation	mean	std. dev.	max. out.	number of out.
64-PAM	n.d.	n.d.	n.d.	n.d.
32-PAM	n.d.	n.d.	n.d.	n.d.
16-PAM	5.32	6.6	37	265
8-PAM	5.54	6.52	37	215
4-PAM	5.19	5.87	31	180
OOK	5.31	5.74	30	157
2-PPM	5.28	5.49	28	148
4-PPM	4.93	5.05	24	150
8-PPM	4.6	4.81	24	149
16-PPM	4.6	4.81	24	149
32-PPM	4.18	4.60	23	141
64-PPM	n.d.	n.d.	n.d.	n.d.

Table A.3: Mean and standard deviation of in hours of Pr_{out} (hours) per month ($z = 1$ km)

Modulation / Month	OOK		4-PAM		8-PAM		16-PAM		4-PPM	
	a	b	a	b	a	b	a	b	a	b
Jan.	5.9	5.2	5.6	5.6	5.55	5.59	5.2	5.2	4.7	5.2
Feb.	6.5	6.8	6.3	6.7	6.26	6.74	7.0	6.9	6.2	6.5
Mar.	5.1	5.1	5.2	5.0	5.2	5.01	5.2	5.3	4.2	4.7
Apr.	5.0	4.0	4.5	3.9	4.5	3.91	5.0	4.1	4.2	4.1
May	7.0	2.8	7.3	2.6	7.3	2.62	7.0	2.8	6.0	3.0
Jun.	3.6	4.7	6.3	8.0	6.2	8.0	3.6	4.7	5.0	5.0
Jul.	4.0	1.0	4.5	0.5	4.5	0.5	4.0	1.0	4.0	1.0
Aug.	2.0	0.0	1.5	0.5	1.5	0.5	2.0	0	2.0	0
Sep.	1.8	1.2	1.8	1.1	1.8	1.1	1.8	1.2	3.0	1.0
Oct.	0.0	0.0	0.0	0.0	0.0	0.0	0	0	0	0
Nov.	4.6	4.2	4.0	4.8	4.0	4.8	4.0	3.2	3.8	3.3
Dec.	5.3	6.8	5.6	6.9	5.6	6.9	4.3	4.4	4.1	4.0

Table A.4: Average rate per year with channel coding for 1 km link distance (Gbps)

Modulation / Code	OOK	4-PAM	8-PAM	16-PAM	32-PAM	64-PAM
RS						
239/255	0.83	1.47	1.25	0.44	0.06	0.00
223/255	0.78	1.41	1.32	0.53	0.08	0.00
191/255	0.67	1.24	1.29	0.63	0.12	0.01
127/255	0.45	0.85	0.99	0.61	0.17	0.02
LDPC						
9/10	0.81	1.52	1.71	0.99	0.25	0.02
8/9	0.80	1.51	1.73	1.02	0.27	0.03
5/6	0.75	1.40	1.77	1.26	0.43	0.07
4/5	0.72	1.39	1.76	1.56	0.56	0.10
3/4	0.68	1.31	1.73	1.50	0.74	0.18
2/3	0.60	1.17	1.6	1.60	1.03	0.35
3/5	0.54	1.05	1.46	1.56	1.01	0.5
1/2	0.45	0.89	1.28	1.49	1.39	0.97

Table A.5: Outage metrics of coded modulations in hours of $\mathrm{Pr_{out}}$ per year ($z = 1$ km)

Outage metrics / Modulation	mean	std. dev.	max. out.	number of out.
RS coded				
OOK 239/255	5.3	5.6	29	151
4-PAM 239/255	4.9	5.7	31	197
8-PAM 223/255	5.6	6.5	37	149
16-PAM 191/255	5.4	6.5	37	241
32-PAM 127/255	n.d.	n.d.	n.d.	n.d.
64-PAM 127/255	n.d.	n.d.	n.d.	n.d.
LDPC coded				
OOK 9/10	5.3	5.4	28	148
4-PAM 9/10	5.2	5.9	31	170
8-PAM 5/6	5.4	6.2	36	203
16-PAM 2/3	5.7	6.6	37	202
32-PAM 1/2	5.7	6.6	37	202
64-PAM 1/2	5.5	6.6	37	221
4-PPM 5/6	4.8	4.5	24	147

B Simulation Programs in Matlab

Most of the work in this thesis was based on simulations which were developed and performed in using a numerical mathematic program, called Matlab [73]. The type of programs range from calculating BER, SER rates for coded/uncoded modulation schemes, data rates simulations, outage and availability calculations to extraction of different types of measured system data. In the following sections a selection of the most important Matlab codes are given for examination.

B.1 Bit error and symbol error curves

BER, SER for uncoded M-PAM

```
    %--- Theoretical and simulated SER and BER results of M-PAM modulation schemes ---
%Choose N for the number of sent symbols (effects the calulation time).
%Choose M (only even) for the modulation order and the symbol rate Rs. If a specific
%bit rate is needed comment Rs line and uncomment Rb line. The constants
%xmin and ymin are the limits of the plot.
%It is a must to include the UsedFunctions folder as a Matlab path !!!
%With *** marked code lines could/should be changed by the user to
%simulated different systems.

%-----------------------------------------%
% Author: Martin Czaputa
% email: martin.czaputa@gmail.com
% version 1.0
% last modified: 29.Jul.2010
% -----------------------------------------%
addpath('/Users/fraggle/Documents/MATLAB/MatlabWork_2010_06_13/UsedFunctions')
clear all; clc;

%--- Initialize needed parameters
N = 10^2;     %number of transmitted symbols ***
M = 16;       %modulation order M-PAM ***
k = log2(M);  %transmitted bits per symbol
P = 1;        %average transmitted power ***
Rs = 10^9; Ts = 1/Rs; Rb = Rs*k; Tb = 1/Rb; %symbol rate, symbol duration,
%bit rate, bit duration ***

%--- Define SNR and calculate n_sigma
xmin = 40; xmax = 70;   %limits of SNRdB plot ***
SNRdB = [xmin:1:xmax];      %10*log((P*sqrt(T))/sigma)
SNR = 10.^(SNRdB/10);     %SNR = (P*sqrt(R))/sigma
n_sigma = P./SNR;        %std. dev. of used AWGN noise

%--- Define M-PAM constellation
mpam = [0:M-1];                       %set PAM symbols
pamnorm = 2*P*sqrt(Ts)/(M-1);         %normalize symbols to satisfy the eye safety
%constraint to E{x}=<P where x are sent symbols
gray_pam = bitxor(mpam,floor(mpam/2));  %connection between normal symbols and
%gray coded symbols
[tt ind] = sort(gray_pam);

%--- Bit to symbol generation
xBit = rand(1,N*k,1)>0.5;                  %random 1's and 0's
bin2DecMatrix = ones(N,1)*(2.^[(k-1):-1:0]) ; %conversion from binary to decimal
xBitReshape =  reshape(xBit,k,N).';          %grouping to N symbols having k bits each

xDec = [sum(xBitReshape.*bin2DecMatrix,2)].'; %decimal to binary
xGrayDec = bitxor(xDec,floor(xDec/2));       %decimal to gray decimal
x = xGrayDec*pamnorm;

for i=1:length(SNR)
    %--- transmission over AWGN channel
    n = n_sigma(i)*randn(1,N);  %white guassian noise, 0dB variance
    y = x + n;                  % channel model, AWGN
```

```
    %--- Demodulation
    x_rec = round(y/pamnorm); %need to rescale to demodulate

    %--- allocate recieved symbols to symbol alphabet, matched filter
    % and threshold detector
    x_rec(find(x_rec > max(mpam))) = max(mpam);
    x_rec(find(x_rec < min(mpam))) = min(mpam);

    %--- convert symbols to decimal
    x_recDec = ind(x_rec+1)-1;

    %--- convert decimal to bin_str to bin_num
    x_recBit = dec2bin(x_recDec).';
    x_recBit = x_recBit(1:end).';
    x_recBit = str2num(x_recBit)';

    %--- determine symbol and bit errors
    errors_bit(i) = sum(abs(xBit-x_recBit)>0);
    errors_sym(i) = sum(abs(xDec - x_recDec)>0);

end

%--- actual simulated BER and SER vector for different SNR values
P_ber_sim = errors_bit/(N*k);    %bit errors divided by sent bits
P_ser_sim = errors_sym/N;        %symbol errors divided by sent smbols

%theoretical bit error and symbol error curves
for i = 1:length(SNR)
    P_ber_theo(i) = Pe_bit_mpam_nB(Rb,M,SNR(i));
end
Pser_rs = zeros(1,length(SNR));
for i = 1:length(SNR)
    P_ser_theo(i) = Pe_sym_mpam_nB(Rs,M,SNR(i));
end


%------------ Plotting analytically and statistically calculated BER,SER-----
%------------------------- curves against SNRdB -----------------------------
figure
semilogy(SNRdB, P_ber_sim, '-+k')
hold on
semilogy(SNRdB, P_ber_theo)
hold off
legend([num2str(M) 'PAM_{estimated}'],[num2str(M) 'PAM_{analy}'])
xlabel('SNRdB in P/sqrt(R_{bit}) to \sigma ')
ylabel('BER')
titlestring{1} = 'The figure shows the bit error rate for ';
titlestring{2} = [num2str(M) 'PAM and the estimated once plotted against optical SNR'];
title(titlestring)
axis([xmin, xmax, 10^(-6), 1])
grid on

figure
semilogy(SNRdB, P_ser_sim, '-+k')
hold on
semilogy(SNRdB, P_ser_theo)
hold off
legend([num2str(M) 'PAM_{estimated}'],[num2str(M) 'PAM_{analy}'])
xlabel('SNRdB in P/sqrt(R_{bit}) to \sigma ')
ylabel('SER')
titlestring{1} = 'The figure shows the symbol error rate for ';
titlestring{2} = [num2str(M) 'PAM and the estimated once plotted against optical SNR'];
title(titlestring)
axis([xmin, xmax, 10^(-6), 1])
grid on
```

BER, SER for uncoded M-PPM

```
%--- Theoretical and simulated SER and BER results of M-PPM modulation schemes ---
%Choose N for the number of sent symbols (effects the calulation time).
%Choose M (only even) for the modulation order and the symbol rate Rs. If a specific
%bit rate is needed comment Rs line and uncomment Rb line. The constants
%xmin and ymin are the limits of the plot.
%It is a must to include the UsedFunctions folder as a Matlab path !!!
%With *** marked code lines could/should be changed by the user to
%simulated different systems.

%---------------------------------------%
% Author: Martin Czaputa
% email: martin.czaputa.gmail.com
% version 1.0
% last modified: 29.Jul.2010
```

```matlab
% ——————————————————————————%
addpath('/Users/fraggle/Documents/MATLAB/MatlabWork_2010_06_13/UsedFunctions')
clear all; clc;

%--- Initialize needed parameters
N = 10^3;      %number of transmitted symbols ***
M = 4;         %modulation order M-PAM ***
k = log2(M);%transmitted bits per symbol
P = 1;         %average transmitted power
%symbol rate, symbol duration, bit rate, bit duration ***
Rs = 10^9/M; Ts = 1/Rs; Rb = Rs*k; Tb = 1/Rb;

%--- Define SNR and calculate n_sigma
xmin=25; xmax=60;        %limits of SNRdB plot ***
SNRdB = [xmin:1:xmax];      %10*log((P*sqrt(T))/sigma)
SNR = 10.^(SNRdB/10);    %SNR = (P*sqrt(R))/sigma
n_sigma = P./SNR;        %std. dev. of used AWGN noise
len = length(n_sigma);

%--- Define M-PPM constelllation
PPM = eye(M);               %modulation scheme M-PPM
ppmnorm = P*sqrt(Ts*M);    %normalization factor to get average power P

%--- Bit to symbol generation
%generate a randome bit sequence with N*k number of bits
xBit = rand(1,N*k)>0.5;
bin2DecMatrix = ones(N,1)*(2.^[(k-1):-1:0]) ;   %conversion from binary to decimal
xBitReshape =   reshape(xBit,k,N).';               %grouping to N symbols having k bits each

xDec = [sum(xBitReshape.*bin2DecMatrix,2)].'; % decimal to binary
%xGrayDec = bitxor(xDec,floor(xDec/2)); %decimal to gray decimal

%--- generate signal
x_sent = PPM(:,xDec+1);       %generates a sequence of N symbols
x_sentn = x_sent*ppmnorm;
a_rec = zeros(M,N);           %recieved symbols
n_rand = randn(M,N);          %M dimensional random vector
errors_sym = zeros(1,len);


for i=1:len
    %--- Transmission over AWGN channel
    n = n_sigma(i)*n_rand;  % white guassian noise, 0dB variance
    y = x_sentn + n;        % channel model, AWGN
    x_rec = zeros(M,N);

    %--- Demodulation (matched filter, here implemented with
    %max(), take highest peak in symbol interval)
    [Y,I] = max(y);

    %--- Convert modulation back to decimal
    x_recDec = I-1;


    %--- convert decimal to bin_str to bin_num
    x_recBit = dec2bin(x_recDec).';
    x_recBit = x_recBit(1:end).';
    x_recBit = str2num(x_recBit)';

    %--- determine bit errors
    errors_bit(i) = sum(abs(xBit-x_recBit)>0);
    errors_sym(i) = sum(abs(xDec - x_recDec)>0);
end
%counted biterrors and symbol errors through all sent bits/symbols
P_ber_sim = errors_bit/(N*k);
P_ser_sim = errors_sym/N;

for i = 1:length(SNR)
    P_ber_theo(i) = Pe_bit_mppm_nB(Rb,M,SNR(i));
end
for i = 1:length(SNR)
    P_ser_theo(i) = Pe_sym_mppm_nB(Rs,M,SNR(i));
end


%——————— Plotting analytically and statistically calculated BER,SER————
%—————————————————— curves agaisnt SNRdB ——————————————————
figure
semilogy(SNRdB,P_ber_sim,'-+k')
hold on
semilogy(SNRdB,P_ber_theo)
hold off
legend([num2str(M) 'PPM_{estimated}'],[num2str(M) 'PPM_{analy}'])
xlabel('SNRdB_in_P/sqrt(R_{bit})_to_\sigma_')
ylabel('BER')
titlestring {1} = 'The_figure_shows_the_bit_error_rate_for ';
titlestring {2} = [num2str(M) 'PPM_and_the_estimated_once_plotted_against_optical_SNR'];
```

```
title(titlestring)
axis([xmin, xmax, 10^(-6), 1])
grid on

figure
semilogy(SNRdB, P_ser_sim, '-+k')
hold on
semilogy(SNRdB, P_ser_theo)
hold off
legend([num2str(M) 'PPM_{estimated}'],[num2str(M) 'PPM_{analy}'])
xlabel('SNRdB_in_P/sqrt(R_{bit})_to_\sigma_')
ylabel('SER')
titlestring {1} = 'The_figure_shows_the_symbol_error_rate_for';
titlestring {2} = [num2str(M) 'PPM_and_the_estimated_once_plotted_against_optical_SNR'];
title(titlestring)
axis([xmin, xmax, 10^(-6), 1])
grid on

%save BER_PPM_.mat P_ber_sim P_ber_theo SNR SNRdB M Rs
%save SER_PPM_.mat P_ser_sim P_ser_theo SNR SNRdB M Rs
\begin{lstlisting}


 \vspace{1 cm}
\subsection{BER, SER for LDPC coded $M$-PAM}

\begin{lstlisting}
%Simulates BER and SER for coded LDPC and uncoded M-PAM modulation schemes. You
%should adjust the parameters with *** in the comment line to simulate
%different systems.
%
%----------------------------------------%
% Author: Martin Czaputa
% email: martin.czaputa@gmail.com
% version 1.0
% last modified: 20.Aug.2010
% ----------------------------------------%
addpath('/Users/fraggle/Documents/MATLAB/MatlabWork_2010_06_13/UsedFunctions')
clear all; clc;
code = 0;    % encoded == 1; uncoded == 0;    ***
%--- Initialize needed parameters
if code==true
    ns = 64800; r = 8/9; ks = ns*r;
    N = ks;
    packets = 1;    %sent ldpc packets of length 64800 --> 64800*packets
else
    N = 10^7;    %number of transmitted symbols ***
    packets = 1;
end
M = 2;        %modulation order M-PAM ***
optDC = (M-1);
k = log2(M);%transmitted bits per symbol
P = 1;        %average transmitted power ***
%symbol rate, symbol duration, bit rate, bit duration ***
Rs = 10^9; Ts = 1/Rs; Rb = Rs*k; Tb = 1/Rb;
%--- Define SNR and calculate n_sigma
xmin = 45; xmax = 53;    %limits of SNRdB plot ***
SNRdB = [xmin:1:xmax];%10*log((P*sqrt(T))/sigma)
SNR = 10.^(SNRdB/10);    %SNR = (P*sqrt(R))/sigma
%normalize symbols to satisfy the eye safety constraint to E{x}=<P where x are sent symbols
pamnorm = 2*P*sqrt(Ts)/(M-1)/2;
n_sigma = (P./SNR)/pamnorm;        %std. dev. of used AWGN noise
errors_bit_l = zeros(1,length(SNRdB));    %init error symbols vector
errors_bit = zeros(1,length(SNRdB));
errors_sym_l = zeros(1,length(SNRdB));    %init error symbols vector
%because the trick with additional loops is used the errors have to be summated
errors_sym = zeros(1,length(SNRdB));

if code == true
    %--- Encoding, Coding ---
    H = dvbs2ldpc(r);
    encLDPC = fec.ldpcenc(H);
    %--- Signal generation ---
    x_bit = randint(1,N,2);
    x_bit_enc = encode(encLDPC, x_bit)';
    decLDPC = fec.ldpcdec(H);
    decLDPC.NumIterations = 30;
    decLDPC.DoParityChecks = 'Yes';
    %decLDPC.DecisionType = 'Soft Decision';
    n = randn(ns/k,1);
else
    %--- Signal generation ---
    n = randn(N,1);
    x_bit = randint(N*k,1,2);
    x_bit_enc = x_bit;
end
```

```matlab
%--- Modulation ---
%modPAM = modem.pammod('M', M, 'SymbolOrder', 'binary','InputType', 'Bit');
modPAM = modem.pammod('M',M,'SymbolOrder','Gray','InputType','Bit');
x_sym = real(modulate(modPAM,x_bit_enc));
if code == true
    x_sym_comp = real(modulate(modPAM,x_bit'));
end
% add DC for optical transmission, smallest symbol constallation amplitude is 0
%x_sy = (x_sym+optDC)*pamnorm;
%x_sy = (x_sym)*pamnorm;
x_sy = (x_sym);
%demodPAMsy = modem.pamdemod(modPAM,'DecisionType','hard decision');
demodPAMsy = modem.pamdemod(modPAM,'DecisionType','hard_decision','SymbolOrder','binary');
demodPAMsy.outputtype = 'integer';
for i = 1:length(SNR)
    for j = 1:packets

        %--- Channel ---
        r_sy_noise = x_sy + n_sigma(i)*n;
        %r_sy_noise = r_sy_noise/pamnorm-optDC;
        %r_sy_noise = r_sy_noise/pamnorm;

        if code == true
            demodPAM = modem.pamdemod(modPAM,'DecisionType','LLR','NoiseVariance',n_sigma(i)^2);
        else
            demodPAM = modem.pamdemod(modPAM,'DecisionType','hard_decision');
        end
        r_bit_enc = demodulate(demodPAM,r_sy_noise);
        r_sy = demodulate(demodPAMsy,r_sy_noise);

        if code == true
            %--- Decoding ---
            r_bit = decode(decLDPC,r_bit_enc');
            r_s = real(modulate(modPAM,r_bit'));
            errors_sym_l(i) = sum(abs(x_sym_comp - r_s )>0);
        else
            r_bit = r_bit_enc;
            errors_sym_l(i) = sum(abs((x_sym+optDC)/2 - r_sy )>0);
        end
        errors_bit_l = sum(abs(x_bit-r_bit)>0);
        errors_bit(i) = errors_bit_l + errors_bit(i);
        errors_sym(i) = errors_sym_l(i) + errors_sym(i);
    end
end
%--- actual simulated BER and SER vector for different SNR values
if code == true
    P_ber_sim = errors_bit/(N*packets);      %bit errors divided by sent bits
    P_ser_sim = errors_sym/(N/log2(M)*packets);         %symbol errors divided by sent smbols
else
    P_ber_sim = errors_bit/(N*k*packets);    %bit errors divided by sent bits
    P_ser_sim = errors_sym/(N*packets);          %symbol errors divided by sent smbols
end

%theoretical bit error and symbol error curves
for i = 1:length(SNR)
    P_ber_theo(i) = Pe_bit_mpam_nB(Rb,M,SNR(i));
end
Pser_rs = zeros(1,length(SNR));
for i = 1:length(SNR)
    P_ser_theo(i) = Pe_sym_mpam_nB(Rs,M,SNR(i));
end


%----------- Plotting analytically and statistically calculated BER,SER----
%------------------------ curves against SNRdB --------------------------
figure
semilogy(SNRdB,P_ber_sim,'-+k')
hold on
semilogy(SNRdB,P_ber_theo)
hold off
legend([num2str(M) 'PAM_{estimated}'],[num2str(M) 'PAM_{analy}'])
xlabel('SNRdB_in_P/sqrt(R_{bit})_to_\sigma_')
ylabel('BER')
titlestring {1} = 'The_figure_shows_the_bit_error_rate_for';
titlestring {2} = [num2str(M) 'PAM_and_the_estimated_once_plotted_against_optical_SNR'];
title(titlestring)
axis([xmin, xmax, 10^(-6), 1])
grid on
figure
semilogy(SNRdB,P_ser_sim,'-+k')
hold on
semilogy(SNRdB,P_ser_theo)
hold off
legend([num2str(M) 'PAM_{estimated}'],[num2str(M) 'PAM_{analy}'])
xlabel('SNRdB_in_P/sqrt(R_{bit})_to_\sigma_')
ylabel('SER')
titlestring {1} = 'The_figure_shows_the_symbol_error_rate_for';
```

```matlab
titlestring {2} = [num2str(M) 'PAM_and_the_estimated_once_plotted_against_optical_SNR'];
title(titlestring)
axis([xmin, xmax, 10^(-6), 1])
grid on
```

BER, SER for LDPC coded M-PPM

```matlab
%--- Theoretical and simulated SER and BER results of LDPC coded M-PPM modulation schemes ---
%Choose N for the number of sent symbols (effects the calulation time).
%Choose M (only even) for the modulation order and the symbol rate Rs. If a specific
%bit rate is needed comment Rs line and uncomment Rb line. The constants
%xmin and ymin are the limits of the plot.
%It is a must to include the UsedFunctions folder as a Matlab path !!!
%With *** marked code lines could/should be changed by the user to
%simulated different systems.

%------------------------------------%
% Author: Martin Czaputa
% email: martin.czaputa.gmail.com
% version 1.0
% last modified: 2.Oct.2010
% ------------------------------------%
addpath('/Users/fraggle/Documents/MATLAB/MatlabWork_2010_06_13/UsedFunctions')
clear all; clc;

%--- Initialize needed parameters
ns = 64800; r = 1/2; ks = ns*r;
N = ks;
packets = 1;        %sent ldpc packets of length 64800 --> 64800*packets
M = 64;             %modulation order M-PAM ***
k = log2(M);        %transmitted bits per symbol
P = 1;              %average transmitted power ***
%symbol rate, symbol duration, bit rate, bit duration ***
Rs = 10^9/M; Ts = 1/Rs; Rb = Rs*k; Tb = 1/Rb;
ppmnorm = sqrt(Ts*M);                           %normalization factor to get average power P

[indx0,indx1] = init_llr_ppm(M);%initialize log-likelihood function parameters
%--- Define SNR and calculate n_sigma
xmin=30; xmax=40;                    %limits of SNRdB plot ***
SNRdB = [xmin:0.1:xmax];             %10*log((P*sqrt(T))/sigma)
SNR = 10.^(SNRdB/10);                %SNR = (P*sqrt(R))/sigma
n_sigma = (P./SNR)/ppmnorm;          %std. dev. of used AWGN noise
len = length(n_sigma);

%--- Encoding, Coding ---
H = dvbs2ldpc(r);
encLDPC = fec.ldpcenc(H);
%--- Signal generation ---
decLDPC = fec.ldpcdec(H);
decLDPC.NumIterations = 30;
decLDPC.DoParityChecks = 'Yes';

%--- Define M-PPM constelllation
 PPM = eye(M);                 %modulation scheme M-PPM


%--- Bit to symbol generation
x_bit = randint(1,N,2);                 %generate a randome bit sequence with N number of bits
x_bit_enc = encode(encLDPC, x_bit)';
bin2DecVec = 2.^[(k-1):-1:0] ;          %conversion from binary to
xBitReshape =  reshape(x_bit_enc',k,ns/k).';  %grouping to N symbols having k bits each
xDec = xBitReshape*bin2DecVec';         %decimal to binary

%--- generate signal
x_sent = PPM(:,xDec+1);          %generates a sequence of N symbols
a_rec = zeros(M,ns/k);           %recieved symbols
n_rand = randn(M,ns/k);          %M dimensional random vector
errors_sym = zeros(1,len);

%--- symbol generation of uncoded bits for smbol error calculation
xBitReshape_2 =  reshape(x_bit,k,ks/k).';
xTX_dec_unc = xBitReshape_2*bin2DecVec';
tic
for i=1:len

    %--- Transmission over AWGN channel
    y = x_sent + n_sigma(i)*n_rand;          % channel model, AWGN

    %llr = llr_ppm(M,y,n_sigma(i));
    llr = llr_ppm_c(y, n_sigma(i),ns, M,PPM,indx0,indx1);
    x_recBit = decode(decLDPC, llr);

    %--- calculate received symbols
```

```matlab
        xBitReshapeRX =   reshape(x_recBit,k,ks/k).';
        xDecRX = xBitReshapeRX*bin2DecVec';

        %--- determine bit errors
        errors_bit(i) = sum(abs(x_bit-x_recBit)>0);
        errors_sym(i) = sum(abs(xTX_dec_unc - xDecRX)>0);
end
%counted biterrors and symbol errors through all sent bits/symbols
P_ber_sim = errors_bit/N;
P_ser_sim = errors_sym/(N/k);
toc


for i = 1:length(SNR)
    P_ber_theo(i) = Pe_bit_mppm_nB(Rb,M,SNR(i));
end
for i = 1:length(SNR)
    P_ser_theo(i) = Pe_sym_mppm_nB(Rs,M,SNR(i));
end

%------------ Plotting analytically and statistically calculated BER,SER----
%--------------------------- curves against SNRdB --------------------------
semilogy(SNRdB,P_ber_sim,'-+k')
hold on
semilogy(SNRdB,P_ber_theo)
hold off
legend([num2str(M) 'PPM_{estimated}'],[num2str(M) 'PPM_{analy}'])
xlabel('SNRdB_in_P/sqrt(R_{bit})_to_\sigma_')
ylabel('BER')
titlestring {1} = 'The_figure_shows_the_bit_error_rate_for';
titlestring {2} = [num2str(M) 'PPM_and_the_estimated_once_plotted_against_optical_SNR'];
title(titlestring)
axis([xmin, xmax, 10^(-6), 1])
grid on
%
figure
semilogy(SNRdB,P_ser_sim,'-+k')
hold on
semilogy(SNRdB,P_ser_theo)
hold off
legend([num2str(M) 'PPM_{estimated}'],[num2str(M) 'PPM_{analy}'])
xlabel('SNRdB_in_P/sqrt(R_{bit})_to_\sigma_')
ylabel('SER')
titlestring {1} = 'The_figure_shows_the_symbol_error_rate_for';
titlestring {2} = [num2str(M) 'PPM_and_the_estimated_once_plotted_against_optical_SNR'];
title(titlestring)
axis([xmin, xmax, 10^(-6), 1])
grid on
```

BER, SER for RS coded M-PAM

```matlab
%--- Theoretical and simulated SER and BER results of LDPC coded M-PAM modulation schemes ---
%--- with additional forward error correction code using Reed Solomon ----
%Choose N for the number of sent symbols (effects the calulation time).
%Choose M (only even) for the modulation order and the symbol rate Rs. If a specific
%bit rate is needed comment Rs line and uncomment Rb line. The constants
%xmin and ymin are the limits of the plot.
%It is a must to include the UsedFunctions folder as a Matlab path !!!
%With *** marked code lines could/should be changed by the user to
%simulated different systems.

%-----------------------------------%
% Author: Martin Czaputa
% email: martin.czaputa.gmail.com
% version 1.1
% last modified: 29.Jul.2010
% -----------------------------------%
addpath('/Users/fraggle/Documents/MATLAB/MatlabWork_2010_06_13/UsedFunctions')
clear all; clc
%--- The simulation is very slow due to a huge amount operations in the main loop ---
%--- Decreasing the sent symbols is faster but inaccurate and doesn't ---
%--- deliver values for higher SNR ---
% symbols should not exceed 10^5 and the outerloop not more than 4
symbols = 1*10^3; %suggestion for sent symbols (truncated because of RS code length)
outterloop = 1; %instead of increasing the symbols vector more loops are faster

%--- Reed-Solomon initialization
n = 255; kl = 127; len = log2(n+1);      %RS(255,127) ***
%n = 255; kl = 223; len = log2(n+1); %RS(255,223) ***
% n = 255; kl = 239; len = log2(n+1);%RS(255,239) ***
enc = fec.rsenc(n,kl);              %RS encoder
dec =  fec.rsdec(enc);             %RS decoder
```

```matlab
%--- Initialize needed parameters
M = 256;            %modulation order M-PAM ***
k = log2(M);        %transmitted bits per symbol
P = 1;                          %average transmitted power
%symbol rate, symbol duration, bit rate, bit duration ***
Rs = 10^9; Ts = 1/Rs; Rb = Rs*k; Tb = 1/Rb;

bits = symbols*k;               %suggested number of bits
kmal = floor(bits/(len*kl));
N = kmal*(len*kl)/k;

%--- Define SNR and calculate n_sigma
xmin = 60; xmax = 80;                  %limits of SNRdB plot ***
SNRdB = [xmin:1:xmax];                 %10*log((P*sqrt(T))/sigma)
SNR = 10.^(SNRdB/10);                  %SNR = (P*sqrt(R))/sigma
n_sigma = P./SNR;                      %std. dev. of used AWGN noise
errors_sym = zeros(1,length(SNRdB));   %init error symbols vector
%because the trick with additional loops is used the errors have to be summated
errors_sym_sum = zeros(1,length(SNRdB));

%--- Define M-PAM constellation
mpam = [0:M-1];                        %set PAM symbols
%normalize symbols to satisfy the eye safety constraint to E{x}=<P where x are sent symbols
pamnorm = 2*P*sqrt(Ts)/(M-1);
gray_pam = bitxor(mpam,floor(mpam/2)); %connection between normal symbols and gray coded symbols
[tt ind] = sort(gray_pam);

%--- Bit to symbol generation
sym = randsrc(1,kl*kmal,[0:n]); %uncoded sent symbols
xDec = dec2dec(sym,k);
xBit = dec2binvec(sym);

%--- Encode msg with the ENCODE function.
sym_rs = encode(enc,sym');         %encode symbols with RS
xBit_rs = dec2binvec(sym_rs);      %convert to binary vetor to calculate BER later
len_sym = length(xBit_rs)/k;


xBit = rand(1,N*k,1)>0.5; % random 1's and 0's
bin2DecMatrix = ones(len_sym,1)*(2.^[(k-1):-1:0]) ; %conversion from binary to decimal
xBitReshape =  reshape(xBit_rs,k,len_sym).';        %grouping to N symbols having k bits each

xDec_rs = [sum(xBitReshape.*bin2DecMatrix,2)].';%decimal to binary
xGrayDec = bitxor(xDec_rs,floor(xDec_rs/2));    %decimal to gray decimal
x = xGrayDec*pamnorm;

for j=1:outterloop
for i=1:length(SNR)

    %--- Transmission over AWGN channel
    n_awgn = n_sigma(i)*randn(1,len_sym);   %white guassian noise, 0dB variance
    y = x + n_awgn;                         %channel model, AWGN

    %--- Demodulation
    x_rec = round(y/pamnorm); %need to rescale to demodulate

    %--- Allocate received symbols to symbol alphabet
    x_rec(find(x_rec > max(mpam))) = max(mpam);
    x_rec(find(x_rec < min(mpam))) = min(mpam);

    %--- Convert symbols from dec to dec_RS
    x_recDec_rs = ind(x_rec+1)-1;            %Convert symbols to decimal
    xRX_sym_rs = dec2dec(x_recDec_rs,len);   %Convert to RS symbols

    %--- Decode and correct RS symbols
    xRX_sym = decode(dec,xRX_sym_rs);

    %--- Convert back to PAM symbols to calculate SER
    x_recDec = dec2dec(xRX_sym,k)';

    errors_sym(i) = sum(abs(xDec' - x_recDec)>0);
    errors_sym_sum(i) = errors_sym(i) + errors_sym_sum(i);
    %----- remove % to calculate also the BER ----
    %---- takes more time
    %--- Convert decimal to bin_str to bin_num
    x_recBit = dec2bin(x_recDec).';
    x_recBit = x_recBit(1:end).';
    x_recBit = str2num(x_recBit)';

%--- Check dismatch of sent and recieved bits
    xBit == x_recBin

%--- Determine bit errors
errors(i) = sum(abs(xBit-x_recBit)>0);

%----------------------------------------------------------------
```

```matlab
    end
  end
  aug = linspace(0.8,1,8);
  %--- actual simulated BER and SER vector for different SNR values
  % % % P_ber_sim = errors/(N*k*outterloop);
  P_ser_sim = errors_sym_sum/(N*outterloop);

  %--- Theoretical bit error and symbol error rate
  for i = 1:length(SNR)
      P_ber_theo(i) = Pe_bit_mpam_nB(Rb,M,SNR(i));
  end
  for i = 1:length(SNR)
      P_ser_theo(i) = Pe_sym_mpam_nB(Rs,M,SNR(i));
  end
  %--- Theoretical Reed Solomon SER after decoder
  Pbit = 0;
  t = floor((n-kl)/2);
  C = nchoosek(n,kl);
  for o=[(t+1):n];
      C(o-t)=nchoosek(n,o);
  end
  for i=1:length(SNR)
          %% HAS TO BE IMPROVED!!!
          P_ser_rs_theo(i) = serrs( n, kl, t, 1-(1-P_ser_theo(i))^(len/k), C);
  end



      % % %------------- Plotting analytically and statistically calculated BER,SER------
      % % %------------------------------- curves against SNRdB ---------------------------
  semilogy(SNRdB,P_ber_sim,'-+k')
  hold on
  semilogy(SNRdB,P_ber_theo)
  hold off
  legend([num2str(M) 'PAM_{estimated}'],[num2str(M) 'PAM_{analy}'])
  xlabel('SNRdB_in_P/sqrt(R_{bit})_to_\sigma_')
  ylabel('BER')
  titlestring {1} = 'The_figure_shows_the_bit_error_rate_for ';
  titlestring {2} = [num2str(M) 'PAM_and_the_estimated_once_plotted_against_optical_SNR'];
  title(titlestring)
  axis([xmin, xmax, 10^(-6), 1])
  grid on

  figure
  semilogy(SNRdB,P_ser_sim,'-+k')
  hold on
  semilogy(SNRdB,P_ser_theo)
  hold on
  semilogy(SNRdB,P_ser_rs_theo,'-r')
  hold off
  legend([num2str(M) 'PAM-RS(' num2str(n) ',' num2str(kl) ')_{simulated}'] ...
  ... ,[num2str(M) 'PAM_{analy}'],[num2str(M) 'PAM-RS(' num2str(n) ',' num2str(kl) ')_{analy}'])
  xlabel('SNRdB_in_P/sqrt(R_{bit})_to_\sigma_')
  ylabel('SER')
  titlestring {1} = ['Theoretical_SER_for_' num2str(M) '_coded_and_uncoded_PAM_as_well'];
  titlestring {2} = ['as_simulated_coded_PAM_curve.'];
  title(titlestring)
  axis([xmin, xmax, 10^(-6), 1])
  grid on
```

B.2 Metrics: Data rates, availability and outages.

Simulation model for M-PAM and M-PPM to calculate data rates.

```matlab
  %--- This simulation is to evaluate the performance of different modulations for
  %latency tolerant traffic applications.
  %--- IP packets with different modulation schemes are here transmitted over
  %an optical channel. Measured historical yearly weather data is used to
  %calculate the average hourly throughput as well as the hourly average rate
  %per day. Channel losses hl, hg and the parameters for hs are loaded from
  %calculated_data_ham_****.mat, which was calculated in waether_extract.m.
  %Plots are done in "Plotting relevant curves".

  %--------------------------------------------%
  % Author: Martin Czaputa
  % email: martin.czaputa.gmail.com
  % version 1.0
  % last modified: 21.Feb.2010
  %--------------------------------------------%

  clear all
```

```matlab
%loads hg=geometric attenuation, hl=atmospheric att. and
%logn_param = mus and sigmas for the lognormal scintillation model

load attenuationData/calculated_data_ham_1000.mat
%--- define transmission values
P = 0.5;          %average transmitting power = 500mW
R = 0.5;          %Responsitivity in A/W
var_n = 10^(-16);%10^(-17)          %variance of AWGN of the optical channel for day
%PRgsig includes geometric losses, the receiver responsitivity and through sigma
PRgsig = P*R*hg/sqrt(var_n);

ms_range = 60*60*1000/10;   %interval in 10ms per hour
%------------ Calculating the IP packet throughput ---------
days = 366;       % Year 2008 had 366 days. Minimum days are two because of the R_b-Tilde calculation
mmodulation = [2,4,8,16,32,64];          %simulated modulation orders
molen = length(mmodulation);
currPerc = 1;     %percentage display for the simulation, gives only an app. of the status of the sim
.
percent = round([1:20]*(days*24)/20);
Rs = 10^9; Ts = 1/Rs;


for i = 1:(24*days) %hours
    if i == percent(currPerc)       %just displays the percentage of time the simulation is running
        disp([num2str(currPerc*5) '%'])
        currPerc = currPerc+1;
    end
    %generate hs in intervals of 10msec from a lognormal distribution
    hs = lognrnd(logn_param(1,i),logn_param(2,i),1,ms_range);
    SNR = PRgsig*hl(i)*hs;  %signal to noise ratio is here a vector with the length of length(hs)


    for j = 1:molen
    %----------- M-PAM --------
    %-------------------------
        M = mmodulation(j); %modulation order
        k = log2(M);            %multiplication factor to calculate the actual bitrate regarding the
        symbol rate
        Rb = Rs*k;
        Tb = 1/Rb;              %bitrate of Rb*k Gbits/s

        %--- calculate the average rate regarding the SER as well as the
        %--- average rate regarding the packet error rate

        %--- average rate <> SER
        mpam_ser = Pe_sym_mpam_nB(Rs,M,SNR);     %symbol error probability every 10ms

        %--- IP packet number per 10ms
        %--- average rate <> per
        mpam_avgr_h_ip(j,i) = mean((1-mpam_ser).^(1024/k))*Rs*k;

    %----------- M-PPM --------
    %-------------------------
        k = log2(M);    %multiplication factor to calculate the actual bitrate regarding the symbol
        rate
        Rsppm = Rs/M;

        %--- calculate the average rate regarding the SER as well as the
        %--- average rate regarding the packet error rate

        %--- average rate <> SER
        mppm_ser = Pe_sym_mppm_nB(Rsppm,M,SNR);
        %The SER which is above the threshold is set 1 = fail. (theoretical SER formular is
        inaccurate)
        ind2 = find(mppm_ser>0.7);
        mppm_ser(ind2)=0.7;

        %--- IP packet number per 10ms
        mppm_avgr_h_ip(j,i) = mean((1-mppm_ser).^(1024/k))*Rsppm*k;
    end
end

%--- Calulating R_b-Tilde per hour in bits
for i = 1:molen
    for j=1:(days*24-23)
        mpam_avgr_h_ipsmo(i,j) = mean(mpam_avgr_h_ip(i,((j-1)+1):j+23));
        mppm_avgr_h_ipsmo(i,j) = mean(mppm_avgr_h_ip(i,((j-1)+1):j+23));
    end
end

%%--- Calulating R_b per hour in bits
% for i = 1:molen
%     for j=1:days
%         mpam_avgr_d_ip(i,j) = mean(mpam_avgr_h_ip(i,((j-1)*24+1):j*24));
%         mppm_avgr_d_ip(i,j) = mean(mppm_avgr_h_ip(i,((j-1)*24+1):j*24));
%     end
% end

%--- Average R_b-Tilde per day in bits
```

```
for i = 1:molen
    for j=1:days-1
        mpam_avgr_d_ipsmo(i,j) = mean(mpam_avgr_h_ipsmo(i,((j-1)*24+1):j*24));
        mppm_avgr_d_ipsmo(i,j) = mean(mppm_avgr_h_ipsmo(i,((j-1)*24+1):j*24));
    end
end


all_modu = [mpam_avgr_h_ip;mppm_avgr_h_ip];
mean_avgr = mean(all_modu');      %average data rate per year of each modulation scheme
[val,ind]=max(all_modu);          %determine the adaptive rate of the given set of modulations
adaptive_avgr = mean(val)

%reliability of each modulation scheme, ???? wrong formular
for i =1:molen*2
    fraction(i) = length(find(ind==i))/length(ind);
    %if data rate is below 1 Mbit/s than the link is assumed to be off
    reliability(i) = 100-length(find(all_modu(i,:)<0.0001))/length(all_modu(1,:))*100;
    end
reliability = reliability ';
save sim_data.mat mpam_avgr_h_ip mpam_avgr_d_ipsmo  mppm_avgr_h_ip ...
...  mppm_avgr_d_ipsmo mpam_avgr_h_ipsmo mppm_avgr_h_ipsmo mean_avgr fraction
save adaptrate_reliability.txt adaptive_avgr reliability -ascii
```

Simulation model for LDPC coded M-PAM and M-PPM to calculate data rates.

```
%--- This simulation is to evaluate the performance of different LDPC coded modulations for
%latency tolerant traffic applications.
%---Different modulation schemes are here transmitted over
%a free space optical channel. Measured historical yearly weather data is used to
%calculate the average hourly rate as well as the hourly average rate
%per day. Channel losses hl, hg and the parameters for hs are loaded from
%calculated_data_ham_****.mat, which was calculated in waether_extract.m.
%Plots are done in "Plotting relevant curves".

%--------------------------------------------%
% Author: Martin Czaputa
% email: martin.czaputa@gmail.com
% version 1.0
% last modified: 14.Oct.2010
%--------------------------------------------%
%addpath('/Ubers/fraggle/Documents/MATLAB/MatlabWork_2010_06_13/UsedFunctions')
%addpath('/Users/fraggle/Documents/MATLAB/MatlabWork_2010_06_13/BER_SER')

clear all; clc;
load attenuationData/calculated_data_ham_1000.mat    %loads hg=geometric attenuation, hl=
    atmospheric att. and logn_param = mus and sigmas for the lognormal scitnillation model
load SER_curves/pam_ldpc_ber_complete_01_01_2011.mat
load SER_curves/ppm_ldpc_ber_complete_01_01_2011.mat

%---define transmission values
P = 0.5;          %average transmitting power = 500mW
R = 0.5;          %Responsitivity in A/W
% var_n = 10^(-17);               %variance of AWGN of the optical channel for day / std =
    10^(-8.5)
var_n = 10^(-16);
PRgsig = P*R*hg/sqrt(var_n);      %PRgsig includes geomtric losses, the reciever responsitivity and
    through sigma

ms_range = 60*60*1000/10;    %interval in 10ms per hour
%ms_range = 100;

%------------ Calculating the IP packet throuput -------
days = 366;      % Year 2008 had 366 days. Minimum days are two because of the R_b-Tilde calculation
mmodulation = [2,4,8,16,32,64];         %simulated modulation orders
% mmodulation = [2,4,8];        %simulated modulation orders

r = 5/6;    %r= [1/2, 3/5, 2/3, 3/4, 4/5, 5/6, 8/9, 9/10];
molen = length(mmodulation);
currPerc = 1;                            %percentage display for the simulation, gives only an app. of
    the status of the sim.
percent = round([1:20]*(days*24)/20);
Rs = 10^9; Ts = 1/Rs;
DLim = 1;%10^(-3);

for i = 1:(24*days) %hours
    if i == percent(currPerc)
        disp([num2str(currPerc*5) '%'])
        currPerc = currPerc+1;
    end
```

```matlab
    hs = lognrnd(logn_param(1,i),logn_param(2,i),1,ms_range);    %generate hs in intervals of 10msec
        from a lognormal distribution
    SNR = PRgsig*hl(i)*hs;  %signal to noise ratio is here a vector with the length of length(hs)


    for j = 1:molen
    %---------- M-PAM ----------
    %--------------------------
        M = mmodulation(j); %modulation order
        k = log2(M);          %multiplication factor to calculate the actual bitrate regarding the
            symbol rate
        Rb = k*Rs;

        %--- average rate <> BER
        mpam_ber = ser_snr( pam_ldpc_ber, pam_ldpc_ber_snr, SNR, r,M);
        %--- IP packet number per 10ms
        mpam_ber(find(mpam_ber>=DLim))=1;
        mpam_avgr_h_ip(j,i) = mean((1-mpam_ber).^(10^5))*Rb*r;


        %---------- M-PPM ----------
        %--------------------------
        k = log2(M);              %multiplication factor to calculate the actual bitrate regarding
            the symbol rate
        Rsppm = Rs/M;

        %--- average rate <> BER
        mppm_ber = ser_snr( ppm_ldpc_ber, ppm_ldpc_ber_snr, SNR, r,M);

        %--- IP packet number per 10ms
        mppm_ber(find(mppm_ber>DLim))=1;
        mppm_avgr_h_ip(j,i) = mean((1-mppm_ber).^(10^5))*Rsppm*k*r;
    end
end

mean(mpam_avgr_h_ip(1,:))
%--- Calulating R_b-Tilde per hour in bits
for i = 1:molen
    for j=1:(days*24-23)
        mpam_avgr_h_ipsmo(i,j) = mean(mpam_avgr_h_ip(i,((j-1)+1):j+23));
        mppm_avgr_h_ipsmo(i,j) = mean(mppm_avgr_h_ip(i,((j-1)+1):j+23));
    end
end


%--- Average R_b-Tilde per day in bits
for i = 1:molen
    for j=1:days-1
        mpam_avgr_d_ipsmo(i,j) = mean(mpam_avgr_h_ipsmo(i,((j-1)*24+1):j*24));
        mppm_avgr_d_ipsmo(i,j) = mean(mppm_avgr_h_ipsmo(i,((j-1)*24+1):j*24));
    end
end


all_modu = [mpam_avgr_h_ip;mppm_avgr_h_ip];
mean_avgr = mean(all_modu')     %average data rate per year of each modulation scheme
[val,ind]=max(all_modu);            %determine the adaptive rate of the given set of modulations
adaptive_avgr = mean(val)
r
save sim_data_LDPC_.mat mpam_avgr_h_ip mpam_avgr_d_ipsmo mppm_avgr_h_ip mppm_avgr_d_ipsmo
    mpam_avgr_h_ipsmo mppm_avgr_h_ipsmo mean_avgr
```

Availability Calculation

```matlab
%--- Availability calculations for various latency tolerant applications as well as
%for adaptive modulation and adaptive coded modulation
%--------------------------------------%
% Author: Martin Czaputa
% email: martin.czaputa.gmail.com
% version 1.0
% last modified: 18.Aug.2010
%--------------------------------------%
clc
clear all
% close all
% load rateAdapt_10-6.mat
% load moduRateAdapt.mat


load sim_data_1000.mat
%load sim_data_ldpc_5_6.mat
% load sim_data_RS_255_210_allMod.mat

%load sim_data_Rs_255_239.mat
% load sim_data_Rs_255_223.mat
%load sim_data_Rs_255_127.mat
```

```
mmodulation = [2,4,8,16,32,64];
%mmodulation = [2,4,8];
molen = length(mmodulation);
days = 366;
linkr = [200,500,1000,2000];
%months = [31,29,31,30,31,30,31,31,30,31,30,31];
months = [1,31,60,91,121,152,182,213,244,274,305,335,366];
plotsign = {'-+k','-..k','--*k','-<k',':dk','-sk'};
plotsign2 = {'-k','--k','--k','--k','--k','--k'};
month_n = {'Jan','Feb','Mar','Apr','May','Jun','Jul','Aug','Sep','Oct','Nov','Dec'}';
range = linspace(0,335,11);


for i = 1:molen
    for j=1:days
        mpam_avgr_d_ip(i,j) = mean(mpam_avgr_h_ip(i,((j-1)*24+1):j*24));
        mppm_avgr_d_ip(i,j) = mean(mppm_avgr_h_ip(i,((j-1)*24+1):j*24));
    end
end

% plot(mpam_avgr_d_ip(1,:))
% hold on
% plot(mppm_avgr_d_ip(6,:),'r')
% hold off


%----------------------------------------------------------
%--- (2) --- Pr[Rate > R0] OOK, PAM and OOK, PPM -------------
%----------------------------------------------------------
%load sim_data_1000.mat
% Ro = 2%*10^9;
Ro = 3;%*10^9;
% range = 0:0.2:Ro;
range = 0:0.01:Ro;
len = length(mpam_avgr_h_ip);
cdf_pam = zeros(molen,length(range));
figure
for i = 1:molen
    for j = 1:length(range)
        cdf_pam(i,j) = length(find(mpam_avgr_h_ipsmo(i,:)/10^9>=range(j)))/len;%/len;
    end
    plot(range,cdf_pam(i,:),plotsign{i})
    hold on
end


%------ plot addit. AM schemes 10^-6
for j = 1:length(range)
    cdf_AM(1,j) = length(find(rate_adapt_h_ipsmo/10^9>=range(j)))/len;%/len;
end
plot(range,cdf_AM,'-*r')
hold on

load rateAdapt_10-3.mat
%------ plot addit. AM schemes 10^-3
for j = 1:length(range)
    cdf_AM(1,j) = length(find(rate_adapt_h_ipsmo/10^9>=range(j)))/len;%/len;
end
plot(range,cdf_AM,'-+r')
hold on

load rateAdapt_10-6_red.mat
%------ plot addit. AM schemes 10^-6red
for j = 1:length(range)
    cdf_AM(1,j) = length(find(rate_adapt_h_ipsmo/10^9>=range(j)))/len;%/len;
end
plot(range,cdf_AM,'-+g')
hold on

%------ plot addit. AMC schemes
for j = 1:length(range)
    cdf_ACM(1,j) = length(find(moduRate_adapt_h_ipsmo/10^9>=range(j)))/len;%/len;
end
plot(range,cdf_ACM,'-*g')
hold on

%[trash, xpos] = min(abs(cdf_pam(1,:) - 0.4))
%plot(cdf_pam(1,xpos),'<')
hold off
axis([0, Ro, 0, 1])
xlabel(' $R_0$ (Gbps)','Interpreter','latex','FontSize',17)
ylabel('$\mathrm{Pr}_{\mathrm{rate}}\,(R_0)=\mathrm{Prob}\,\,_{_\{_\tilde{R_{b}}_\geq_R_{0}_\}$','
    Interpreter','latex','FontSize',17)
set(gca,'XTick',0:0.25:Ro)
set(gca,'FontSize',14)
legend('OOK','4-PAM','8-PAM','16-PAM','32-PAM','64-PAM','AM-10^{-6}','AM-10^{-3}','AM-10^{-6}_red')
%xlabel('Average daily rate $R_0$ per hour (Gbps)','Interpreter','latex','FontSize',12)
```

```
%ylabel('Probability [$\tilde{R_b} > R_0$]','Interpreter','latex','FontSize',12)
%exportfig(gcf,['./plottet/rate_pam_prob.eps'])
```

Outage calculation for various modulation schemes.

```
%--- Calculating the outage probability for various simulated systems ---
% (Latency tolerant applications, AM, ACM)
%--------------------------------------------%
% Author: Martin Czaputa
% email: martin.czaputa@gmail.com
% version 1.0
% last modified: 21.Feb.2010
% --------------------------------------------%

clear all; clc; close all;

load sim_data_1000.mat
% load rateAdapt_LDPC_5_6.mat
%load sim_data_Rs_255_239_allMod.mat
%load sim_data_Rs_255_223_allMod.mat
%load sim_data_Rs_255_127_allMod.mat
% load rateAdapt.mat

plotsign = {'-.ok','--*k','-+k','-k','-dk','k'};
plotsign2 = {'-.ok','--*b','-+r','-k','-dk','k'};
%--- PAM ---
% signal(1,:) = rate_adapt;  %AM

signal(1,:) = mpam_avgr_h_ip(1,:);   %OOK
signal(2,:) = mpam_avgr_h_ip(2,:);   %4-PAM
signal(3,:) = mpam_avgr_h_ip(3,:);   %8-PAM
signal(4,:) = mpam_avgr_h_ip(4,:);   %16-PAM
% signal(5,:) = mpam_avgr_h_ip(5,:);   %32-PAM
% signal(6,:) = mpam_avgr_h_ip(6,:);   %64-PAM


%--- PPM ---
signal(5,:) = mppm_avgr_h_ip(1,:);   %2-PPM
signal(6,:) = mppm_avgr_h_ip(2,:);   %4-PPM
signal(7,:) = mppm_avgr_h_ip(3,:);   %8-PPM
signal(8,:) = mppm_avgr_h_ip(4,:);  %16-PPM
signal(9,:) = mppm_avgr_h_ip(5,:);  %32-PPM
% signal(10,:) = mppm_avgr_h_ip(6,:);  %64-PPM




[leny,len] = size(signal);
outage = zeros(leny,len);

rate_lim = 10^8;

for i = 1:leny
    wahr(i) = length(find(signal(i,:)>=rate_lim)) ;
end


for k = 1:leny
    temp_s = signal(k,:) < rate_lim;
    len_out(k) = length(find(signal(k,:) < rate_lim));
    counter = 0;
    onoff = 0;

    for i = 1 : len +1
        if i < (len +1)
            if temp_s(i) == 1
                counter = counter +1;
                onoff = 1;
            else% temp_s(i) == 0
                if onoff == 1
                    outage(k,counter) = outage(k,counter) + 1;
                    counter = 0;
                    onoff = 0;
                end
            end
        else
            if onoff == 1
                outage(k,counter) = outage(k,counter) + 1;
                counter = 0;
                onoff = 0;
            end
        end
    end
end
```

```matlab
%−−−−− Outage Probability with characterized by "mean and std" −−−−−

normf = sum(outage')';        %norm factor for outage, = number of events
for i = 1:leny
    outage_pr(i,:) = outage(i,:)/normf(i);   %calculate outage pr.
end
mean = outage_pr*[1:len]';                      %mean values of outage pr.
for j = 1:leny
    var(j) = sum(([1:len]−mean(j)).^2*outage_pr(j,:)');   %var values of outage pr.
end
%disp('OOK,')
disp('OOK_4−PAM__4−PPM')
mean = mean'
std = sqrt(var)

%−−−
figure(2)
for j = 1:2
    plot(outage_pr(j,:),plotsign{j})
    hold on
end
%   plot(outage_pr(4,:),plotsign{4})
xlabel('$t_{\mathrm{out}}$_[hours]','Interpreter','latex','FontSize',17)
ylabel('$\mathrm{Pr_{\mathrm{out}}}\,\,(t_{\mathrm{out}})$','Interpreter','latex','FontSize',17)
set(gca,'XTick',1:2:31)
set(gca,'FontSize',14)
axis([1,31,0,0.4]);
legend('OOK','4−PAM','4−PPM')

[a,b] = size(outage)
for j=1:a
    outageMax(j) = max(find(outage(j,:)>0));
end
outageMax
```

Monthly outage calculation for various schemes.

```matlab
%−−− Calculating the outage probability for various simulated systems and various months −−−
% (Latency tolerant applications, AM, ACM)

%−−−−−−−−−−−−−−−−−−−−−−−−−−−−−−−%
% Author: Martin Czaputa
% email: martin.czaputa@gmail.com
% version 1.0
% last modified: 23.Aug.2010
% −−−−−−−−−−−−−−−−−−−−−−−−−−−−−−%

clear all;, clc;
rate_lim = 10^6;     %normal 10^8 !!!!!!!!!!!!!!!!!!!

% load rateAdapt_10−6.mat
load sim_data_1000.mat
%load sim_data_Rs_255_239_allMod.mat
%load sim_data_Rs_255_223_allMod.mat
%load sim_data_Rs_255_127_allMod.mat
plotsign = {'−.ok','−−*k','−+k','−k','−dk','k'};
meanMonth = zeros(12,5); varMonth = zeros(12,5);

for p = 0:11
    %−−− PAM −−−
    signal(1,:) = mpam_avgr_h_ip(1,(1:732)+p*732);   %OOK
    signal(2,:) = mpam_avgr_h_ip(2,(1:732)+p*732);   %4−PAM
    signal(3,:) = mpam_avgr_h_ip(3,(1:732)+p*732);   %8−PAM

    %−−− PPM −−−
    signal(4,:) = mppm_avgr_h_ip(2,(1:732)+p*732);   %4−PPM
    signal(5,:) = mppm_avgr_h_ip(4,(1:732)+p*732);   %16−PPM
%   signal(6,:) = mppm_avgr_h_ip(5,(1:732)+p*732);   %32−PPM

    %−−− AM −−−
%   signal(5,:) = rate_adapt_h((1:732)+p*732);  %AM

    %len = length of the signal in hours, leny count of different modulations OOK,4PAM usw
    [leny,len] = size(signal);
    %defined outage length equal to signal length, signal could be off all the time
    outage = zeros(leny,len);

    for i = 1:leny
        wahr(i) = length(find(signal(i,:)>=rate_lim)) ;
    end
```

```matlab
for k = 1:leny
    temp_s = signal(k,:) < rate_lim;
    len_out(k) = length(find(signal(k,:) < rate_lim));
    counter = 0;
    onoff = 0;

    for i = 1 : len +1
        if i < (len +1)
            if temp_s(i) == 1
                counter = counter +1;
                onoff = 1;
            else% temp_s(i) == 0
                if onoff == 1
                    outage(k,counter) = outage(k,counter) + 1;
                    counter = 0;
                    onoff = 0;
                end
            end
        else
            if onoff == 1
                outage(k,counter) = outage(k,counter) + 1;
                counter = 0;
                onoff = 0;
            end
        end
    end
end

%------ Outage Probability with characterized by "mean and std" ------

normf = sum(outage')';   %norm factor for outage, = number of events
normf(normf == 0)=1; %avoid division by zero when calculating the outages(by setting the value
    to 1)
for i = 1:leny
    outage_pr(i,:) = outage(i,:)/normf(i);   %calculate outage pr.
end
meanMonth(p+1,:) = (outage_pr*[1:len]')';                         %mean values of outage pr.
for j = 1:leny
    varMonth(p+1,j) = sum(([1:len]-meanMonth(p+1,j)).^2*outage_pr(j,:)');   %var values of
        outage pr.
end

end
disp('OOK  4-PAM  8-PAM  4-PPM  AM  ')
stdMonth = sqrt(varMonth)
meanMonth

figure(2)
for j = 1:3
    plot(outage_pr(j,:),plotsign{j})
    hold on
end
%    plot(outage_pr(4,:),plotsign{4})
xlabel('$t_{\mathrm{out}}$_[hours]','Interpreter','latex','FontSize',17)
ylabel('$\mathrm{Pr_{\mathrm{out}}}\,\,(t_{\mathrm{out}})$','Interpreter','latex','FontSize',17)
set(gca,'XTick',1:2:31)
set(gca,'FontSize',14)

axis([1,31,0,0.4]);
legend('OOK','4-PAM','4-PPM')
```

B.3 AM and ACM model

Adaptive modulation model

```matlab
%---   This simulates an "adaptive modulation" system where the modulation
% is changing according to the estimated channel state
%Measured historical yearly weather data is used to
%calculate the average hourly throughput as well as the hourly average rate
%per day. Channel losses hl, hg and the parameters for hs are loaded from
%calculated_data_ham_****.mat, which was calculated in waether_extract.m.
%Plots are done in "Plotting relevant curves".

%-------------------------------------------%
% Author: Martin Czaputa
% email: martin.czaputa@gmail.com
% version 1.0
% last modified: 11.Oct.2010
%-------------------------------------------%
```

89

```matlab
clear all; clc;
load /Users/fraggle/Documents/MATLAB/MatlabWork_2010_06_13/Simulations/attenuationData/
    calculated_data_ham_1000.mat     %loads hg=geometric attenuation, hl=atmospheric att. and
    logn_param = mus and sigmas for the lognormal scitnillation model
load /Users/fraggle/Documents/MATLAB/MatlabWork_2010_06_13/Simulations/SER_curves/BER_LIMIT_10-3.
    mat
%---define transmission values
P = 0.5;          %average transmitting power = 500mW
R = 0.5;          %Responsitivity in A/W
var_n = 10^(-17);                    %variance of AWGN of the optical channel for day / std = 10^(-8.5)
PRgsig = P*R*hg/sqrt(var_n);      %PRgsig includes geomtric losses, the reciever responsitivity and
    through sigma

%ms_range = 60*60*1000/10;   %interval in 10ms per hour
ms_range = 300;

%------------ Calculating the IP packet throuput -------
days = 366;       % Year 2008 had 366 days. Minimum days are two because of the R_b-Tilde calculation

currPerc = 1;                          %percentage display for the simulation, gives only an app. of
    the status of the sim.
percent = round([1:20]*(days*24)/20);
Rs = 10^9; Ts = 1/Rs;
packetL = 1024;
rate_adapt_ms = ones(1,ms_range)*(-100);
rate_adapt = zeros(1,ms_range*24*days);
chosenModu = cell(2,ms_range*24*days);


for i = 1:(24*days) %hours
    if i == percent(currPerc)
        disp([num2str(currPerc*5)  '%'])
        currPerc = currPerc+1;
    end
    hs = lognrnd(logn_param(1,i),logn_param(2,i),1,ms_range);   %generate hs in intervals of 10msec
        from a lognormal distribution
    SNR = PRgsig*hl(i)*hs;  %signal to noise ratio is here a vector with the length of length(hs)

    moduArt = getModulation( SNR, Pber_limit_rec, Pber_modul);

    for j = 1:ms_range
        if isequal(moduArt{1,j},'PAM')
            M = moduArt{2,j};
            k = log2(M);
            mpam_ber = Pe_bit_mpam_nB(Rs*k,M,SNR(j));
            rate_adapt_ms(j) = (1-mpam_ber)*Rs*k;
        elseif isequal(moduArt{1,j},'PPM')
            M = moduArt{2,j};
            k = log2(M);
            Rsppm = Rs/M;
            mppm_ber = Pe_bit_mppm_nB(Rsppm*k,M,SNR(j));
            ind2 = find(mppm_ber>0.8);             %The BER which is above the threshold is set 1 =
                fail. (theoretical SER formular is inaccurate)
            mppm_ber(ind2)=0.8;
            rate_adapt_ms(j) = (1-mppm_ber)*Rsppm*k;
        elseif isequal(moduArt{1,j},'dead')
            rate_adapt_ms(j) = 0;
        else
            rate_adapt_ms(j) = -999;
        end
        rate_adapt(j+(i-1)*ms_range) = rate_adapt_ms(j);
        chosenModu(1,j+(i-1)*ms_range) = moduArt(1,j);
        chosenModu(2,j+(i-1)*ms_range) = moduArt(2,j);
    end

end

 for i=1:days*24
        rate_adapt_h(i) = mean(rate_adapt(ms_range*(i-1)+1:i*ms_range));
 end

 for j=1:(days*24-23)
     rate_adapt_h_ipsmo(j) = mean(rate_adapt_h(((j-1)+1):j+23));
 end


save rateAdapt.mat rate_adapt rate_adapt_h rate_adapt_h_ipsmo chosenModu
```

Adaptive coded modulation model.

```matlab
%---   This simulates an "adaptive coded modulation" system where the modulation
% and code structure is changing according to the estimated channel state
```

```
%Measured historical yearly weather data is used to
%calculate the average hourly throughput as well as the hourly average rate
%per day. Channel losses hl, hg and the parameters for hs are loaded from
%calculated_data_ham_****.mat, which was calculated in waether_extract.m.
%Plots are done in "Plotting relevant curves".

%——————————————————————————————%
% Author: Martin Czaputa
% email: martin.czaputa@gmail.com
% version 1
% last modified: 15.Oct.2010
%——————————————————————————————%

clear all; clc;
load /Users/fraggle/Documents/MATLAB/MatlabWork_2010_06_13/Simulations/attenuationData/
    calculated_data_ham_1000.mat
% load /Users/fraggle/Documents/MATLAB/MatlabWork_2010_06_13/Simulations/SER_curves/BER_LIMIT.mat
load capacityPAMPPM_complete2.mat
load /Users/fraggle/Documents/MATLAB/MatlabWork_2010_06_13/Simulations/SER_curves/
    ppm_ldpc_ber_complete_01_01_2011.mat
load /Users/fraggle/Documents/MATLAB/MatlabWork_2010_06_13/Simulations/SER_curves/
    pam_ldpc_ber_complete_01_01_2011.mat


%———define transmission values
P = 0.5;          %average transmitting power = 500mW
R = 0.5;          %Responsitivity in A/W
var_n = 10^(-17);              %variance of AWGN of the optical channel for day / std = 10^(-8.5)
PRgsig = P*R*hg/sqrt(var_n);    %PRgsig includes geomtric losses, the reciever responsitivity and
    through sigma

%ms_range = 60*60*1000/10;   %interval in 10ms per hour
ms_range = 100;

%————————— Calculating the IP packet throuput ————————
days = 366;     % Year 2008 had 366 days. Minimum days are two because of the R_b-Tilde calculation

currPerc = 1;                          %percentage display for the simulation, gives only an app. of
    the status of the sim.
percent = round([1:20]*(days*24)/20);
Rs = 10^9; Ts = 1/Rs;
packetL = 1024;

moduRate_adapt_ms = ones(1,ms_range)*(-100);
moduRate = zeros(1,ms_range*24*days);
%rate_v = [1/2, 3/5, 2/3, 3/4, 4/5, 5/6, 8/9, 9/10];

for i = 1:(24*days) %hours
    if i == percent(currPerc)
        disp([num2str(currPerc*5) '%'])
        currPerc = currPerc+1;
    end
    hs = lognrnd(logn_param(1,i),logn_param(2,i),1,ms_range);   %generate hs in intervals of 10msec
        from a lognormal distribution
    SNR = PRgsig*hl(i)*hs;  %signal to noise ratio is here a vector with the length of length(hs)

    %——— simulation start ————
    RateModulation_ms = getModulationRate( SNR, SNR_cap, C_curve, modPAM, modPPM);

    %——— 1 = PAM, 0 = PPM, 2 = Dead

    for j = 1:ms_range
        if RateModulation_ms(1,j) == 1
            M = RateModulation_ms(2,j);
            r = RateModulation_ms(3,j);
            k = log2(M);
            mpam_ber = ser_snr( pam_ldpc_ber, pam_ldpc_ber_snr, SNR(j), r,M);      %symbol error
                probability every 10ms
            moduRate_adapt_ms(j) = (1-mpam_ber)*Rs*k*r;
        elseif RateModulation_ms(1,j) == 0
            M = RateModulation_ms(2,j);
            r = RateModulation_ms(3,j);
            k = log2(M);
            Rsppm = Rs/M;
            mppm_ber = ser_snr( ppm_ldpc_ber, ppm_ldpc_ber_snr, SNR(j), r,M);
            moduRate_adapt_ms(j) = (1-mppm_ber)*Rsppm*k*r;
        elseif RateModulation_ms(1,j) == 2
            moduRate_adapt_ms(j) = 0;
        else
            moduRate_adapt_ms(j) = -999;
        end

        moduRate_adapt(j+(i-1)*ms_range) = moduRate_adapt_ms(j);

    end
end
```

```matlab
for i=1:days*24
        moduRate_adapt_h(i) = mean(moduRate_adapt(ms_range*(i-1)+1:i*ms_range));
end


for j=1:(days*24-23)
    moduRate_adapt_h_ipsmo(j) = mean(moduRate_adapt_h(((j-1)+1):j+23));
end


save moduRateAdapt.mat moduRate_adapt moduRate_adapt_h moduRate_adapt_h_ipsmo
```

B.4 Weather data extraction.

```matlab
%——————————— Extract weather data out of csv files ———————————————
% This script merges 12 files(months) of weather data extracted from the
% canadian history weather data records. The 12 files have to be saved by
% hand in a CSV file format. In the CSV files everything has to be deleted
% what is not data until the header of the starting CSV file (Januar) like in
% the folder "ham". If different parameters of hg, link distance are needed
% this script should run once a time. Than you can comment this script from
% the start until "save model_param.mat vis_model vis_range;". All needed
% parameters are saved in model_param.mat. The parameters
% hl hg logn_param are finally saved in "calculated_data" for further
% usage. hs is not calculated here because it needs too much memory if
% calculated at once for a whole year.
% ————————————————————————————————————————————————————————————————

%————————————————————————————————————————————%
% Author: Martin Czaputa
% email: martin.czaputa.gmail.com
% version 1.0
% last modified: 21.Feb.2010
% ————————————————————————————————————————————%

clear all

%path(path,'/Users/fraggle/Documents/MATLAB/MatlabWork_2010_02_23/UsedFunctions');
%——— Linux, Unix, MAC OS command which merges the files ham_00.csv to ham_12.csv into one csv
%——— file
! cat ./ham/ham_01.csv ./ham/ham_02.csv ./ham/ham_03.csv ./ham/ham_04.csv ./ham/ham_05.csv ./ham/
    ham_06.csv ./ham/ham_07.csv ./ham/ham_08.csv ./ham/ham_09.csv ./ham/ham_10.csv ./ham/ham_11.csv
    ./ham/ham_12.csv > mergedData.csv

%%——— for Win PC use this one instead of the line above (.csv files have to be in the folder of the
    script)
% copy *.csv mergedData.csv

%——— textRep replaces all " symbols in the file. otherwise it is more
%——— difficult to deal with the csv data
textRep('mergedData.csv','mergedData_rep.csv');

%——— csvimport imports csv files into matlab --> cell structure
csvi = csvimport('mergedData_rep.csv');
temp1 = csvi(:,16);                      %extract visibility data in km
vis_range = cell2mat(temp1(2:end))';
vis_range(find(vis_range==0)) = 0.1;     %here i set the zero visibility to some small value to
    counterface hl=0

%——— take out three coloumns of weather data, discard the fourth waether
%——— coloumn
vis_mode = csvi(:,[24:26]);
vis_mode = vis_mode([2:end],:);   %first entry is the title,header

len = length(vis_mode);
%——— All different kind of weather situations are brought together to 5
%——— different weather conditions. For the model only one weather
%——— condition is chosen per hour. It is always the worst one chosen. For
%——— example if the weather data  says it is foggy and snowing than the snow
%——— model is chosen. The scintillation loss is always present.
%——— Clear=1,Fog=2, Rain=3, Snow=4, Dense Snow = 5
for k = 1:3
    for i = 1:len
        switch vis_mode{i,k}
            case{'Clear','Mainly_Clear','Mostly_Cloudy','Cloudy','Tornado','Waterspout','
                Thunderstorms','Heavy_Thunderstorms','Funnel_Cloud','Blowing_Sand','Blowing_Dust','
                Dust'}
                %vis_mode{i,k} = 'Clear';
                vis_mode{i,k} = 1;
            case{'Fog','Ice_Fog','Smoke','Haze','Freezing_Fog'}
                %vis_mode{i,k} = 'Fog';
                vis_mode{i,k} = 2;
```

```matlab
            case{'Rain','Light_Rain','Moderate_Rain','Heavy_Rain','Ice_Pellets_Showers','Ice_Pellet
               _Showers','Ice_Pellets','Ice_Crystals','Rain_Showers','Light_Rain_Showers','
               Moderate_Rain_Showers','Heavy_Rain_Showers','Drizzle','Freezing_Rain','Light_
               Freezing_Rain','Moderate_Freezing_Rain','Heavy_Freezing_Rain','Freezing_Drizzle','
               Snow_Pellets','Snow_Grains'}
               %vis_mode{i,k} = 'Rain';
               vis_mode{i,k} = 3;
            case{'Snow','Light_Snow','Heavy_Snow','Snow_Showers','Light_Snow_Showers','Blowing_Snow
               '}
               %vis_mode{i,k} = 'Snow';
               vis_mode{i,k} = 4;
            case{'Moderate_Snow','Moderate_Snow_Showers','Heavy_Snow_Showers','Hail'}
               %vis_mode{i,k} = 'Dense Snow';
               vis_mode{i,k} = 5;
            case{''}
               vis_mode{i,k} = 1;
        end
    end
end
vis_model = max(cell2mat(vis_mode)');

%--- If there is no measurement data available for a/more hours an
%--- exemption is thrown
if find(isnan(vis_model)>0)
    errRecord = MException('NaN_value_in_vis_model','Make_sure_there_each_entry_of_"visibility"_has
        _a_value');
    throw(errRecord);
end
save model_param.mat vis_model vis_range;
load model_param.mat;
len = length(vis_model);

%------------------- Model h calculations and specifications ------------
%----------------------------------------------------------------------
z = 1000;              %link distance in m
d_rlens = 0.2;         %d_recieving_lens = 0.2 m (20cm) --> aperture diameter
phi = 2*10^(-3);       % phi = 2*10^(-3)rad -> 2mrad, divergence angle
d_beam =z*phi;         %beam width at propagation distance z in m

K = 1.23;              %for a planar otpical field, 0.5 for a radial field,but be careful because
       sigma_x (0.30 ...to ) changes than too
lambda = 1550;         %wavelength in 1550 nm
k = 2*pi/(lambda*10^(-9));  %wave number, uses lambda in m


%--------------------- Calculate hl in respect to the -----------------
%------------ visibility(vis_range) and the weather condition (vis_model)--
%-KIM model, Snow and Rain model were used, one model is picked at one time

z_vis = z/1000; %the atmosphere loss uses z in km, so z must be also in km
%--- calculate q
q = zeros(1,len);
ind = find(vis_range >=50);
q(ind) = 1.6;
ind = find(6<=vis_range & vis_range <50);
q(ind) = 1.3;
ind = find(1<=vis_range & vis_range <6);
q(ind) = vis_range(ind)*0.16+0.34;
ind = find(0.5<=vis_range & vis_range <1);
q(ind) = vis_range(ind)-0.5;
ind = find(vis_range <0.5);
q(ind) = 0;

for i = 1:len
    switch vis_model(i)
        case{1,2}
            atten_atm = (3.91/vis_range(i))*(lambda/550)^(-q(i));   %clear,haze,fog
        case{3}
            atten_atm = 2.9/vis_range(i);         %rain
        case{4}
            atten_atm = 15*(2.9/vis_range(i)); %snow
        case{5}
            atten_atm = 20*(2.9/vis_range(i)); %dense snow
    end
    hl(i) = exp(-atten_atm*z_vis); %Beers-Lambert Law
end


%--------------------- Calculate hg ----------------------------------
%----------------------------------------------------------------------
hg = ((d_rlens)/d_beam)^2;   %ratio of reviece aperture area to spread beam area
hg_dB = 10*log10(hg);        %hg in dB

%--------------------- Calculate hs in respect to the ----------------
%--------------------------- visibility(vis_range) ---------------------
```

```matlab
logn_param = zeros(2,len);          %saves sigma and mu per hour calculated by Cn_2, used for lognormal
        distribution in the main simulation

%--- Cn_2 is chosen according to the visibility
for i = 1:len
    a = vis_range(i);
    switch logical(true)
        case a>=10
            Cn_2 = 2*10^(-14);
        case (a>=4) & (a<10)
            Cn_2 = 1.8*10^(-14);
        case (a>=2) & (a<4)
            Cn_2 = 1.5*10^(-14);
        case (a>=1) & (a<2)
            Cn_2 = 1*10^(-14);
        case (a<1)
            Cn_2 = 0.5*10^(-14);
    end

    %--- sig_r_2 = 1.23*k^(7/6)*Cn_2*z^(11/6) is the Rytrov variance
    sig_x_2 = 0.30545*k^(7/6)*Cn_2*z^(11/6);    %lognormal variance is approximately sig_r/4
    sig_x = sqrt(sig_x_2);                      %lognormal std deviation
    logn_param(1,i) = -2*sig_x_2;               %sig and mu for the matlab implemented lognormal
        distrib.
    logn_param(2,i) = 2*sig_x;

end

save calculated_data hl hg logn_param
```

B.5 Calculate information rates

```matlab
%--- This file plots the capacity C in BIT/T (= BIT/channel use) for M-PAM
%and M-PPM. It uses Ungerboecks numerical formular with the help of Monte
%Carlo method to calculate the capacity curves.

%------------------------------------------------%
% Author: Martin Czaputa
% email: martin.czaputa@gmail.com
% version 1.0
% last modified: 20.Sept.2010
% ------------------------------------------------%

clear all;clc;
xmin=-10; xmax=20;
SNRdB = xmin:1:xmax;
SNR = 10.^(SNRdB/10);
P = 1;
sigma = (P./SNR);
lenSNR = length(sigma);
% plotsign = {'-.ok','--*r','-+b','-c','-dk','-<k','-sm','->','-.vm','-h','-s','-^','-h'};
% plotsign = {'-.ok','--*k','-+k','-k','-dk','-k'};
plotsign = {'-k','-k','-k','-k','-k','-k'};
plotv = 1;
Rs = 1; Ts = 1/Rs;      % symbol-rate for PAM

legPlot = cell(1);
switch_pam = 'on';
switch_ppm = 'on';

% modPAM = [64,32,16,8,4,2];
% modPPM = [2,4,8,16,32,64];
modPAM = [2,4];
modPPM = [2];
C_curve = zeros(length(modPAM)+length(modPPM),lenSNR);


% ------------- M-PAM -------------
% figure
if strcmpi(switch_pam,'on')
for M = modPAM
    PAM = [0:M-1];
    constPAM = PAM*2*P*sqrt(Ts)/(M-1);
    for i = 1: lenSNR                           %calculating the capacity curve
        C_curve(plotv,i) = capMontePAM(constPAM, sigma(i));
    end
    plot(SNRdB, C_curve(plotv,:),plotsign{plotv})
    hold on
    legPlot{plotv}= [num2str(M) '-PAM'];
    plotv = plotv + 1;
end
end
```

```matlab
% ———————— M–PPM ————————

if strcmpi(switch_ppm,'on')
for M = modPPM
    Rsppm = Rs/M; Tsppm = 1/Rsppm;
%       Rsppm = Rs; Tsppm = 1/Rsppm;
    PPM = eye(M);
    constPPM = PPM*P*sqrt(Tsppm*M);
    for i = 1: lenSNR                                    %calculating the capacity curve
        C_curve(plotv,i) = capMontePPM(constPPM, sigma(i))/M;
    end
    plot(SNRdB, C_curve(plotv,:),plotsign{plotv})
    hold on
    legPlot{plotv}= [num2str(M) '–PPM'];
    plotv = plotv + 1;
end
end
hold off
%——— Plotting curves ———
% xlabel('SNR  $P/\sqrt{\sigma^2*T}\,\,\,$  [dB]','Interpreter','latex','FontSize',12)
% ylabel('C $[\mathrm{bits}\,\,\,/T_s]$','Interpreter','latex','FontSize',12)
% title('Information Rate of different modulation schemes vs. SNR [dB]')
xlabel('SNR__$P/\sigma\,\,\,$__[dB]','Interpreter','latex','FontSize',12)
ylabel('$I$_$[\mathrm{bits_/_channel_use}]$','Interpreter','latex','FontSize',12)
% $[\mathrm{bits}\,\,\,/T_s]$','Interpreter','latex','FontSize',12)
% grid on
legend(legPlot{:},'Location','NorthWest')
axis([xmin,xmax,0,1.2])
hold off
SNR_cap = SNR;
save capacityPAMPPM.mat modPAM modPPM C_curve SNR_cap


function C_star = capMontePAM(modart,sigma)

%intitialization
C_star = 0;
C_sum_k = 0;
C_sum_exp = 0;
N = length(modart);

%create a normal distributed real one dimension variable w with sigma^2 and
%a variable w for complex two dimension with 2*sigma^2
monte_leng = 10^4;

if imag(modart)==0
    w = sigma*randn(1,monte_leng);
else
    a = sigma*randn(1,monte_leng);
    b = sigma*randn(1,monte_leng);
    w = a+j*b;
end


for k=0:N-1
    C_sum_exp = 0;
    %expectation is done over Monta Carlo averaging
    for mo=1:monte_leng
        C_sum_i = 0;
        %sum over the the different exponntial functions
        for i =0:N-1
            C_sum_i = C_sum_i + exp(-(abs(modart(k+1)+w(mo)-modart(i+1))^2-abs(w(mo))^2)/(2*sigma^2))
                ;
        end
        C_sum_exp = C_sum_exp + log2(C_sum_i);
    end
    C_sum_k = C_sum_k + (1/monte_leng)*C_sum_exp;
end

C_star = log2(N)-1/N*C_sum_k;


function C_star = capMontePPM(modart,sigma)

%intitialization
C_star = 0;
C_sum_k = 0;
C_sum_exp = 0;
N = length(modart);

%create a normal distributed real one dimension variable w with sigma^2 and
%a variable w for complex two dimension with 2*sigma^2


monte_leng = 2000;
ppm_l = length(modart);
w = sigma*randn(ppm_l,monte_leng);
```

```
for k=0:N-1
    C_sum_exp = 0;
    %expectation is done with Monta Carlo averaging
    for mo=1:monte_leng
        C_sum_i = 0;
    %sum over the the different expontial functions
    for i=0:N-1
        C_sum_i = C_sum_i + exp(-((skap(modart(:,k+1)+w(:,mo)-modart(:,i+1)))-(skap(w(:,mo))))
            /(2*sigma^2));
        %C_sum_i = C_sum_i + exp(-skap(((modart(:,k+1)+w(:,mo)-modart(:,i+1))).^2-(w(:,mo)).^2)
            /(2*sigma^2));
    end
        C_sum_exp = C_sum_exp + log2(C_sum_i);
    end
    C_sum_k = C_sum_k + (1/monte_leng)*C_sum_exp;
end

C_star = log2(N)-1/N*C_sum_k;
```